MOLECULAR AND GENETIC STUDIES OF IRON HOMEOSTASIS IN ARABIDOPSIS

A Dissertation
Presented to
the Faculty of the Graduate School
University of Missouri-Columbia

In Partial Fulfillment
of the Requirements for the Degree

Doctor of Philosophy

---

by

ALBERTO MAURER

Dr. Elizabeth E. Rogers Dissertation Supervisor

MAY 2006

The undersigned, appointed by the Dean of the Graduate School, have examined the dissertation entitled

MOLECULAR AND GENETIC STUDIES OF IRON HOMEOSTASIS IN ARABIDOPSIS

Presented by ALBERTO MAURER

A candidate for the degree of Doctor of Philosophy

And hereby certify that in their opinion it is worthy of acceptance

_____
Dr. Elizabeth E. Rogers

_____
Dr. Michael Petris

_____
Dr. John C. Walker

_____
Dr. Walter Gassmann

_____
Dr. Joseph C. Polacco

ACKNOWLEDGEMENTS

First of all, I would like to thank my advisor, Dr. Elizabeth E. Rogers, for giving me the opportunity to complete my Ph.D. degree in her lab. I was only able to finish this thesis thanks to her patience and guidance.

Second, I would like to thank all the people and organizations that were able to support my studies in the form of assistantships: The Genetics Area Program and its former director Dr. Donald Riddle for my first-year assistantship; Dr. Douglass Randall and the Interdisciplinary Plant Group for the support given to me in the form of a 3-year assistantship; Dr. Elizabeth E. Rogers who supported my studies for 2 years; and to the Monsanto Corporation, who awarded me a senior grad-student assistantship. Thanks to all of you I was able to complete my degree.

I will be forever thankful to Dr. Donald Riddle, Dr. Joseph Polacco, and Dr. Kim Won-Seok for their enormous support while confronting difficult times in the middle of my degree.

Many thanks to the past and present members of my Graduate Committee: you were always supportive and ready with suggestions and help for my research and graduate career: Dr. Michael Petris, Dr. John C. Walker, Dr. Walter Gassmann, Dr. David Eide, and especially Dr. Joseph Polacco.

I need to thank my lab mates Mr. Timothy Durrett and Dr. Dirk Charlson. They were next to me in the trenches of our daily battle for good results and sound science. All their advice, suggestions, and help were primordial in the research that led to this thesis and my degree. I would like to include here all the rotation students, undergraduates, and

visiting scholars, that in one way or another helped me complete experiments and projects: Lorena DaPonte, Timothy Pouland, Juan Gutierrez, Kareema Smith, and Sandhya Tondhapu. Your help was more valuable than you could ever imagine.

A project as long and arduous as a Ph.D. degree in Genetics would have been impossible for me to attain without the unconditional support of my friends Miguel and Alicia Rodriguez, Moises Cortes-Cruz, Jason Meyer, Thomas Campbell, Juan Jose Gutierrez, Anna Glazkova, Carine Tannous, and many others that if mentioned, would fill many pages like this one. Thanks to you all.

Finally, the most important thanks of all: to my family. Thanks for your encouragement, support, and patience. This degree is dedicated to you.

TABLE OF CONTENTS

LIST OF TABLES

LIST OF FIGURES

MOLECULAR AND GENETIC STUDIES OF IRON HOMEOSTASIS IN ARABIDOPSIS

Alberto Maurer

Dr. Elizabeth E. Rogers, Dissertation Supervisor

ABSTRACT

Iron is an essential element for plant survival. However, in excess, it is deleterious to the organism, thus iron concentration is tightly regulated *in planta*. The first point in the iron regulation system is acquisition, and plants have evolved two different strategies to obtain it from the soil. Dicots and non-graminaceous monocots use Strategy I to obtain iron from soil, whereas grasses use a chelation-based mechanism termed Strategy II (Marschner, 1995 and see Chapter 1). In the present thesis, we describe two different approaches to increase our understanding of iron homeostasis in the Strategy I model plant *Arabidopsis thaliana*: a functional genomic approach (Chapter 2 and Chapter 3) and a mutant screen (Chapter 4).

For the functional genomic approach, Affymetrix ATH-1 microarrays were hybridized with RNA extracted from shoots and roots of *Arabidopsis thaliana* Col-0 plants grown under iron-sufficient or -deficient conditions. The resulting datasets were screened, analyzed, and ten genes were chosen for further studies. In Chapter 2, we describe the initial characterization of eight of the ten genes, which included a metallothionein, a putative sugar transporter, three P-Type ATPases, and three

cytochrome P450s. None of these genes appeared to have a direct effect on iron homeostasis in Arabidopsis. We also present possible future research projects using the microarray dataset as a starting point.

In Chapter 3, we show the initial characterization of the other two genes selected from the microarray dataset. Both belong to a small sub-family of four genes of the basic helix-loop-helix transcription factor family of genes. All four were up-regulated in shoots and roots of iron-deficient plants. We focused our research on *bHLH101*, which was expressed in root and shoot meristems, in cotyledons, and in the root vasculature. Since individual T-DNA lines did not show a visible phenotype under the conditions tested, and all four show similar increases in mRNA levels under iron-deficiency, we hypothesized that all four TFs provide redundancy to each other, possibly due to homo- or hetero-dimerizing within the group. At the end of Chapter 3, we propose possible functions of these transcription factors.

Finally, in Chapter 4, we show the screening of mutant plants with potential disruptions in iron-homeostasis system. The selected mutant showed variegated chlorosis and delayed induction of iron deficiency-inducible ferric-chelate reductase activity. The mutation was mapped to locus At2g34740, which encodes AtATase2 (EC 2.4.2.14). The mutation disrupted the chloroplastic purine biosynthesis pathway, which resulted in damaged chloroplasts. The chloroplast is a major site for metal use and storage in plants. Therefore, alterations in the chloroplast are hypothesized to affect metal homeostasis throughout the plant. We provide the first direct evidence linking disruption of chloroplast function with defects in general metal homeostasis in Arabidopsis.

CHAPTER 1

INTRODUCTION AND LITERATURE REVIEW

Iron is essential for living organisms

Iron is commonly found in nature. It easily changes oxidation states. Organisms take advantage of both characteristics and utilize iron in reduction/oxidation reactions and as part of certain biological structures. Plants utilize iron in respiration, chlorophyll synthesis, photosynthesis and other important processes. Its key importance in chlorophyll synthesis is one of the reasons why low iron availability makes plants chlorotic. On the other hand, iron can be dangerous to plants since it is able to catalyze the creation of reactive oxygen species through the Fenton reaction (Winterbourn, 1995). This dual nature of iron: essential, yet possibly dangerous, makes organisms regulate its uptake and storage tightly (Spiller and Terry, 1980; Terry and Low, 1982; Pushnik et al., 1984; Henle and Linn, 1997).

Iron deficiency affects 30% of the world's population (Lucca et al., 2000; Lucca et al., 2001) because even though plants produce most of the proteins and carbohydrates consumed by mankind, most of them do not store enough iron to supply our dietary needs (Grusak and DellaPenna, 1999). In some cases, plants cannot obtain enough iron to cover their nutritional needs because of certain soil conditions that make iron difficult to obtain. There has been considerable effort to increase the amount of bioavailable iron in plants to improve the diet of people affected by iron deficiency. One way to address this problem

involves using iron-based soil or foliar fertilizers with the aim to eliminate plant iron deficiency and increase their internal iron storage. The use of these fertilizers have either a limited effect on nutritive status of the plant, or are effective but too expensive to be considered for use in field crops (Hecht-Buchholz and Ortmann, 1986; Hüve et al., 2003). The most efficient way to increase iron content in plants is to genetically modify their complex mechanisms of iron acquisition and storage (Welch, 2002). In this way, the modified plants could become a more substantial source of iron for human nutrition.

To make plants a source of iron to satisfy human needs, we need to improve our understanding of iron homeostasis in plants before we can efficiently modify their iron homeostasis system. Therefore our main goal is to increase the knowledge about iron homeostasis in the model plant *Arabidopsis thaliana*. We chose Arabidopsis because its genome is completely sequenced, a large scientific community is dedicated to its study, and parts of its iron homeostasis mechanism have already been described. We hope our research could someday be used to increase total iron content in crop plants to help reduce iron deficiency in human nutrition.

Iron homeostasis in plants has been studied for a long time. We now know that plants can obtain iron from the soil in two possible ways. Grasses (e.g. maize, wheat, rice) utilize what is called Strategy II, and all other plants (e.g. Arabidopsis, potato, grape) utilize what is called Strategy I (Marschner and Romheld, 1994; Marschner, 1995). We will proceed to briefly describe both processes.

Strategy II

Strategy II plants produce phytosiderophores, which are small organic iron chelators, and release them from the roots. The synthesis of phytosiderophores begins with the conversion of methionine into nicotianamine (NA) by nicotianamine synthase (NAS). All plants contain *NAS* genes; and these genes show root-specific and iron-inducible expression in some Strategy II plants (Higuchi et al., 1999; Inoue et al., 2003; Mizuno et al., 2003). Once NA is synthesized it can be further modified resulting in a range of phytosiderophores including mugineic acid (MA) and 2'- deoxy mugineic acid (DMA). Once secreted by the roots, phytosiderophores chelate Fe(III) (Higuchi et al., 1999; von Wiren et al., 2000; Reichman and Parker, 2002; Schaaf et al., 2004a), creating a complex which is acquired by root epidermal cells through a specific importer called *YS1* (for Yellow Stripe 1) in maize or *YSL* (for Yellow Stripe-Like) in other species. *YS1* belongs to the OPT (for Oligo-Peptide Transporter) class of transporters (Yen et al., 2001). OPTs are capable of importing iron-chelator complexes through biological membranes (Curie et al., 2001; Roberts et al., 2004; Schaaf et al., 2004b). The expression of *YS1* is upregulated in shoots and roots under iron deficiency (Curie et al., 2001). It is capable of transporting several phytosiderophore-chelated metals such as Cu, Zn, Cd, Ni, Mn, Fe(II), and Fe(III), as shown in the zinc uptake-defective yeast mutant *zap1* (Schaaf et al., 2004b). Genes with homology to *YS1* have been cloned in rice (another Strategy II plant), which possess at least 18 similar genes (Koike et al., 2004). Interestingly, Arabidopsis, which is not known for importing Fe-phytosiderophore compounds into its

roots, contains at least eight genes similar to *YS1* in its genome (Walker, 2002) with possible iron-chelator transport functions inside the plant (see later).

Strategy I

Strategy I plants are characterized by three root-localized molecular responses to iron deficiency. One of these three responses consists of the induction of an unidentified ATP-dependent proton transporter whose activity will lower the pH of the rhizosphere (Romheld et al., 1984; Santi et al., 2005). This pH reduction increases Fe(III) solubility in the soil. The second response consists of increasing the transcription of a membrane-bound, root-expressed ferric-chelate reductase (Romheld and Marschner, 1983; Romera et al., 2003). It has been proposed that iron reduction is a rate-limiting step for iron acquisition in some Strategy I plants (Grusak et al., 1990). In Arabidopsis, the root epidermal reductase is encoded by the gene *FRO2*. The FRO2 protein is a flavocytochrome that transports electrons across membranes to reduce solubilized Fe(III) to Fe(II) (Robinson et al., 1999). *FRO2* belongs to a family of eight genes with tissue-specific expression including root, shoot, flower, cotyledons, trichomes, pollen grains and leaf veins (Robinson et al., 1999; Connolly et al., 2003; Wu et al., 2005; Mukherjee et al., 2006). It has been proposed that iron moves through the plant as a Fe(III)-citrate complex, which will be reduced to Fe(II) by one of the eight plant reductases before being imported into the cell as a Fe(II)-NA (Mukherjee et al., 2006). *FRO2* is coordinately regulated with *IRT1* at the transcriptional and post-transcriptional level

(Connolly et al., 2002). While *FRO2* is transcriptionally regulated by Fe, Zn, and Cd, it is only capable of reducing Fe(III) and Cu(II) (Connolly et al., 2003).

The importance of *FRO2* in Arabidopsis plants has been called into question by studies with the mutant Arabidopsis line *frd1* (for Ferric Reductase Defective 1). *frd1* plants cannot express their root ferric-chelate reductase under activity due to mutations in the *FRO2* gene (Yi and Guerinot, 1996, Robinson et al., 1999). The mutations in *FRO2* do not affect the activity of other members of the Strategy I response: under iron-deficiency conditions *IRT1* is still up-regulated and roots can still acidify the rhizosphere. *frd1* plants, when grown on soil, over-accumulate Mn and Zn, and have WT levels of iron. Plants become iron deficient only when placed in artificial media containing a strong Fe(III) chelator (Yi and Guerinot, 1996). The is an apparent contradiction between reports qualifying the ferric-chelate reductase activity as essential in *Pisum sativum* (Grusak et al., 1990), but not in *Arabidopsis thalinana* (Yi and Guerinot, 1996). From these reports, we can hypothesize that legumes require higher amounts of iron than Arabidopsis. Arabidopsis can thrive without a functional *FRO2*, since the minute amounts of Fe(II) already present in the soil are enough for the plant to survive (Yi and Guerinot, 1996), but the same conditions do not provide Pisum (Grusak et al., 1990) and possibly other legumes with enough iron to use and store.

The third molecular response to iron deficiency in Strategy I plants is the up-regulation of *IRT1* (Iron-Regulated Transporter 1) which is the essential Fe(II) importer into the root of Strategy I plants (Henriques et al., 2002, Varotto et al., 2002; Vert et al., 2002). *IRT1* belongs to the ZIP gene family of transporters, which has at least 15 members in Arabidopsis (Eide et al., 1996; Maser et al., 2001). It was cloned by

functional complementation of a yeast strain defective in iron uptake (Eide et al., 1996). Although IRT1 transports mainly Fe(II), it also has the ability to transport other divalent metals like Zn(II), Mn(II), and Cd(II). *IRT1* expression is induced in the root epidermis under low Fe, Zn, and Cd conditions, and it is regulated post-transcriptionally by Fe and Zn (Vert et al., 2001; Connolly et al., 2002).

In Arabidopsis, *IRT1* has a paralog called *IRT2* that is located ~3,000 bp away from *IRT1*. *IRT2* is similar to *IRT1* in several ways, including its iron-inducible expression in the root epidermis and its ability to transport Fe and Zn, and its ability to complement a yeast mutant defective in iron uptake (Vert et al., 2001). But there are differences between both: *IRT1*, but not *IRT2*, can transport Mn or Cd in yeast (Vert et al., 2001). Plants with mutations that make *IRT1* non-functional show lethal phenotypes whereas plants with mutations that disrupt *IRT2* appear normal. Additionally, the promoter of *IRT1* is 100-fold stronger (Vert et al., 2002), yet over-expressing *IRT2* in a plant line where *IRT1* is non-functional does not rescue the mutant plants (Varotto et al., 2002). These data imply that although both *IRT1* and *IRT2* import iron from the soil into the root of Arabidopsis plants, *IRT2* plays a secondary role in this process (Varotto et al., 2002; Vert et al., 2002).

Regulation of iron-deficiency responses

Iron-deficiency responses in Strategy I plants, including the regulation of *IRT1* and *FRO2*, respond to independent signals from both the root and the shoot (Vert et al., 2003). The local (root) iron-deficiency signal regulates modifications in the root

architecture (Schikora and Schmidt, 2001). These modifications include the increase of transfer cells in sugar beet (*Beta vulgaris*) (Landsberg, 1994), the ethylene-dependent increase in number of root hairs in *A. thaliana* (Schmidt and Schikora, 2001), and the ethylene-independent increase of transfer cells and root hairs in tomato (*Lycopersicum esculentum*) (Schikora and Schmidt, 2002).

The hypothesis that there is a long distance signal originating in the shoots that regulates iron uptake in roots of Strategy I plants was proposed after characterizing the pea mutants *dgl* (DeGenerate Leaves) and *brz* (from its BRonZe-colored leaves). Both mutant pea lines contain non-allelic mutations in a single locus, and both constitutively express their iron-deficiency responses and over-accumulate iron (Grusak, 1994). Both mutant plant lines show the presence of electron-dense particles in the mitochondria, cytoplasm, and endoplasmatic reticulum, but not the chloroplast (Becker et al., 1998). These particles are mostly iron precipitates, but include manganese and zinc (Becker et al., 1998). Reciprocal graft experiments between *dgl* and WT suggest that the up-regulation of the root iron-deficiency responses depends on the genotype of the shoot (Grusak and Pezeshgi, 1996). This implies that although the root is the organ that will acquire iron from the environment, it depends on a long-distance signal sent by the shoot to activate its iron-deficiency responses. This also implies that even though iron is required throughout the plant, iron levels are sensed in the shoot regardless of iron nutrition status elsewhere. The presence of this long-distance signal has been confirmed at the molecular level by quantifying *FRO2* and *IRT1* mRNA levels in roots on each side of split-root experiments (Vert et al., 2003). The nature of the local signal and its interaction with the systemic signal remains complex (Vert et al., 2003).

Much of what we know about iron homeostasis in eukaryotic organisms comes from studies conducted in the model organism *S. cerevisiae.* Iron is necessary and potentially toxic for yeast, and its acquisition is tightly regulated through a transcription factor that may be an iron sensor (Yamaguchi-Iwai et al., 1995; Yamaguchi et al., 1996). This transcription factor (TF) has been named Aft1 (Activator of Ferrous Transport 1) and its localization inside the yeast cell is iron-dependent: during iron deficiency conditions, Aft1p re-localizes from the cytosol to the nucleus. Once in the nucleus, Aft1p binds to promoters of genes used by the high-affinity iron-acquisition system, inducing their expression (Yamaguchi-Iwai et al., 2002). Intense research has focused on how Aft1p reacts to the presence/absence of iron. Early theories proposed that Aft1p exposed its NLS when iron was absent and hid it when iron was present (Yamaguchi-Iwai et al., 2002). A more recent hypothesis proposed that Aft1p binds iron in the form of Fe-S clusters made in the mitochondria (Chen et al., 2004). Fe-S clusters are known to interact with proteins to change their three-dimensional conformation (Beinert et al., 1997; Rouault and Tong, 2005). Recently, it has been proposed that Aft1p does not bind a Fe-S cluster, but rather an unknown signal coming from the mitochondrial Fe-S cluster synthesis pathway (Rutherford et al., 2005).

The cloning of *LeFER,* a basic helix-loop-helix (bHLH) TF mutated in the tomato line *T3238fer (Fer)* plants uncovered for the first time one of the regulators of iron-deficiency responses in Strategy I plants. This semi-lethal mutation makes *fer* tomato plants incapable of inducing its iron-deficiency responses (Brown et al., 1971; Brown and Ambler, 1974). *LeFER* is expressed in roots of WT tomato plants at basal levels and expression increases when plants become iron deficient, showing iron-dependent

transcriptional regulation (Brumbarova and Bauer, 2005). Study of 35S::*LeFER* plants show LeFER protein being down-regulated under high iron conditions, showing post-transcriptional regulation by iron (Brumbarova and Bauer, 2005). *LeFER* shows post-translational regulation as well, possibly because it may need to bind an unknown factor to become active (Ling et al., 1996; Ling et al., 2002). The master regulator and the iron sensor in plants are yet to be discovered.

The homolog of *LeFER* in Arabidopsis is AtbHLH029. This transcription factor has been described as *FRU1* (Fer-like Regulator of iron Uptake 1) and was found by doing similarity searches with the *LeFER* sequence (Jakoby et al., 2004). This TF was also described as *FIT1* (Fe-deficiency Induced Transcription factor 1) after analyzing microarray data of WT and *frd3* mutant plants grown under iron-deficiency or complete conditions (see Chapter 2) (Colangelo and Guerinot, 2004). As in the case of *LeFER*, *FRU1/FIT1* is constitutively expressed in roots and its expression increases in root epidermal cells under iron-deficiency conditions. Under normal conditions, it is weakly expressed in leaves, trichomes, and flowers, and shows no expression in siliques or cotyledons (Jakoby et al., 2004). Independent research showed that *FRU1/FIT1* is expressed in the root differentiation zone, but not in the elongation or meristematic zones (Colangelo and Guerinot, 2004). Mutant *A. thaliana* plants with a non-functional copy of this gene are conditionally lethal, chlorotic, and need to be supplied with extra iron to survive. Also, the mutant cannot increase expression levels of *FRO2* under iron-deficiency conditions (Jakoby et al., 2004). *fit1* mutant plants increase transcript levels of *IRT1* when under iron-deficiency conditions, but IRT1 protein is absent (Colangelo and Guerinot, 2004). Finally, the roots of the same mutant plants accumulate about half the

normal amount of iron, suggesting transcriptional regulation of *FRO2* and post-transcriptional regulation of *IRT1* by the same TF (Colangelo and Guerinot, 2004). Plants over-expressing *FRU1/FIT1* grown under normal conditions show similar *FRO2* mRNA levels and twice the chlorophyll levels than WT controls (Jakoby et al., 2004). When the over-expressing lines are placed under iron-deficiency conditions, both their ferric-chelate reductase activity and their *IRT1* mRNA levels are higher than WT controls grown under the same conditions (Jakoby et al., 2004). Curiously, shoots of *FRU1/FIT1* over-expressing plants show up-regulation of both *FRO2* and *IRT1* when placed in iron-deficient media (Jakoby et al., 2004). Since *FRU1/FIT1* can complement the *fer* tomato mutant, it has been suggested that *LeFER* and *FRU1/FIT1* represent a TF that is a universal Strategy I regulator (Yuan et al., 2005).

Iron transport inside the plant

Once iron is inside the root, it needs to be transported into the vasculature and to all tissues in the plant, especially iron sink organs such as pollen, seeds and leaves. Once iron reaches a particular organ/tissue, it needs to be imported into the cells. Some insights into iron translocation come from studies with the Arabidopsis mutant *frd3*. *frd3* plants constitutively express iron-deficiency responses (Rogers and Guerinot, 2002). These mutant plants over-accumulate Mn, and depending on the growth conditions, they may over-accumulate Cu, Mg, S, and Zn, in leaves and roots, and Fe in roots only (Delhaize, 1996). Excess iron is accumulated in the vascular tissue in *frd3* plants. Interestingly, *FRD3* encodes a putative transporter of small organic molecules and is expressed in cells

surrounding the root vasculature (Green and Rogers, 2004). It seems that *frd3* mutant plants cannot transport an essential factor or iron chelator into the xylem, and the absence of this hypothetical factor impedes the efficient transport of iron out of the xylem and into leaf cells (Rogers and Guerinot, 2002; Green and Rogers, 2004). Finding the substrate of *FRD3* is the focus of intense research in our lab.

Other members of the iron transport system inside the plant are the eight *YS1* homologs present in the Arabidopsis genome. It has been shown that *YS1* transports phytosiderophore-Fe(II) complexes into the roots of maize plants (Schaaf et al., 2004b) and in Arabidopsis they have been named *AtYSL1-8* (Curie et al., 2001). *AtYSL2* is the closest homolog to *ZmYS1* and it is expressed in roots and shoots where its expression is regulated by iron- and zinc-deficiency, and by copper excess (DiDonato et al., 2004; Schaaf et al., 2005). *AtYSL2* is able to transport Fe(II)-NA, Fe(II)-MA, and Cu(II)-NA when tested in yeast (DiDonato et al., 2004). Because of the localization of the expression of this gene *in planta*, it has been proposed to have a role transporting NA-Fe and NA-Cu laterally from the xylem into tissues away from the xylem (DiDonato et al., 2004; Koike et al., 2004), pointing at NA as an iron chelator inside the plant.

Iron transport inside the cell

Iron needs to enter the cell and be distributed into and out of all organelles, vesicles, cytoplasm, and any other region inside the cell. Many transporters would be required to provide the cell with an efficient cellular iron homeostasis system. So far only NRAMP (Natural Resistance Associated Macrophage Protein) transporter proteins have

been shown to participate in intracellular iron distribution (Curie et al., 2000; Guerinot, 2000; Thomine et al., 2000; Maser et al., 2001; Curie and Briat, 2003; Hall and Williams, 2003).

NRAMPS were first discovered in mammals as part of defense against microorganisms. Homologues of mammalian *NRAMP* genes were found in *D. melanogaster*, *C. elegans*, and *S. cerevesiae*. Their function as possible metal transporters was discovered in yeast (Cellier et al., 1995; Belouchi et al., 1997; Zhou and Yang, 2004). The Arabidopsis genome contains six *NRAMP* genes, of which only three (*AtNRAMP-1, -3,* and *-4*) have been partially characterized. *AtNRAMP-1, -3,* and *-4* are mainly iron transporters their transcription is induced under iron-deficiency conditions, although they also transport Zn, Mn, and Cd. Their expression localization is at times overlapping and varies during normal plant development (Curie et al., 2000; Thomine et al., 2000; Maser et al., 2001; Hall and Williams, 2003; Thomine et al., 2003; Lanquar et al., 2004). Evidence collected so far points to the involvement of *NRAMP* genes in intracellular metal homeostasis by transporting iron and other metal ions into or out of different organelles (Curie et al., 2000; Thomine et al., 2000; Thomine et al., 2003; Zhou and Yang, 2004). Specifically, *AtNramp3* and *AtNramp4* have been shown to be partially redundant, but when both are absent, Arabidopsis seeds fail to retrieve iron from the vacuole. This shows, for the first time, the role of the plant vacuole as a major iron storage place. It also shows the first iron exporters from the plant vacuole (Lanquar et al., 2005).

Iron chelators

Iron needs to be chelated to keep it in solution and at the same time to keep it from creating harmful free radicals through the Fenton reaction. There are several possible iron chelators inside plants, including malate and citrate, which are two organic acids that increase their concentration inside the plant under iron-deficient conditions (Abadia et al., 2002) and are able to form stable complexes with Fe(II) and Fe(III) (Lopez-Millan et al., 2000, 2001; Abadia et al., 2002; Hider et al., 2004). Another putative iron chelator in plants is ITP (Iron Transport Protein). ITP was discovered bound to iron in phloem exudates of *Ricinus comunis* (Kruger et al., 2002). ITP belongs to a group of late embryogenesis abundant (LEA) proteins called dehydrins. Arabidopsis has over 10 dehydrins and they are either constitutively expressed or induced under environmental stresses like cold, drought, salt stress, or ABA treatment (Puhakainen et al., 2004). It is possible that the Arabidopsis genome contains an ITP homolog (Kruger et al., 2002). Another possible plant iron chelator is NA, a ubiquitous non-proteinoic amino acid (Scholz et al., 1992; Higuchi et al., 1999) that forms stable complexes with both Fe(II) and Fe(III), and is an intermediate compound in the synthesis of phytosiderophores in Strategy II plants (Stephan and Scholz, 1990; von Wiren et al., 1999; Hider et al., 2004). Iron-deficient plants have increased NA concentrations in their roots relative to iron-sufficient plants (Stephan and Scholz, 1990; Pich et al., 2001). Additional evidence for the role of NA as an iron chelator comes from studies of the tomato mutant *chloronerva*. *chloronerva* plants have a mutation in their only NAS gene, rendering it non-functional. These plants have constitutive iron-deficiency responses, over-

accumulate iron, and show elevated activity of antioxidant enzymes and iron precipitates in vacuoles and mitochondria (Herbik et al., 1996; Yoshimura et al., 2000; Liu et al., 2002). Unlike tomato, *A. thaliana* possesses four NAS genes with possible overlapping functions, which may explain the lack of *chloronerva*-like mutants in this species (Suzuki et al., 1999; Suzuki et al., 2001).

Iron storage

The ferritin protein is found in plants and many other living organisms. Its function is to store iron, making ferritin a key member of iron detoxification and storage pathways. Twenty-four ferritin subunits will form a hollow shell with capacity to store up to 4,500 Fe(III) atoms. In vertebrates, these subunits can be divided in two types (H- and L-), whereas plants and bacteria have only one type (H-). All ferritins in nature share many properties, including their three-dimensional structure, but there are species- and cell-specific differences in how ferritin subunits are organized, and their transcription and post-transcriptional regulation show complex individual genetic regulation for each ferritin gene. The presence of Iron Regulatory Elements (IRE) found in the 5'-UTR of vertebrate ferritin mRNA is one of the most striking differences with plant ferritins (Theil, 1987; Harrison and Arosio, 1996). Under iron starvation conditions, IRP1 and IRP2 (Iron Regulatory Protein) regulate ferretin mRNA translation by binding to IREs, which in turn inhibits its translation. Each IRP shows specific transcriptional and post-transcriptional regulation, giving the system flexibility to adjust under different iron nutritional statuses (Pantopoulos**,** 2004).

Arabidopsis has four ferritin genes: *AtFer1-4*. Different factors regulate their transcription: iron overload and H_2O_2 up-regulate transcript levels of *AtFer1* and *AtFer3* whereas ABA induces the expression of AtFer2 (Petit et al., 2001). In maize, ABA (Lobreaux et al., 1993) and Ser/Thr phosphatases (Savino et al., 1997) have been implied in the regulation of ferritins (for a review see Briat et al., 1999). *AtFer1* is the most ubiquitously expressed of the four (Gaymard et al., 1996; Petit et al., 2001). These characteristics make ferritin useful to modify the total iron content in plants: by over-expressing ferritin, researchers were able to increase total iron in rice seeds two- to three-fold (Goto et al., 1999; Lucca et al., 2001) and in lettuce by up to 70% (Goto et al., 2000) when compared to controls. In addition, high levels of ferritin made tobacco plants more tolerant to oxidative stress, virus, and fungal attacks (Deák et al., 1999), and increased total plant height and weight (Yoshihara et al., 2003).

Iron is necessary for plant growth and development. Iron needs to be acquired from the soil, transported into the root vasculature, moved to the places where it is required, used, or stored. Efforts by several groups around the world have been able to help us understand how all these different mechanisms work and interact with each other. As mentioned in this review, this knowledge points to even more unanswered questions that need to be addressed. We still do not know how iron moves from the root epidermal cells to the root vasculature. What is the factor or iron chelator transported into the vasculature by FRD3? What is the oxidation state of iron while inside the vasculature or when inside the cell? How is iron distributed inside the plant and inside the cell? What is the iron sensor that directs the up-regulation of the iron acquisition process? Which transcription factor regulates the expression of *FRU1/FIT1*? What is the nature of the

shoot–to-root signal? The answer to these questions will increase our knowledge of iron homeostasis in plants, which will help us reach the ultimate goal of increasing bioavailable iron in crops.

REFERENCES

Abadia, J., Lopez-Millan, A.-F., Rombola, A., and Abadia, A. (2002). Organic acids and Fe deficiency: a review. Plant and Soil **241,** 75-86.

Becker, R., Manteuffel, R., Neumann, D., and Scholz, G.n. (1998). Excessive iron accumulation in the pea mutants dgl and brz: subcellular localization of iron and ferritin. Planta **207,** 217-223.

Beinert` H., Holm, R.H., and Munck, E. (1997). Iron-sulfur clusters: nature's modular, multipurpose structures. Science **277,** 653-659.

Belouchi, A., Kwan, T., and Gros, P. (1997). Cloning and characterization of the OsNramp family from Oryza sativa, a new family of membrane proteins possibly implicated in the transport of metal ions. Plant Molecular Biology **33,** 1085-1092.

Briat, J.-F., Lobreaux, S., Grignon, N., and Vansuyt, G. (1999). Regulation of plant ferritin synthesis: how and why. Cellular and Molecular Life Sciences **56,** 155-166.

Brown, J.C., and Ambler, J.E. (1974). Iron-stress response in tomato (*Lycopersicum esculentum*). 1. Sites of iron reduction, absorption, and transport. Physiologia Plantarum **31,** 221-224.

Brown, J.C., Chaney, R.L., and Ambler, J.E. (1971). A new tomato mutant inefficient in the transport of iron. Physiologia Plantarum **25,** 48-53.

Brumbarova, T., and Bauer, P. (2005). Iron-mediated control of the basic helix-loop-helix protein FER, a regulator of iron uptake in tomato. Plant Physiology **137,** 1018-1026.

Cellier, M., Prive, G., Belouchi, A., Kwan, T., Rodrigues, V., Chia, W., and Gros, P. (1995). Nramp defines a family of membrane proteins. Proceedings of the National Academy of Sciences of the United States of America **92,** 10089-10093.

Chen, O.S., Crisp, R.J., Valachovic, M., Bard, M., Winge, D.R., and Kaplan, J. (2004). Transcription of the yeast iron regulon responds not directly to iron but

rather to iron-sulfur cluster biosynthesis. Journal of Biological Chemistry **279,** 29513.

Colangelo, E.P., and Guerinot, M.L. (2004). The essential basic helix-loop-helix protein FIT1 is required for the iron deficiency response. Plant Cell **16,** 3400-3412.

Connolly, E.L., Fett, J.P., and Guerinot, M.L. (2002). Expression of the IRT1 metal transporter is controlled by metals at the levels of transcript and protein accumulation. Plant Cell **14,** 1347-1357.

Connolly, E.L., Campbell, N.H., Grotz, N., Prichard, C.L., and Guerinot, M.L. (2003). Overexpression of the FRO2 ferric chelate reductase confers tolerance to growth on low iron and uncovers posttranscriptional control. Plant Physiology **133,** 1102-1110.

Curie, C., and Briat, J.-F. (2003). Iron transport and signaling in plants. Annual Reviews in Plant Biology **54,** 07.01-07.24.

Curie, C., Alonso, J.M., Le Jean, M., Ecker, J.R., and Briat, J.-F. (2000). Involvement of NRAMP1 from *Arabidopsis thaliana* in iron transport. Biochemical Journal **347,** 749-755.

Curie, C., Panaviene, Z., Loulergue, C., Dellaporta, S.L., Briat, J.-F., and Walker, E.L. (2001). Maize yellow stripe1 encodes a membrane protein directly involved in Fe(III) uptake. Nature **409,** 346-349.

Deák, M., Horváth, G.V., Davletova, S., Török, K., Sass, L., Vass, I., Barna, B., Király, Z., and Dudits, D. (1999). Plants ectopically expressing the iron binding protein, ferritin, are tolerant to oxidative damage and pathogens. Nature Biotechnology **17,** 192-197.

Delhaize, E. (1996). A metal-accumulator mutant of Arabidopsis thaliana. Plant Physiology **111,** 849-855.

DiDonato, R.J., Roberts, L.A., Sanderson, T., Eisley, R.B., and Walker, E.L. (2004). Arabidopsis Yellow Stripe-Like2 (YSL2): a metal-regulated gene encoding a plasma membrane transporter of nicotianamine-metal complexes. Plant Journal **39,** 403-414.

Eide, D., Broderius, M., Fett, J.P., and Guerinot, M.L. (1996). A novel iron-regulated metal transporter from plants identified by functional expression in yeast. Proceedings of the National Academy of Sciences of the United States of America **93,** 5624-5628.

Gaymard, F., Boucherez, J., and Briat, J.-F. (1996). Characterization of a ferritin mRNA from Arabidopsis thaliana accumulated in response to iron through an oxidative pathway independent of abscisic acid. Biochemical Journal **318,** 67-73.

Goto, F., Yoshihara, T., and Saiki, H. (2000). Iron accumulation and enhanced growth in transgenic lettuce plants expressing the iron- binding protein ferritin. Theoretical and Applied Genetics **100,** 658-664.

Goto, F., Yoshibara, T., Shigemoto, N., Toki, S., and Takaiwa, F. (1999). Iron fortification of rice seed by the soybean ferritin gene. Nature Biotechnology **17,** 282-286.

Green, L.S., and Rogers, E.E. (2004). FRD3 controls iron localization in Arabidopsis. Plant Physiology **136,** 2523-2531.

Grusak, M.A. (1994). Iron transport to developing ovules of *Pisum sativum* (I. seed import characteristics and phloem iron-loading capacity of source regions). Plant Physiology **104,** 649-655.

Grusak, M.A., and Pezeshgi, S. (1996). Shoot-to-root signal transmission regulates root Fe(III) reductase activity in the *dgl* mutant of pea. Plant Physiology **110,** 329-334.

Grusak, M.A., and DellaPenna, D. (1999). Improving the nutrient composition of plants to enhance human nutrition and health. Annual Review of Plant Physiology and Plant Molecular Biology **50,** 133-161.

Grusak, M.A., Welch, R.M., and Kochian, L.V. (1990). Does iron deficiency in *Pisum sativum* enhance the activity of the root plasmalemma iron transport protein? Plant Physiology **94,** 1353-1357.

Guerinot, M.L. (2000). The ZIP family of metal transporters. Biochimica et Biophysica Acta (BBA) - Biomembranes **1465,** 190-198.

Hall, J.L., and Williams, L.E. (2003). Transition metal transporters in plants. Journal of Experimental Botany **54,** 2601-2613.

Harrison, P.M., and Arosio, P. (1996). The ferritins: molecular properties, iron storage function and cellular regulation. Biochimica et Biophysica Acta (BBA) - Bioenergetics **1275,** 161-203.

Hecht-Buchholz, C., and Ortmann, U. (1986). Effect of foliar iron application on regreening and chloroplast development in iron-chlorotic soybean. Journal of Plant Nutrition **9,** 647-659.

Henle, E.S., and Linn, S. (1997). Formation, prevention, and repair of DNA damage by iron/hydrogen peroxide. Journal of Biological Chemistry **272,** 19095-19098.

Henriques, R., Jasik, J., Klein, M., Martinoia, E., Feller, U., Schell, J., Pais, M.S., and Koncz, C. (2002). Knock-out of Arabidopsis metal transporter gene *IRT1* results in iron deficiency accompanied by cell differentiation defects. Plant Molecular Biology **50,** 587-597.

Herbik, A., Giritch, A., Horstmann, C., Becker, R., Balzer, H.-J., Baumlein, H., and Stephan, U.W. (1996). Iron and copper nutrition-dependent changes in protein expression in a tomato wild type and the nicotianamine-free mutant chloronerva. Plant Physiology **111,** 533-540.

Hider, R.C., Yoshimura, E., Khodr, H., and von Wiren, N. (2004). Competition or complementation: the iron-chelating abilities of nicotianamine and phytosiderophores. New Phytologist **164,** 204-208.

Higuchi, K., Suzuki, K., Nakanishi, H., Yamaguchi, H., Nishizawa, N.-K., and Mori, S. (1999). Cloning of nicotianamine synthase genes, novel genes involved in the biosynthesis of phytosiderophores. Plant Physiology **119,** 471-479.

Hüve, K., Remus, R., Lüttschwager, D., and Merbach, W. (2003). Transport of foliar applied iron (59Fe) in *Vicia faba*. Journal of Plant Nutrition **26,** 2231-2242.

Inoue, H., Higuchi, K., Takahashi, M., Nakanishi, H., Mori, S., and Nishizawa, N.K. (2003). Three rice nicotianamine synthase genes, *OsNAS1*, *OsNAS2*, and *OsNAS3* are expressed in cells involved in long-distance transport of iron and differentially regulated by iron. Plant Journal **36,** 366-381.

Jakoby, M., Wang, H.-Y., Reidt, W., Weisshaar, B., and Bauer, P. (2004). *FRU (BHLH029)* is required for induction of iron mobilization genes in *Arabidopsis thaliana*. FEBS Letters **577,** 528-534.

Koike, S., Inoue, H., Mizuno, D., Takahashi, M., Nakanishi, H., Mori, S., and Nishizawa, N.K. (2004). OsYSL2 is a rice metal-nicotianamine transporter that is regulated by iron and expressed in the phloem. Plant Journal **39,** 415-424.

Kruger, C., Berkowitz, O., Stephan, U.W., and Hell, R. (2002). A metal-binding member of the late embryogenesis abundant protein family transports iron in the pholem of *Ricinus communis* L. Journal of Biological Chemistry **28,** 25062-25069.

Landsberg, E.-C. (1994). Transfer cell formation in sugar beet roots induced by latent Fe deficiency. Plant and Soil **165,** 197-205.

Lanquar, V., Lelievre, F., Barbier-Brygoo, H., and Thomine, S. (2004). Regulation and function of AtNRAMP4 metal transporter protein. Soil Science and Plant Nutrition **50,** 1141–1150.

Lanquar, V., Lelièvre, F., Bolte, S., Hamès, C., Alcon, C., Neumann, D., Vansuyt, G., Curie, C., Schröder, A., Krämer, U., Barbier-Brygoo, H., and Thomine, S. (2005). Mobilization of vacuolar iron by AtNRAMP3 and AtNRAMP4 is essential for seed germination on low iron. EMBO Journal **24,** 4041-4051.

Ling, H.-Q., Pitch, A., Scholz, G., and Ganal, M.W. (1996). Genetic analysis of two tomato mutants affected in the regulation of iron metabolism. Molecular and General Genetics MGG **252,** 87-92.

Ling, H.-Q., Bauer, P., Bereczky, Z., Keller, B., and Ganal, M. (2002). The tomato *fer* gene encoding a bHLH protein controls iron-uptake responses in roots. Proceedings of the National Academy of Sciences of the United States of America **99,** 13938-13943.

Liu, Z., Shen, J., Carbrey, J.M., Mukhopadhyay, R., Agre, P., and Rosen, B.P. (2002). Arsenite transport by mammalian aquaglyceroporins AQP7 and AQP9. Proceedings of the National Academy of Sciences of the United States of America **99,** 6053-6058.

Lobreaux, S., Hardy, T. and Briat, J. F. (1993) Abscisic acid isinvolved in the iron-induced synthesis of maize ferritin. EMBO Journal **12,** 651–657.

Lopez-Millan, A.F., Morales, F., Abadia, A., and Abadia, J. (2000). Effects of iron deficiency on the composition of the leaf apoplastic fluid and xylem sap in sugar beet. Implications for iron and carbon transport. Plant Physiology **124,** 873-884.

Lopez-Millan, A.F., Morales, F., Abadia, A., and Abadia, J. (2001). Changes induced by Fe deficiency and Fe resupply in the organic acid metabolism of sugar beet (*Beta vulgaris*) leaves. Physiologia Plantarum **112,** 31-38.

Lucca, P., Hurrell, R., and Potrykus, I. (2001). Approaches to improving the bioavailability and level of iron in rice seeds. Journal of the Science of Food and Agriculture **81,** 828-834.

Lucca, P., Wunn, J., Hurrell, R., and Potrykus, I. (2000). Development of iron-rich rice and improvement of its absortion in humans by genetic engineering. Journal of Plant Nutrition **23,** 1983-1988.

Marschner, H. (1995). Mineral nutrition of higher plants, second edition. Academic Press, London.

Marschner, H., and Romheld, V. (1994). Strategies of plants for iron acquisition of iron. Plant and Soil **165,** 261-274.

Maser, P., Thomine, S., Schroeder, J.I., Ward, J.M., Hirshi, K., Sze, H., Talke, I.N., Amtmann, A., Maathuis, F.J.M., Sanders, D., Harper, J.F., Tchieu, J., Gribskov, M., Persans, M.W., Salt, D.E., Kim, S.A., and Guerinot, M.L. (2001). Phylogenetic relationships within cation transporter families of Arabidopsis. Plant Physiology **126,** 1646-1667.

Mizuno, D., Higuchi, K., Sakamoto, T., Nakanishi, H., Mori, S., and Nishizawa, N.K. (2003). Three nicotianamine synthase genes isolated from maize are

differentially regulated by iron nutritional status. Plant Physiology **132,** 1989-1997.

Mukherjee, I., Campbell, N., Ash, J., and Connolly, E. (2006). Expression profiling of the Arabidopsis ferric chelate reductase (*FRO*) gene family reveals differential regulation by iron and copper. Planta**,** in press.

Pantopoulos, K. (2004). Iron metabolism and the IRIE/IRP regulatory system: an update. Annals of the New York Academy of Sciences **1012,** 1–13

Petit, J.-M., Briat, J.-F., and Lobreaux, S. (2001). Structure and differential expression of the four members of the *Arabidopsis thaliana* ferritin gene family. Biochemical Journal **359,** 575-582.

Pich, A., Manteuffel, R., Hillmer, S., Scholz, G.n., and Schmidt, W. (2001). Fe homeostasis in plant cells: Does nicotianamine play multiple roles in the regulation of cytoplasmic Fe concentration? Planta **213,** 967-976.

Puhakainen, T., Hess, M.W., Makela, P., Svensson, J., Heino, P., and Palva, E.T. (2004). Overexpression of multiple dehydrin genes enhances tolerance to freezing stress in Arabidopsis. Plant Molecular Biology **54,** 743-753.

Pushnik, J.C., Miller, G.W., and Manwaring, J.H. (1984). The role of iron in higher plant chlorophyll biosynthesis, maintenance and chloroplast biogenesis. Journal of Plant Nutrition **7,** 733-758.

Reichman, S.M., and Parker, D.R. (2002). Revisiting the metal-binding chemistry of nicotianamine and 2'-deoxymugineic acid. Implications for iron nutrition in Strategy II plants. Plant Physiology **129,** 1435-1438.

Roberts, L.A., Pierson, A.J., Panaviene, Z., and Walker, E.L. (2004). Yellow Stripe1. Expanded roles for the maize iron-phytosiderophore transporter. Plant Physiology **135,** 112-120.

Robinson, N.J., Procter, C.M., Connolly, E.L., and Guerinot, M.L. (1999). A ferric-chelate reductase for iron uptake from soils. Nature **397,** 694-697.

Rogers, E.E., and Guerinot, M.L. (2002). FRD3, a member of the multidrug and toxin efflux family, controls iron deficiency responses in Arabidopsis. Plant Cell **14,** 1787-1799.

Romera, F.J., Frejo, V.M., and Alcantara, E. (2003). Simultaneous Fe- and Cu-deficiency synergically accelerates the induction of several Fe-deficiency stress responses in Strategy I plants. Plant Physiology and Biochemistry **41,** 821-827.

Romheld, V., and Marschner, H. (1983). Mechanism of iron uptake by peanut plants. Plant Physiology **71,** 949-954.

Romheld, V., Muller, C., and Marschner, H. (1984). Localization and capacity of proton pumps in roots of intact sunflower plants. Plant Physiology **76,** 603-606.

Rouault, T.A., and Tong, W.-H. (2005). Iron-sulphur cluster biogenesis and mitochondrial iron homeostasis. Nature Reviews Molecular Cell Biology **6,** 345-351.

Rutherford, J.C., Ojeda, L., Balk, J., Muhlenhoff, U., Lill, R., and Winge, D.R. (2005). Activation of the Iron Regulon by the Yeast Aft1/Aft2 Transcription Factors Depends on Mitochondrial but Not Cytosolic Iron-Sulfur Protein Biogenesis. Journal of Biological Chemistry **280,** 10135-10140.

Savino, G., Briat, J. F. and Lobreaux, S. (1997) Inhibition of the iron-induced ZmFer1 maize ferritin gene expression by antioxidants and Ser:Thr phosphatase inhibitors. J. Biol. Chem. **272**, 33319–33326.

Santi, S., Cesco, S., Varanini, Z., and Pinton, R. (2005). Two plasma membrane H+-ATPase genes are differentially expressed in iron-deficient cucumber plants. Plant Physiology and Biochemistry **43,** 287-292.

Schaaf, G., Erenoglu, B.E., and von Wiren, N. (2004a). Physiological and biochemical characterization of metal-phytosiderophore transport in graminaceous species. Soil Science and Plant Nutrition **50,** 989–995.

Schaaf, G., Ludewig, U., Erenoglu, B.E., Mori, S., Kitahara, T., and von Wiren, N. (2004b). ZmYS1 functions as a proton-coupled symporter for phytosiderophore- and nicotianamine-chelated metals. Journal of Biological Chemistry **279,** 9091-9096.

Schaaf, G., Schikora, A., Haberle, J., Vert, G., Ludewig, U., Briat, J.-F., Curie, C., and von Wiren, N. (2005). A putative function for the Arabidopsis Fe-phytosiderophore transporter homolog AtYSL2 in Fe and Zn homeostasis. Plant Cell Physiology **46,** 762-774.

Schikora, A., and Schmidt, W. (2001). Iron stress-induced changes in root epidermal cell fate are regulated independently from physiological responses to low iron availability. Plant Physiology **125,** 1679-1687.

Schikora, A., and Schmidt, W. (2002). Formation of transfer cells and H+-ATPase expression in tomato roots under P and Fe deficiency. Planta **215,** 304-311.

Schmidt, W., and Schikora, A. (2001). Different pathways are involved in phosphate and iron stress-induced alterations of root epidermal cell development. Plant Physiology **125,** 2078-2084.

Scholz, G., Becker, R., Pich, A., and Stephan, U.W. (1992). Nicotianamine - a common constituent of strategies I and II of iron acquisition by plants: a review. Journal of Plant Nutrition **15,** 1647-1665.

Spiller, S., and Terry, N. (1980). Limiting factors in photosynthesis. Plant Physiology **65,** 121-125.

Stephan, U.W., and Scholz, G. (1990). Nicotianamine concentrations in iron sufficient and iron deficient sunflower and barley roots. Journal of Plant Physiology **136,** 631-634.

Suzuki, K., Nakanishi, H., Nishizawa, N.K., and Mori, S. (2001). Analysis of upstream region of nicotianamine synthase gene from *Arabidopsis thaliana*: presence of putative ERE-like sequence. Bioscience, Biotechnology, and Biochemistry **65,** 2794-2797.

Suzuki, K., Higuchi, K., Nakanishi, H., Nishizawa, N.K., and Mori, S. (1999). Cloning of nicotianamine synthase genes from *Arabidopsis thaliana*. Soil Science and Plant Nutrition **45,** 993-1002.

Terry, N., and Low, G. (1982). Leaf chlorophyll content and its relation to the intracellular localization of iron. Journal of Plant Nutrition **5,** 301-310.

Theil, E.C. (1987). Ferritin: structure, gene regulation, and cellular function in animals, plants, and microorganisms. Annual Review of Biochemistry **56,** 289-315.

Thomine, S., Wang, R., Ward, J.M., Crawford, N.M., and Schroeder, J.I. (2000). Cadmium and iron transport by members of a plant metal transporter family in Arabidopsis with homology to Nramp genes. Proceedings of the National Academy of Sciences of the United States of America **97,** 4991-4996.

Thomine, S., Lelievre, F., Debardelieux, E., Schroeder, J.I., and Barbier-Brygoo, H. (2003). AtNRAMP3, a multispecific vacuolar metal transporter involved in plant responses to iron deficiency. Plant Journal **34,** 685-695.

Varotto, C., Maiwald, D., Pesaresi, P., Jahns, P., Salamini, F., and Leister, D. (2002). The metal ion transporter IRT1 is necessary for iron homeostasis and efficient photosynthesis in *Arabidopsis thaliana*. Plant Journal **31,** 589-599.

Vert, G., Briat, J.-F., and Curie, C. (2001). Arabidopsis *IRT2* gene encodes a root-periphery iron transporter. Plant Journal **26,** 181-189.

Vert, G., Grotz, N., Dedaldechamp, F., Gaymard, F., Guerinot, M.L., Briat, J.-F., and Curie, C. (2002). IRT1, an Arabidopsis transporter essential for iron uptake from the soil and for plant growth. Plant Cell **14,** 1223-1233.

Vert, G.A., Briat, J.-F., and Curie, C. (2003). Dual regulation of the Arabidopsis high-affinity root iron uptake system by local and long-distance signals. Plant Physiology **132,** 796-804.

von Wiren, N., Khodr, H., and Hider, R.C. (2000). Hydroxylated phytosiderophore species possess an enhanced chelate stability and affinity for Iron(III). Plant Physiology **124,** 1149-1157.

von Wiren, N., Klair, S., Bansal, S., Briat, J.-F., Khodr, H., Shioiri, T., Leigh, R.A., and Hider, R.C. (1999). Nicotianamine chelates both Fe(III) and Fe(II). Implications for metal transport in plants. Plant Physiology **119,** 1107-1114.

Walker, E.L. (2002). Functional analysis of the Arabidopsis yellow stripe-like (YSL) family. Heavy metal transport and partitioning via metal-nicotanamine (NA) complexes. Plant Physiology **129,** 431-432.

Welch, R.M. (2002). The impact of mineral nutrients in food crops on global human health. Plant and Soil **247,** 83-90.

Winterbourn, C.C. (1995). Toxicity of iron and hydrogen peroxide: the Fenton reaction. Toxicology Letters **82-83,** 969-974.

Wu, H., Li, L., Du, J., Yuan, Y., Cheng, X., and Ling, H.-Q. (2005). Molecular and biochemical characterization of the Fe(III) chelate reductase gene family in *Arabidopsis thaliana*. Plant Cell Physiology **46,** 1505-1514.

Yamaguchi, Y., Heiny, M.E., Suzuki, M., and Gitlin, J.D. (1996). Biochemical characterization and intracellular localization of the Menkes disease protein. Proceedings of the National Academy of Sciences of the United States of America **93,** 14030-14035.

Yamaguchi-Iwai, Y., Dancis, A., and Klausner, R.D. (1995). AFT1: a mediator of iron regulated transcriptional control in *Saccharomyces cerevisiae*. EMBO Journal **14,** 1231-1239.

Yamaguchi-Iwai, Y., Ueta, R., Fukunaka, A., and Sasaki, R. (2002). Subcellular localization of Aft1 transcription factor responds to iron status in *Saccharomyces cerevisiae*. Journal of Biological Chemistry **277,** 18914-18918.

Yen, M-R., Tseng, Y-H., and Saier, M.H., Jr. (2001). Maize *Yellow Stripe1*, an iron-phytosiderophore uptake transporter, is a member of the oligopeptide transporter (OPT) family. Microbiology **147,** 2881-2883.

Yi, Y., and Guerinot, M.L. (1996). Genetic evidence that induction of root Fe(III) chelate reductase activity is necessary for iron uptake under iron deficiency. Plant Journal **10,** 835-844.

Yoshihara, T., Masuda, T., Jiang, T., Goto, F., Mori, S., and Nishizawa, N.K. (2003). Analysis of some divalent metal contents in tobacco expressing the exogenous soybean ferritin gene. Journal of Plant Nutrition **26,** 2253-2265.

Yoshimura, E., Sakaguchi, T., Nakanishi, H., Nishizawa, N.K., Nakai, I., and Mori, S. (2000). Characterization of the chemical state of iron in the leaves of wild-type tomato and of a nicotianamine-free mutant chloronerva by X-ray absortion near edge structure (XANES). Phytochemical Analysis **11,** 160-162.

Yuan, Y.X., Zhang, J., Wang, D.W., and Ling, H.Q. (2005). *AtbHLH29* of *Arabidopsis thaliana* is a functional ortholog of tomato *FER* involved in controlling iron acquisition in strategy I plants. Cell Research **15,** 613-621.

Zhou, X., and Yang, Y. (2004). Differential expression of rice Nramp genes in response to pathogen infection, defense signal molecules and metal ions. Physiological and Molecular Plant Pathology **65,** 235-243.

CHAPTER 2

FUNCTIONAL GENOMIC ANALYSIS OF IRON HOMEOSTASIS IN *Arabidopsis thaliana*

ABSTRACT

Iron acquisition and regulation is a complex and not well-understood process. In order to increase our knowledge of plant iron homeostasis, Drs. Elizabeth E. Rogers and Mary Lou Guerinot (Dartmouth College) hybridized Affymetrix ATH-1 microarrays with RNA extracted from shoots and roots of *Arabidopsis thaliana* Col-0 plants grown under iron-sufficient or -deficient conditions. Ten genes were chosen for further study. These genes were selected based on their modification of transcriptional activity under iron-deficient conditions or on their possible involvement in iron homeostasis as inferred from their annotation. Individual T-DNA insertion lines for each of the ten genes were obtained from the Arabidopsis Biological Resources Center (ABRC). All the homozygous T-DNA lines appeared similar to control plants under the conditions tested. The initial characterization of two genes encoding bHLH transcription factors is described in Chapter 3. The remaining eight genes included a metallothionein, a putative sugar transporter, three P-Type ATPases, and three cytochrome P450s. The three cytochrome P450s are closely related to each other, making them potentially functionally redundant. RNAi lines are in the process of being obtained to reduce or eliminate the expression of the three simultaneously.

INTRODUCTION

Iron is plentiful in soils in the insoluble Fe(III) form, which is difficult for plants to acquire and utilize. Therefore iron is one of the three nutrients most commonly limiting plant growth, after nitrogen and phosphorous (Marschner, 1995). To acquire iron from the soil, non-graminaceous plants like *Arabidopsis thaliana* (also called Strategy I plants) activate three iron-deficiency responsive genes. One, an unidentified proton pump, is expressed in root epidermal cells and extrudes protons into the rhizosphere. This pH reduction increases the solubility of Fe(III). Solubilized Fe(III) is reduced to Fe(II) by a root epidermal ferric-chelate reductase encoded by the gene *AtFRO2*. Reduced iron is directly taken into the plant using the main root iron importer, AtIRT1.

Iron homeostasis is a process that is still not fully understood (for a review see Chapter 1). To increase our knowledge of iron sensing, acquisition, and regulation, Dr. Elizabeth E. Rogers in collaboration with Dr. Mary Lou Guerinot at Dartmouth College started a genomics effort aimed at identifying and characterizing novel genes involved in the iron homeostasis system of *A. thaliana*. This effort started with the hybridization of Affymetrix ATH-1 microarrays with RNA from shoots and roots of iron-sufficient and -deficient *Arabidopsis thaliana* Col-0 plants.

Thanks to the sequencing of the *A. thaliana* genome (The Arabidopsis Genome Initiative, 2000) and the development of the Affymetrix ATH-1 high-density microarray, we were able to measure the global gene expression of this plant in response to iron deprivation (Aharoni and Vorst, 2002; Coughlan et al., 2004). The Affymetrix chip is sensitive, with a detection limit of 1/100,000 RNA transcripts (Ishii et al., 2000), and its

ability to quantify transcript abundance is similar to that of RNA blots (Meyers et al., 2004). The Affymetrix ATH-1 whole genome microarray contains probes for ~24,000 (Meyers et al., 2004) of the 26,207 genes annotated at the latest release (Haas et al., 2005), providing us with the tools to accelerate our transition from raw data to broader understanding (Wisman and Ohlrogge, 2000) of iron homeostasis. We proceeded to use the concept of co-regulation (cluster analysis), where genes showing similar expression patterns may be functionally related and under the same genetic control mechanism (Aharoni and Vorst, 2002; Buckhout and Thimm, 2003; Kennedy and Wilson, 2004).

Different types of arrays have been previously used to investigate plant iron homeostasis. The first report was published in 2001 and used a 6,300 cDNA spotted array. The spotted array was hybridized with iron-sufficient and iron-deficient WT Arabidopsis mRNA at one, three, and seven days after iron withdrawal (Thimm et al., 2001). Of the total amount of genes spotted on the array, 4.6%, 45.4%, and 18.2% showed alt-erations in transcript levels in shoots one, three, and seven days after iron withdrawal. In roots, 2.5%, 24.5, and 14.0% of the total amount of genes spotted on the array showed statistically significant changes in transcript levels one, three, and seven days after iron withdrawal, as compared with the control. In a more detailed study of transcripts level of enzymes involved in the glycolysis, tricarboxylic acid cycle (TCA), and the oxidative pentose (OPP) pathways in roots, it was shown that all were affected by iron-deficiency conditions in either roots or shoots in at least one of their three time points, although statistical analysis was not performed, therefore we cannot know if the differences were significant. (Thimm et al., 2001). In another case, the researchers used their own high-density microarray with 1,280 spots representing genes expressed in

tomato roots. The tomato plants were grown in a hydroponic solution and RNA extracted after iron had been withdrawn from a few hours to up to two days. Both phosphate and iron nutrition pathways showed close molecular relationships, including extensive crosstalk between members of iron and phosphate signal transduction (Wang et al., 2002). The first study using a standardized microarray (Affymetrix 8.3 k), concluded that although the metal transporters studied had a wide substrate specificity, only a few metals regulated their transcription.

Here we present the initial analysis of datasets from Affymetrix ATH-1 microarrays hybridized with RNA extracted from shoots and roots of iron-sufficient and -deficient *A. thaliana* plants. The analysis revealed many genes with modified expression under iron-deficiency conditions. Ten novel iron-regulated genes ere chosen for further study based on their annotation. Results of these studies for two bHLH transcription factors are presented in Chapter 3, whereas the results for the other eight are presented here.

RESULTS

Affymetrix dataset mining

Affymetrix ATH-1 microarrays were hybridized with RNA obtained independently from shoots and roots of plants grown under iron-sufficient and -deficient conditions. Since only one (out of two) microarray dataset was analyzed, no statistical analysis is given. Comparisons were made between iron-deficient and -sufficient shoot

and root datasets. Results were screened; genes were ranked according to the increase or decrease of their transcript level under iron-deficiency conditions. The 91 genes showing at least a two-fold variation are shown in Table 2.1.

Analysis of iron-sufficient and –deficient shoots

Eight genes in shoots with at least a two-fold expression increase, are shown in Table 2.1.a. Of the eight, four had no known function and the other four were a zinc-finger protein, an oligopeptide transporter (*AtOPT3*) that has been characterized before as being critical for embryo development and is expressed in the plant vasculature (Koh et al., 2002, Stacey et al., 2002, Stacey et al., 2006), an expansin precursor, and a Ser/Thr kinase. Of the four without annotation, At1g48300 increased its expression the most (three-fold). It is a single-copy gene in Arabidopsis, and the N-terminal of its predicted protein weakly resembled a ferredoxin. The predicted protein may be targeted to an endomembrane. The second gene without annotation was up-regulated 2.5-fold (At3g56360). This gene has no other copies in the genome, predicted to be localized to the chloroplast, and does not resemble any other proteins present in the databases. Iron-deficient conditions in shoots induced a 2.4-fold increase in transcript levels of At3g22240. The predicted protein may be targeted to the mitochondrion, and has five homologs in the Arabidopsis genome. Finally, At2g25660 was up-regulated two-fold, encodes a 238 kDa protein predicted to be directed to the chloroplast, is a unique gene in Arabidopsis, and has two orthologs in the public databases: one in rice and another in the blue-green alga *Synechococcus elongatus*.

Table 2.1.b shows 10 genes that were down-regulated at least two-fold in iron-deficient shoots. Ferritin is the main iron-storage protein in plants, and plants would be expected to deplete iron reserves in the absence of available iron. This was consistent with ferritins being the top three down-regulated genes. Since iron can create dangerous radicals through the Fenton reaction, its absence may down-regulate stress and oxidation-related genes (superoxide dismutase, Heat Shock Proteins, Stromal ascorbate peroxidase). This was indeed observed in Table 2.1.b. *AtYSL1*, proposed to be an iron-chelate transporter into the Arabidopsis seed (LeJean et al., 2005) shows a -2.5-fold decreased change in transcript level in iron-deficient shoots (explained in more detail below). Finally, gene At5g50335 shows decreased expression in iron-deficient shoots (-2.6-fold), encodes an 8.5 kDa protein, had no homologs in the Arabidopsis genome, and no orthologs in public databases.

Analysis of iron-sufficient and –deficient roots

Table 2.1.c shows the 50 genes that were up-regulated at least two-fold in iron-deficient roots. Several were genes directly involved in iron-acquisition. Both iron importers of the root are represented, with *IRT1* being up-regulated 12-fold, and *IRT2* up-regulated five-fold. *FRO2*, a well-characterized iron-deficiency inducible ferric-chelate reductase expressed in the root epidermis, was not present on the microarray. The transcription factor *bHLH039* was up-regulated in iron-deficient roots 10-fold (Table 2.1.c and Chapter 3). Another bHLH transcription factor, *FIT1*, is present in the list and was up-regulated 2.5-fold. *FIT1* regulates *FRO2* at the transcriptional level and *IRT1* post-transcriptionally (Colangelo and Guerinot, 2004). Iron-starvation may have

pleiotropic effects on other metal-regulated genes like Zn- (7.6-fold) and Cu- (5.0-fold) transporters. The most up-regulated gene was an In2-like gene (17.6-fold), with possible glutathione-S-transferase activity, and predicted to be a transmembrane Ser/Thr receptor protein kinase.

Four of the genes that showed up-regulation in iron-deficient roots have not been previously characterized. The first one was At5g04730, which was up-regulated 3.7-fold under iron-deficiency conditions, and is predicted to have five transmembrane domains. It belongs to a small family of six genes in the Arabidopsis genome and has slight (25% identity, 44% similarity) resemblance to one protein encoded in the rice genome. The second one, At2g36120, is a gene that encodes a protein of 256 amino acids, of which 152 (60%) are glycines. Transcripts of this gene were increased 3.5-fold. Its protein sequence showed no similarity to other proteins in public databases. The third gene, At3g06890, encodes a small 129 amino acid protein. This gene is unique in the Arabidopsis genome and there is one similar protein in rice. Finally, At3g25950 encodes a five trans-membrane domain protein and belongs to a small family of three genes in Arabidopsis. It has no orthologs in other species, and protein analysis reveals a protein domain with slight resemblance to a DNA-binding motif.

Table 2.1.d lists the 23 genes with at least two-fold down-regulation of expression in roots under iron-deficiency. As expected under iron withdrawal, transcript levels of two ferritins and two oxidative-stress defense genes (peroxidase and superoxide dismutase) drop dramatically. Of the remaining 19 genes, four belong to the glycosyl hydrolase protein family (At4g08160, -2.3-fold; At5g34940, -2.3-fold; At5g55180, -2.0-fold, and At5g14650, -2.0-fold), two are expansins (At4g38770, -2.3-fold; At1g65680, -

2.1-fold), one is a leucine-rich repeat protein kinase with one transmembrane domain (At5g49770, -2.0-fold), one is induced by cold and ABA and may function as an anti-freeze protein (At5g15960, -4.4-fold), one is a putative nodulin that belongs to a small family of five members in Arabidopsis (At1g21140, -2.5-fold), one is a xyloglucan hydrolase (At4g37800, -2.2-fold), one is a enoyl-CoA reductase that may be involved in very long chain fatty acid elongation reactions required for cuticular wax synthesis (At3g55360, -2.2-fold), one belongs to the non-apical meristem (NAM) family of transcription factors required for pattern formation in embryos (At4g28530, -2.1-fold), one is a plant defensin and protease inhibitor (At2g02120, -2.1-fold), one is a protein phosphatase without homologs in the Arabidopsis genome (At3g16560, -2.1-fold), one is a small nucleolar ribonucleoprotein involved in mRNA processing (At1g76860, -2.0-fold), one is involved in lipid metabolism (At4g18550, -2.0-fold), and three are hypothetical, predicted, or unknown genes. One of the three hypothetical proteins (At1g49660, -2.3-fold) had low similarity with a lipase and belongs to a family of at least ten genes in the Arabidopsis genome. The second hypothetical protein (At4g09550, -2.1-fold) has 72 amino acids and two homologs in Arabidopsis. The third hypothetical protein has a DNA-binding motif (At5g54700, -2.1-fold) and has neither homologs in Arabidopsis nor any similarity with proteins from other species.

Affymetrix data confirmation

To confirm that the microarray data closely reflected the actual iron-starved condition of *A. thaliana* plants, we compared transcript levels of three iron-responsive

genes present in the microarray dataset with the transcript level of the same genes obtained from similar plants (*A. thaliana* Columbia *gl-1)* that were grown under similar iron-deficient conditions. *IRT1* was run and hybridized first to confirm the plants used to extract RNA for RNA blots were indeed iron-deficient. *IRT1* is the main iron importer into the root and is a well-characterized iron-responsive gene (Korshunova et al., 1999; Connolly et al., 2002; Henriques et al., 2002, Varotto et al., 2002; Vert et al., 2002). As seen in Figure 2.1.a, *IRT1* levels increased in iron-deficient roots as expected and to levels similar to the microarray. Once we confirmed the RNA reflected iron-deficient conditions in Arabidopsis, we chose two of the ten selected genes to compare transcript induction in RNA blots with microarray data. The genes chosen were the iron-responsive transcription factor *bHLH039* (see Chapter 3) and the putative sugar transporter At5g13740. Transcriptional activity of these two selected genes was similar between RNA blots and microarray datasets in both shoots and roots for either iron-nutritional status (Figure 2.1.b and Figure 2.1.c).

Transcript analysis of 43 iron-related genes

Transcript levels of 43 known and suspected iron-regulated and iron-related genes were identified in the microarray dataset, and presented in Tables 2.2.a and 2.2.b. An additional five members of the ferric-chelate reductase family of genes were absent from the microarray and not used in the analysis.

Figure 2.1.a. *IRT1* transcript levels.

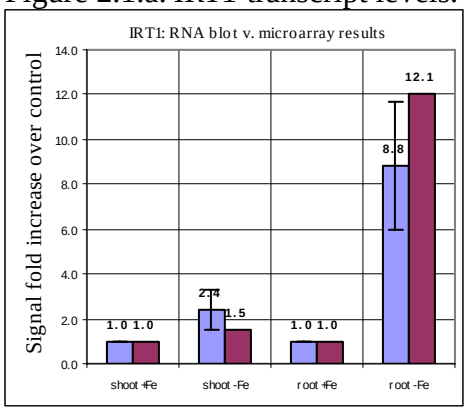

Figure 2.1.b. *bHLH039* (At3g56980) transcript levels.

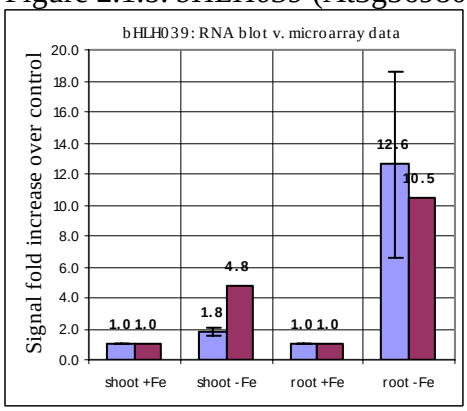

Figure 2.1.c. Putative sugar transporter (At5g13740) transcript levels.

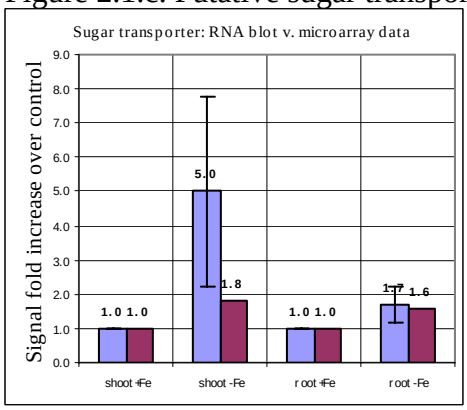

Figure 2.1. Comparison of transcript levels as detected for genes in the microarray or in RNA blots.
RNA blot and microarray results for a. *IRT1*, b. bHLH039 and c. At5g13740. Light grey bar = RNA blot. Dark grey bar = microarray data.
Shoots and roots of iron-sufficient and iron-deficient plants were harvested separately and their RNA used for RNA blots. The experiment was done four times, independently. Signal strength is given after standardization with *UBQ5*. Bars show fold increase of the transcript levels under iron-deficiency conditions in RNA blots (blue) or in the microarray (red). Transcript levels in iron-sufficient tissue was set to one and lines at the top of the blue bars represent the standard deviation. Figure 2.1.a. Results for IRT1. Figure 2.1.b. Results for bHLH039. Figure 2.1.c. Results for At5g13740.

Ferritins

As expected, most (four out of five) ferritin genes show down-regulation in iron-deficient shoots, although some more (*AtFer1;* -4.6 fold) than others (*AtFer3;* -1.5 fold). In general, all ferritins show a two-fold higher expression in shoots than in roots. When placed in iron-deficient conditions, ferritin transcript levels decrease dramatically in both shoots (-3.7 fold) and roots (-2.2 fold). *AtFer2* is expressed mainly in seeds (Petit et al., 2001), and its expression level in roots and shoots under either nutritional status is below the detection limit of the technique.

Ferric-chelate reductases

Of the eight ferric-chelate reductases present in the Arabidopsis genome; only three were present in the Affymetrix ATH1 microarray. *FRO3* had increased expression in both shoots (1.4 fold) and roots (2.9 fold) of iron-starved plants, confirming previously published information (Wu et al., 2005). Both *FRO6* and *FRO8* showed high expression levels in iron-sufficient shoots and the level of mRNA increased slightly under iron-deficiency conditions.

Nicotianamine synthase

Nicotianamine synthase (NAS) expression in iron-deficient shoots was complex. They respond to iron-deficiency conditions by down-regulating transcript levels of one member of the family (*AtNAS3*; -1.7 fold) while up-regulating the expression of another (*AtNAS4;* 2.2 fold). Roots show a complex behavior as well, with *AtNAS1* up-regulated in

iron-deficient roots (1.7 fold), while the expression of both *AtNAS2* and *AtNAS4* remained stable under iron-deficient conditions.

YSL (Yellow-Stripe Like)

It has been suggested that the eight YSL genes in Arabidopsis transport Fe(II)-NA into cells (Walker, 2002). Our results show that the eight genes show tissue-specific expression in Arabidopsis shoots and roots. *AtYSL1* seems to have shoot-specific expression, which is down-regulated under iron-deficiency conditions (-2.5 fold). *AtYSL2* may have root-specific expression that is down-regulated under iron-deficient conditions (-1.3 fold). *AtYSL3* had the strongest-expression gene in the family in both shoots and roots, and its regulation may be independent of iron-nutrition conditions. *AtYSL4* and *AtYSL7* expression levels were below detection limits, at least in shoots and roots. *AtYSL5*, *AtYSL6*, and *AtYSL8* did not modify their expression levels under either iron-nutrition condition in both shoots and roots.

ZIP (Zrt- and Irt-related Protein) family of proteins

IRT1 and *IRT2* are the main iron importers of the root; and the absence of expression in shoots was expected for both. In iron-deficient roots, both genes show a marked increase in expression (12- and 5-fold, respectively). *IRT3*, which is a potential divalent cation transporter with similarity to *ZIP4*, is yet to be characterized. It showed high transcriptional activity in iron-sufficient shoots (signal of ~1,800 units) and roots (signal of ~4,800 units). It was down-regulated -1.6 fold in both iron-deficient shoots and roots. Even when *IRT3* was down-regulated in iron-deficient roots, its expression level

was still 50% higher than the induced expression of *IRT2*. IRTs belong to the ZIP gene family of transporters with at least 15 members in Arabidopsis. ZIP family members appear to have a broad metal ion substrate specificity and although some have been implicated in copper (Wintz et al., 2003) or zinc homeostasis (Grotz et al., 1998), none of them, besides the IRTs, have been implicated in iron transport (Guerinot, 2000; Maser et al., 2001). *AtZIP2*, *AtZIP3*, *AtZIP6*, and *AtZIP9* seem to be root-specific, with just background expression levels in shoots. *AtZIP10* has no detectable expression in either roots or shoots in the microarray and may be a pseudogene since no ESTs for this gene were found in the GeneBank database (accessed online March 1, 2006, data not shown). *AtZIP4* showed down-regulation in roots of iron-deficient plants (-1.5 fold), and *AtZIP5* showed a -1.4 fold reduction in expression levels in both iron-deficient roots and shoots.

AtNRAMPS (Natural Resistance Associated Macrophage Protein)

AtNRAMPS are transporters that are proposed to play an important role in iron distribution inside the cell. *AtNRAMP4* is implicated in the export of iron from the vacuole (Lanquar et al., 2004), therefore the 1.4- to 1.5-fold transcript increase in iron-starved shoots and roots is consistent with supplying iron to the rest of the cell. *AtNRAMP3* may act in concert with *AtNRAMP4* (Lanquar et al., 2005) even though it does not seem to be affected by iron-deficiency in our study. Shoot expression levels of *AtNRAMP1* were twice as high as in roots, but indifferent to iron-deficiency conditions. *AtNRAMP5* and *AtNRAMP6* may be expressed in other tissues since they are below detection limits in both roots and shoots.

Ferroportin-like genes

Ferroportins are iron-transporter genes characterized for the first time in zebrafish (Donovan et al., 2000). In plants, they may be involved in the transport of iron from the epidermal roots cells to the vasculature (Mary Lou Guerinot, personal communication). *Fpt1* and *Fpt3* show minimal levels of transcriptional activity in shoots, whereas *Fpt2* transcript levels in shoots were below the detection limit of the microarray. None of the three modify their transcriptional activity in iron-deficient shoots. They all showed strong transcriptional activity in iron-sufficient roots. When roots were placed under iron-deficient conditions, *Fpt1* had increased transcript levels by 1.5-fold, *Fpt2* increased by 3.2-fold, and *Fpt3* by 1.8-fold.

Calcium exchanger

CAX genes encode high-affinity calcium antiporters present in the vacuole (Hirschi et al., 1996). *CAX1* is expressed at significantly higher levels in shoots than in roots, and it showed a 1.3-fold transcript increase in iron-deficient shoots. The transcriptional activity of *CAX2* is not affected by iron-deficiency conditions in either shoots or roots.

P-Type ATPases and V-Type H-ATPases

ATPases are pumps that transport ions across membranes and against electro-chemical gradients using ATP (Axelsen and Palmgren, 2001). The response of V-Type H-ATPases and P-Type ATPases to iron deficiency was studied. The H-Type ATPase family has eight members in *A. thaliana* whereas P-Type ATPases are 45 genes divided

into five subfamilies (Axelsen and Palmgren, 2001). All of them were present in the microarray, but only three P-Type ATPases belonging to the P1B ATPase sub-family seemed to respond to iron-deficiency conditions (see later). Expression levels of the eight H-Type APases and the 42 other P-Type ATPases were not modified under iron-deficiency conditions (data not shown).

Selection of ten iron-deficiency responsive genes

Selection process

A set of ten genes present in the microarray was chosen for further studies. The selection of these genes was based on several of the following factors: showing differential expression under iron-deficiency conditions as shown in any of our microarray datasets (see later), having a functional annotation that suggested a direct or indirect role in iron homeostasis, and have not been reported in the literature. The characterization of two of the ten genes is described in more detail in Chapter 3. The other eight genes include a metallothionein, a putative sugar transporter, three cytochrome P450s, and three P-Type ATPases (Table 2.3). Even though most of them showed transcript induction under iron-deficiency conditions, the level of transcript increase may or may not be biologically relevant. We analyzed this hypothesis on a case-by-case basis.

Differential expression of selected genes in response to iron deficiency

Metallothioneins are metal chelators (Cobbett and Goldsbrough, 2002). The expression of metallothionein *MT1a* was up-regulated in both shoots (1.3-fold) and roots (1.1-fold) of iron-deficient plants relative to iron-sufficient controls (Tables 2.4.a and 2.4.b). Similar results were found in the second microarray set (data not shown). This increase in expression under iron deficiency is small in percentage (10-30% depending on the tissue), but this comparison was done with transcript baselines that were already high (~13,800 units in iron-sufficient shoots and ~17,400 in iron-sufficient roots). This means that under iron-deficient conditions, *MT1a* transcript levels increased ~5,000 units in shoots and ~2,200 units in roots. We ran a BLAST search using the protein sequence of MT1a and five similar genes present in the Arabidopsis genome were found. One of them was not represented in the microarray, and transcript levels of the other four were not altered by iron-deficiency conditions (data not shown).

A putative sugar transporter, At5g13740, was up-regulated in shoots (1.8-fold) and in roots (1.6-fold) during iron-deficiency conditions (Tables 2.4.a and 2.4.b). Shoot transcript induction of 2.4-fold and root induction of 1.9-fold were found in the second microarray dataset. Two homologous genes in the Arabidopsis genome show expression levels that remain unaltered under iron-deficiency conditions (data not shown).

Three ATPases showed altered expression in response to iron deficiency: *HMA2*, *HMA3*, and *HMA4* (Tables 2.4.a and 2.4.b). None of them had detectable transcript levels in shoots, as is the case in the second microarray dataset (data not shown). *HMA2* and *HMA4* transcripts were present in iron-sufficient roots, and their transcript levels were reduced 1.3 and 1.6 fold in iron-deficient roots, respectively. In the second microarray

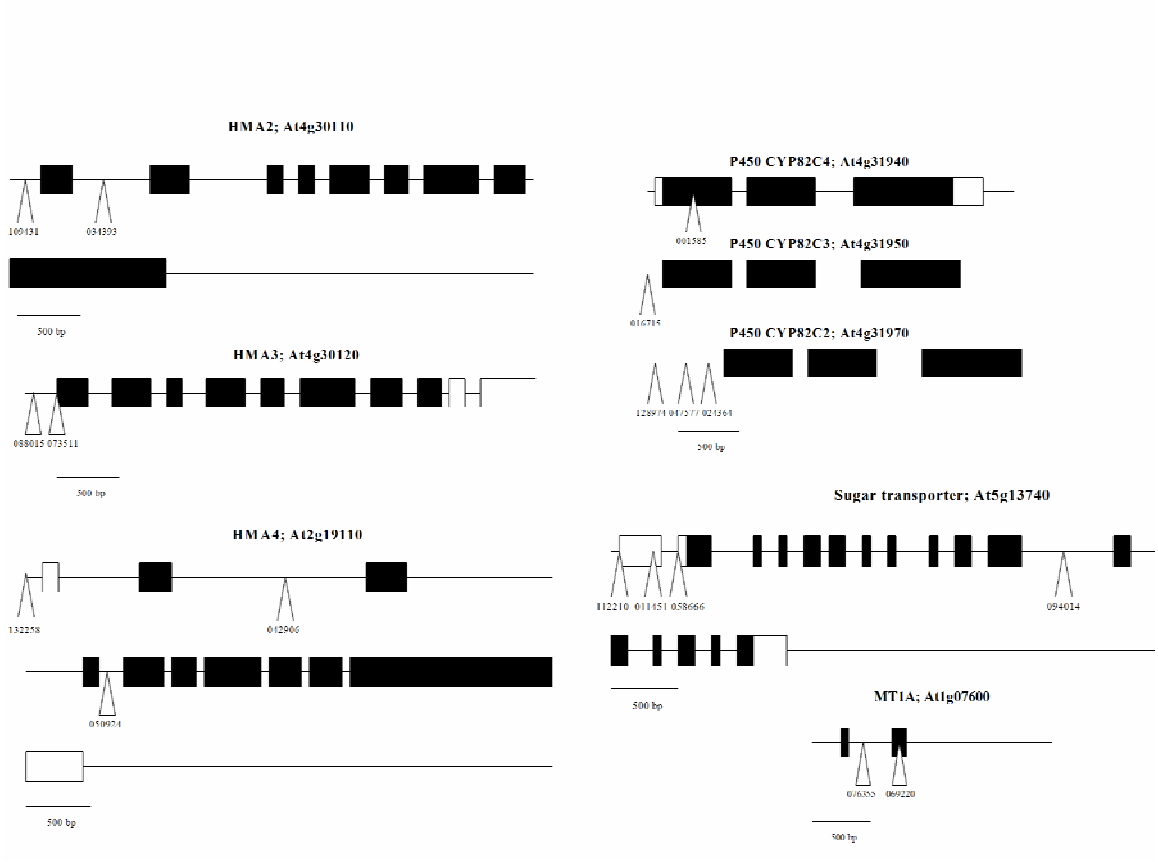

Figure 2.2.
Illustrations representing the arrangement of introns, exons, and T-DNA insertions in eight selected genes. Thin line represents the promoter, the intergenic region, and introns. Exons are represented by filled boxes. 5'- and 3'- UTR regions are represented by empty boxes. T-DNA insertions are represented by inverted triangles with the T-DNA code number written next to them. AGI code is given in the top of each cartoon. Scale of the drawing is given.

dataset, *HMA2* expression in roots was barely above background levels and *HMA4* expression level was reduced 2.3-fold in iron-deficient roots (data not shown). *HMA3* had below-background signal levels in iron-sufficient roots, whereas in iron-deficient roots it had a signal of 383, which, although above background levels, is still considered low. In the second microarray dataset, transcript levels of *HMA3* were below background under either iron nutritional condition (data not shown). All three belong to the P1B subfamily of P-Type ATPases, which has eight members. *HMA8* was not present in the microarray and the other four members of the sub-family did not modify their expression under iron-deficiency conditions (data not shown).

Cytochrome P450s are a large family of genes in Arabidopsis with multiple and versatile functions. Cytochrome P450 *CYP82C4* (At4g31940) has two homologs in the Arabidopsis genome: *CYP82C2* (At4g31970) and *CYP82C3* (At4g31950). In this particular case, we selected them after analyzing microarrays hybridized with RNA extracted from iron-sufficient and -deficient shoots and roots of *frd3* mutant plants, which are plants with constitutive iron-deficiency responses. All three were expressed in iron-sufficient *frd3* roots, with the signal for *CYP82C2* being 4,564, which is considered high. For *CYP82C3*, the signal of 282 is considered low and barely above the background cutoff of 200. Finally, *CYP82C4* showed a signal of 450, which is considered low. When *frd3* roots were placed under iron-deficient conditions, *CYP82C2* showed a 1.4-fold transcript increase, *CYP82C3* showed a 1.2-fold transcript decrease, and *CYP82C4* showed a 1.5-fold decrease (Table 2.4.c). These expression levels, although high for one and low for the other two, stand in stark contrast with the expression levels of the same genes in the WT arrays, which were below or barely above the background signal cutoff.

All three genes have iron-binding motifs inferred from electronic annotation as presented in www.arabidopsis.org. None of them had transcript levels above the background cutoff in shoots of either *frd3* or WT microarrays (data not shown). In the iron-deficient WT root microarray, only *CYP82C4* had a signal level barely above background levels (Table 2.4.c). The second set of WT microarrays showed that none of the three Cytochrome P450s had transcript levels above background in either iron-sufficient or –deficient shoots or roots (data not shown).

T-DNA insertion lines

After the eight genes were selected (the metallothonein MT1a; the sugar transporter At5g13740; the three P-Type ATPases: HMA2, HMA3, and HMA4; and the three Cytochrome P450s: CYP82C2, CYP82C3, and CYP82C4), individual T-DNA insertion lines for each one were ordered (Table 2.3). The insertion position of each T-DNA and the general arrangement of exons and introns for each selected gene are given in Figure 2.2. All homozygous T-DNA lines were grown on plates and soil using standard conditions, but none of the T-DNA insertion lines showed a visual phenotype (Table 2.3).

Elemental analysis

All homozygous T-DNA lines were sent for elemental analysis to the lab of David Salt at Purdue University. Results showed that the lines had elemental profiles similar to the controls and within a standard deviation (data not shown), with the exception of *HMA4*. All three T-DNA mutant alleles of *HMA4* showed approximately half the zinc

content of controls (Table 2.5), which has been reported before (Hussain et al., 2004). This confirms other reports that characterize *HMA4* as a zinc and cadmium effluxer (Mills et al., 2003; Mills et al., 2005). Disruptions in *HMA4* did not alter iron accumulation in Arabidopsis grown under normal soil conditions (Table 2.5).

Gene silencing approach for the three highly-related P450s

RNAi approach

All homozygous T-DNA lines for the three P450s showed WT phenotypes when grown under standard conditions and their elemental profile was similar to the controls (data not shown). An amino acid sequence alignment showed extensive similarity among the three of them, suggesting possible functional redundancy (Table 2.3). These genes are tightly linked, making it difficult to isolate double and/or triple T-DNA mutant lines. To reduce or eliminate their expression simultaneously, an RNAi approach was used.

RNAi targets

As seen in Figure 2.3, all three selected P450s have many common sequence regions. 29 of the homologous sequences were analyzed as RNAi targets, as seen in Table 2.6.a (for complete instructions and references, see Materials and Methods). Table 2.6.b shows the selection process used to define the one sequence used as RNAi target out of the seven final candidates. All seven were at least 26 bases long and were cropped to reach 23 bases, taking into consideration the restrictions posed by the second screening

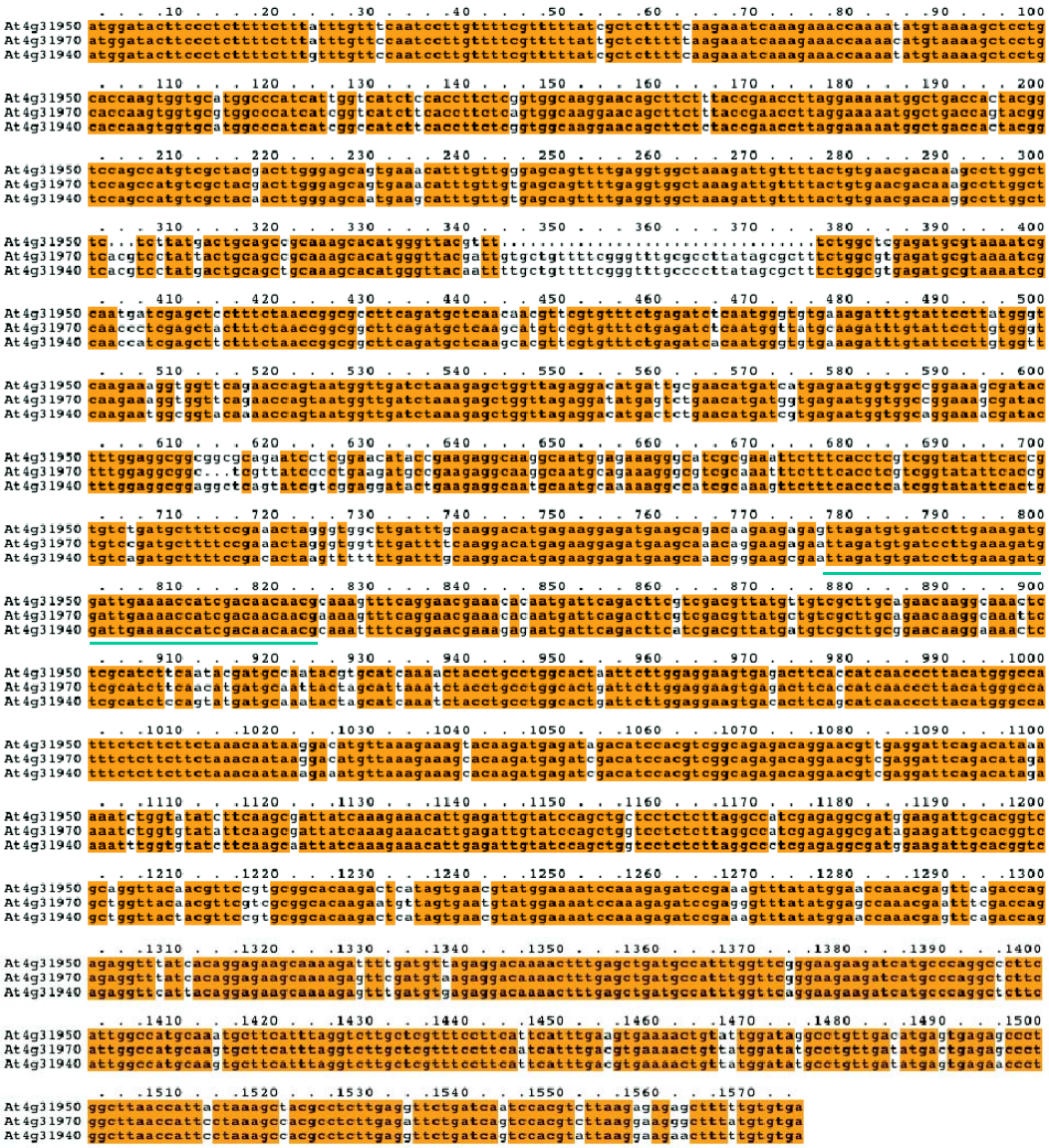

Figure 2.3. Identity among three P450 genes.
The three P450 genes are 91% identical to each other at the nucleotide level. Shaded boxes represent areas of identical sequence. 29 of the common areas were selected and further analyzed to be used as targets of RNAi. After the analysis, seven were identified as useful targets for RNAi and the underlined sequence was used to design oligos for RNAi.

process. The selected sequence was inserted into the pFGC5941 vector using appropriate restriction sites. The finished construct will be used to transform WT Arabidopsis plants.

DISCUSSION

Affymetrix ATH-1 microarrays were hybridized with RNA extracted from iron-sufficient and -deficient roots and shoots from WT plants. RNA blots and microarray results were similar, confirming the quality of the data generated by the microarray (Figure 2.1). Initial analysis of the data revealed several genes that showed transcript up- or down-regulation in iron-deficient roots and shoots. Many genes present in Table 2.1 have been characterized before and behaved as expected in the microarray dataset, including ferritins (*AtFer1*, *AtFer3*, *AtFer4*), iron transporters (*IRT1*, *IRT2*, *AtYSL1*, *AtFpt2*), and ferric-chelate reductases (*AtFRO3*, *AtFRO6*). It is known that de-regulation of one metal ion can bring the de-regulation of several other metals in the organism (Shaul, 2002). This was shown in the microarray dataset when transcript levels for the zinc transporter *MTPA2* and the copper transporter *COPT2* showed 7.6- and 5.0-fold up-regulation in iron-deficient roots, respectively. Previous reports have shown pleiotropic effects of iron in the regulation of phosphate (Wang et al., 2002) and zinc or copper (Wintz et al., 2003).

Several new genes were found that showed iron-deficiency transcript regulation. These included expansins/extensins and members of signal transduction cascades. It is known that iron-deficiency conditions bring dramatic changes in root physiology, increasing secondary roots and the formation of root hairs and transfer cells in the root

epidermis increase in number (Schikora and Schmidt, 2001; Schmidt, 2003). Under iron-deficiency stress, roots show a marked increase in growth rate. If the iron-deficiency stress continues, root growth will slow down and eventually stop. At the same time, plant resources would be directed towards reproductive organs (Schikora and Schmidt, 2001; Schmidt, 2003). These physiological effects of iron-starvation in root physiology were reflected in the complex change in transcriptional activity of root expansins/extensins. Two showed increase transcriptional activity under iron-deficient conditions: one in shoots and the other in roots; while two others showed reduced expression in iron-deficient roots.

Fifteen of the 91 genes (~15%) that showed at least a two-fold up- or down-regulation under iron-deficient conditions were hypothetical/predicted proteins without known or inferred functions, giving us possible leads for future work. Some are present in rice, indicating that they may be common for both iron acquisition strategies (see Chapter 1). Some of them do not have homologs in other plant species (as of April 1, 2006), suggesting that these genes are unique to Arabidopsis.

It is interesting to note that out of the 91 genes that showed at least a two-fold differential expression under iron-deficient conditions, eighteen (~20%) were present in shoots and 73 (~80%) in roots. There is a complex relationship between roots and shoots in iron homeostasis (see Chapter 1). Even though iron is needed and stored in both, it is acquired by the roots. Shoots sense iron and under iron-deficiency they send a long-distance signal to the roots to up-regulate iron-deficiency responses. Roots sense iron in the media directly by a local signal system and respond to the long-distance signal from shoots (Vert et al., 2003). It is possible that the marked difference in number of genes

affected by iron deficiency in either shoots or roots may be just a reflection of our standard iron-starvation conditions, where plants are grown for fourteen days and then placed under iron-deficient conditions for three days. It is also possible that there is a different organ-specific response, at the transcript level, during different stages of iron-deficiency in plants. It is also possible that the iron-acquisition and signaling occurring in roots shows a more complex reaction to iron deficiency than shoots. This may be reflected by the greater number of genes with differential transcript levels under iron deficiency in roots (Table 2.1). In a previous microarray project to identify iron-deficiency regulated genes, *Arabidopsis thaliana* Langsberg *erecta* was grown in a hydroponic solution with several nutrients, but iron-deficiency conditions did not include ferrozine. The inclusion of this iron chelator in our experiments ensures that traces of contaminating iron are not available to the plant. Under their conditions, the expression of ~3,000 genes was affected by iron-deficient conditions in shoots, whereas the expression of only ~1,500 genes was affected in roots (Thimm et al., 2001). We cannot directly compare results from different microarrays (Buckhout and Thimm, 2003; Coughlan et al., 2004; Kennedy and Wilson, 2004), as the conditions of their experiment are markedly different from ours. One striking difference between our results concerns the expression of *FRO2*. Their one-month-old hydroponic plants induced 1.2-, 3.1-, and 6.3-fold at one, three, and seven days after iron withdrawal, respectively, which contradicts other published reports about *FRO2* (Connolly et al., 2003). This difference may be due to the absence of the iron chelator ferrozine. The absence of ferrozine in their trial may leave traces of iron in the media, which would be taken up by the iron-starving plant, delaying the up-regulation of *FRO2* transcripts.

In addition to *FRO2*, Thimm et al., (2001) compared published results of ten other iron-regulated genes and predicted their activity in the array. These genes included one ferritin, ferredoxin, catalase, aconitase, lipoxygenase, iron superoxide dismutase, an H-ATPase, formate dehydrogenase, lysyl-tRNA synthetase, and adenine phosphoribosyltransferase. Of these, only ferritin and ferredoxin behaved as predicted, whereas transcriptional activity of all others did not reflect previously published data. In addition, their data variability between experimental repeats was as large as between treatments (Thimm et al., 2001). These results stand in contrast with the information provided by Wintz et al. (2003). Wintz et al. (2003) grew plants for five weeks in media similar to ours (two week-old plants) and then transferred them to iron-deficient media for five days, as opposed to three days. In spite of different growth conditions between our experiments, we can see several similarities between the later report (Wintz et al., 2003) and our microarray results, including iron-regulated transcription activity of *IRT2*, *FRO3*, *AtFer1*, *AtFer4*, *ZIP5*, *AtNAS1*, and *AtNAS2*. Although the similarities between the datasets were many, we detected some differences between them in the shoot expression of *ZIP4* (stable in our dataset, down-regulated in theirs), in the shoot expression of *ZIP9* (below detection limits in our dataset, up-regulated in theirs), and in the root expression of *AtNAS3* (not detectable in our dataset, up-regulated in theirs). In a study of tomato plants, RNA from iron-deficient roots was used to hybridize a custom-made spotted array (Wang et al., 2002). 17 genes that showed differential expression under iron-deficiency conditions, including four signaling genes, one transcription factor, one cell elongation gene, and one Pi (inorganic phosphate) transporter were identified (Wang et al., 2002). It is interesting to note that the Arabidopsis genome contains iron-

regulated homologs of some of the 17 genes they described (data not shown), suggesting new leads for future work.

After analysis of the microarrays, ten genes were chosen for further study. The characterization of two to of the genes is described in more detail in Chapter 3. Three of the remaining eight were P-Type ATPases. P-Type ATPases transport small cations across membranes using ATP while forming a phosphorylated intermediate. They are involved in maintaining the electrochemical gradient used as the driving force for the secondary transporters (H^+-ATPases in plants), cellular signaling (Ca^{2+}-ATPases), the transport of essential micronutrients (Zn^{2+}, and Cu^{2+}-ATPases) and extrusion of the same ions if they accumulate in excess (Axelsen and Palmgren, 2001). The *A. thaliana* genome contains 45 P-Type ATPases that can be divided into five subfamilies based on the ions transported (Axelsen and Palmgren, 2001). The P1B heavy metal transporter subfamily has eight members and is divided into two groups: monovalent cation transporters of Cu^+/Ag^+, and divalent cation transporters of $Zn^{2+}/Co^{2+}/Cd^{2+}/Pb^{2+}$ (Williams and Mills, 2005). The three iron-regulated P-Type ATPases found through the Affymetrix microarrays were divalent P1B P-Type ATPase transporters.

None of the three T-DNA lines for the chosen P-type ATPases showed an obvious, visible phenotype; an observation confirmed by others (Hussain et al., 2004). During the initial phases of this project, several reports characterizing these three P-Type ATPases were published. *AtHMA2* was characterized as a Zn^{2+} and Cd^{2+} exporter that is responsible for the efflux of both ions from cells, and is expressed throughout the plant (Eren and Arguello, 2004). *AtHMA3* has stronger expression in roots than in other organs and is localized to the vacuole, where it imports Cd^{2+} from the cytosol (Gravot et al.,

2004). *AtHM4* has been shown to transport Zn^{2+}, Cd^{2+} (Mills et al., 2003), and Pb^{2+} when tested in heterologous systems (Verret et al., 2004). The protein localizes to the plasma membrane of cells in the root vasculature, where it plays a role in the loading mechanism of Zn^{2+} and Cd^{2+} into the xylem (Verret et al., 2004). Double *hma2hma4* and single *hma4* mutants showed disruptions in zinc (Hussain et al., 2004) but not iron homeostasis (Table 2.5). One explanation for the up-regulation of these three genes under iron-deficiency conditions takes into account the up-regulation of the main iron importer *IRT1* under those conditions. *IRT1* has been shown to import other divalent cations like Cd^{2+}, Co^{2+}, Zn^{2+}, and Mn^{2+}, besides Fe^{2+} (Connolly et al., 2002; Vert et al., 2002); therefore, it is possible that presence of the extra Zn^{2+} and Cd^{2+} in the plant would require the up-regulation of both *HMA2* and *HMA4* to detoxify the high levels of these cations.

The metallothionein *MT1a* is another gene chosen from the microarray to further investigate its contribution to iron homeostasis. Metallothioneins are a class of cysteine-rich, low molecular mass (4-8 kDa) proteins that contain two metal-binding domains (Harmer et al., 2000; Cobbett and Goldsbrough, 2002). The seven MTs present in the Arabidopsis genome (Robinson et al., 1999; Cobbett and Goldsbrough, 2002) are expressed throughout the plant including roots, shoots, fruits, embryos, trichomes, leaves, germinating seeds, and senescing leaves (Cobbett and Goldsbrough, 2002). In plants, MT expression is induced by several environmental factors, including some heavy metals like Al, Cd, Fe (Hsieh et al., 1995; Snowden et al., 1995; Lee et al., 2004), Cu (Snowden et al., 1995; Guo et al., 2003) and others (Murphy and Taiz, 1995). It has been proposed that metallothioneins are part of a general stress response, a defense against toxic ions, or the general metal homeostasis in the plant (Garcia-Hernandez et al., 1998; Guo et al., 2003).

A T-DNA insertion in *MT1a* did not show an obvious phenotype. It is possible that another metallothionein is functionally redundant to *MT1a*. It is also possible that the contribution of *MT1a* to iron regulation is small; therefore its absence may pass unnoticed. Finally, it is also possible that the up-regulation of *MT1a* in iron-starved plants follows the same explanation given for P-Type ATPases: the increase in Cd^{2+} uptake by an up-regulated *IRT1* could trigger the activation of plant Cd^{2+}-toxicity defenses, including the up-regulation of *Mt1a* for its metal-chelating characteristics.

The putative sugar transporter At5g13740 also showed up-regulation in shoots and roots of iron-deficient plants. Sugar transport inside the plant is complex and relies mainly on active sucrose transporters because photosynthetically active cells must produce enough carbohydrates to supply their own needs and to serve as a source for all sink cells and plant organs, like roots or seeds (Williams et al., 2000; Truernit, 2001). In addition to their essential roles as substrates in carbon and energy metabolism, sugars have important hormone-like functions as primary messengers in signal transduction, affecting gene expression and plant development (Williams et al., 2000; Rolland et al., 2002). It is known that iron-deficiency conditions reduce chlorophyll content in plants, therefore also reduce the amount of photosynthate (carbohydrate) production in the plant. It is interesting that under the mentioned conditions, A5g13740 showed transcriptional up-regulation when one would predict the opposite behavior. The gene product might be involved in carbohydrate signal transduction associated with iron levels in the plant. A T-DNA insertion line did not show an obvious phenotype and had elemental levels similar to control plants (data not shown).

Finally, we discovered one cytochrome P450 that was up-regulated in iron-deficient WT roots from being below background levels to having a signal of 238, which is close to the cutoff value of 200 (Table 2.4.c). This P450 is closely related to two others and all three showed high expression levels in microarrays hybridized with RNA from iron-sufficient roots of the mutant Arabidopsis line *frd3*. P450 proteins are ubiquitous in living organisms (Paquette et al., 2000); and the P450 superfamily in *A. thaliana* comprises 246 full-length and 26 pseudo genes (Nelson et al., 2004). Plant P450s are involved in the synthesis of many plant metabolites (Xu et al., 2001; Narusaka et al., 2004; Nelson et al., 2004). Interestingly, some P450s are induced by pathogen inoculation and by heavy metal treatment (Xu et al., 2001).

The three cytochrome P450s used in this study have iron-binding motifs (www.arabidopsis.org) and one (CYP82C3; At4g31950) is involved in arabinogalactan synthesis and stress (Guan and Nothnagel, 2004). None of them, when mutated, showed an obvious visual phenotype. The high sequence similarity between the three suggestgs that they may be functionally redundant to one another. Obtaining double or triple KOs will be difficult as the three genes are tightly linked in the genome (1,002 bases between At4g31940 and At4g31950, and 5,286 bases between At4g31950 and At4g31970). Instead, to reduce or eliminate the expression of the three genes simultaneously an RNAi approach has been initiated (Elbashir et al., 2001b; Elbashir et al., 2001a; Reynolds et al., 2004).

FUTURE RESEARCH

The functional genomics approach used in this project provided us with several new leads for future work, including many uncharacterized genes with increased or decreased transcripts in response to iron-deficiency conditions. It would be advisable to focus future research efforts on those iron-deficiency responsive genes that are single-copy genes in the Arabidopsis genome. It is less likely for these single-copy genes to show redundancy, therefore increasing the likelihood of finding a phenotype.

The microarray dataset also revealed possible iron-regulation for members of gene families that are partially or completely characterized. This information could allow us to study previously-characterized families of genes and establish their connection, if any, with iron homeostasis. The families of genes that could be studied, just as an example, could include transcription factors, the MATE (Multidrug And Toxic compound Extrusion) family of transporters, OPTs (OligoPeptide Transporter), members of signal transduction cascades, and others.

Finally, the Affymetrix microarray dataset can help us further understand iron homeostasis in Arabidopsis by allowing us compare the promoters of those genes up- or down-regulated in either shoots or roots looking for common motifs or sequence signatures that may indicate co-regulation.

Table 2.1. Affymetrix microarray results showing iron-regulated genes in shoots and roots of *Arabidopsis thaliana* Col-0 plants.

Table 2.1.a. Up-regulated genes in shoots. Eight genes increasing their expression in shoots at least 2X under -Fe shown.

	WT shoots under +Fe		WT shoots under -Fe			
AGI	**Signal[1]**	**Call[2]**	**Signal[1]**	**Call[2]**	**Fold[3] Under -Fe**	**Basic annotation**
At1g48300	2517	P	7500	P	3.0	Hypothetical protein.
At3g56360	2372	P	6023	P	2.5	Putative protein. Directed to the chloroplast.
At5g53450	882	P	2157	P	2.4	Putative protein. ORG1. Ser/thr kinase. Chloroplast.
At3g22240	8899	P	21527	P	2.4	Unknown protein. Mitochondrion.
At3g18290	796	P	1797	P	2.3	Zinc finger protein. Chloroplast. Ubiquitin ligase complex.
At4g16370	629	P	1355	P	2.2	AtOPT3, oligopeptide transporter.
At1g20190	336	P	717	P	2.1	Alpha expansin S2 precursor. AtEXPA11.
At2g25660	214	P	422	P	2.0	Unknown protein. Chloroplast. Embryo defective 2410.

Table 2.1.b. Down-regulated genes in shoots. Ten genes decreasing their expression in shoots at least 2X under -Fe shown.

	WT shoots under +Fe		WT shoots under -Fe			
AGI	**Signal[1]**	**Call[2]**	**Signal[1]**	**Call[2]**	**Fold[3] Under -Fe**	**Basic annotation**
At5g01600	7533	P	1642	P	-4.6	Ferritin 1 precursor. AtFer1.
At3g56090	1570	P	472	P	-3.3	Putative ferritin precursor. AtFer3.
At2g40300	2403	P	843	P	-2.8	Putative ferritin. AtFer4.
At3g43670	594	P	221	P	-2.7	Copper amine oxidase -like protein.
At3g12580	589	P	224	P	-2.6	Heat shock protein 70. Cytosolic.
At5g50335	733	P	286	P	-2.6	Expressed protein.
At4g24120	1189	P	481	P	-2.5	AtYSL1.
At5g07010	1019	P	467	P	-2.2	Steroid sulfotransferase-like protein.
At4g25100	9581	P	4474	P	-2.1	FSD1; Fe-Superoxide dismutase.
At4g08390	709	P	333	P	-2.1	Stromal ascorbate peroxidase.

Table 2.1.c. Up-regulated genes in roots. 50 genes increasing their expression in roots at least 2X under -Fe shown.

	WT roots under +Fe		WT roots under -Fe			
AGI	Signal[1]	Call[2]	Signal[1]	Call[2]	Fold[3] Under -Fe	Basic annotation
At5g02780	229	P	4034	P	17.6	Putative protein In2 - GST-like. Receptor kinase.
At4g19690	591	P	7126	P	12.1	IRT1 Fe(II) transporter protein.
At3g07720	1213	P	12394	P	10.2	Unknown protein. Kelch repeat-containing protein.
At3g58810	432	P	3262	P	7.6	Zinc transporter - like protein. MTPA2.
At5g36890	308	P	2232	P	7.3	Glycosyl hydrolase - like protein.
At4g19680	378	P	2008	P	5.3	IRT2 Fe(II) transporter protein.
At1g34760	244	P	1215	P	5.0	14-3-3 protein GF14omicron (grf11).
At3g46900	447	P	2226	P	5.0	Copper transport protein. COPT2.
At2g43150	354	P	1451	P	4.1	Putative extensin.
At3g50740	1246	P	4941	P	4.0	UTP-glucose glucosyltransferase.
At5g38820	287	P	1116	P	3.9	Transporter - like protein. Amino acid permease.
At1g74760	899	P	3424	P	3.8	Hypothetical protein. Zinc finger, protein ubiquitination.
At5g04730	453	P	1665	P	3.7	Putative protein.
At3g13610	2819	P	10174	P	3.6	Oxidoreductase, 2OG-Fe(II) oxygenase family protein.
At4g17600	212	P	765	P	3.6	Chloroplast transcription factor Lil3:1.
At2g36120	280	P	970	P	3.5	Unknown protein.
At5g03570	1231	P	3976	P	3.2	Ferroportin 2.
At5g45070	885	P	2771	P	3.1	Putative disease resistance protein (TIR class).
At2g34390	221	P	650	P	2.9	Putative aquaporin NIP2.
At1g23020	747	P	2182	P	2.9	FRO3.
At3g61410	260	P	755	P	2.9	Putative protein kinase.
At1g14190	213	P	611	P	2.9	Glucose-methanol-choline (GMC) oxidoreductase family.
At1g80440	1790	P	5139	P	2.9	Kelch repeat-containing F-box family protein.
At3g06890	325	P	898	P	2.8	Hypothetical protein.
At2g01880	1375	P	3772	P	2.7	Putative purple acid phosphatase.
At3g21070	271	P	724	P	2.7	NADK1. ATP-NAD kinase family protein.
At5g45080	358	P	955	P	2.7	Disease resistance protein-related.
At2g28160	1091	P	2747	P	2.5	Putative bHLH transcription factor. FIT1.
At3g53480	2683	P	6627	P	2.5	PDR5-like ABC transporter.
At5g11920	631	P	1474	P	2.3	Fructosidase - like protein.
At3g47040	394	P	890	P	2.3	Beta-D-glucan exohydrolase.
At1g22930	1439	P	3244	P	2.3	T-complex protein 11.
At5g61250	825	P	1806	P	2.2	Similar to beta-glucuronidase.
At5g41280	386	P	843	P	2.2	Receptor-like GPI-anchored protein (Duf26).
At3g48450	386	P	820	P	2.1	Nitrate-responsive NOI protein, putative.
At3g60330	719	P	1515	P	2.1	Plasma membrane H+-ATPase. AHA7.
At1g15670	3209	P	6756	P	2.1	Kelch repeat-containing F-box family protein.
At5g01800	1761	P	3585	P	2.0	Saposin B domain-containing protein.
At4g21680	297	P	601	P	2.0	Proton-dependent oligopeptide transport protein (POT).
At4g38680	567	P	1145	P	2.0	Glycine-rich protein 2 (GRP2).
At1g80360	1021	P	2051	P	2.0	Putative aspartate aminotransferase. Mitochondrion.
At2g46740	1148	P	2295	P	2.0	FAD-binding domain protein. Mitochondrion.
At5g01960	414	P	826	P	2.0	Chloroplast-localized zinc-finger protein.
At5g53450	533	P	1055	P	2.0	Putative protein. ORG1. Ser/thr kinase. Chloroplast.
At4g34950	579	P	1146	P	2.0	Nodulin family protein.
At4g29220	877	P	1728	P	2.0	Phosphofructo-1-kinase-like protein.
At3g25950	247	P	486	P	2.0	Hypothetical protein.
At3g26610	210	P	412	P	2.0	Putative polygalacturonase.
At1g18910	846	P	1659	P	2.0	Zinc finger protein. Ubiquitin ligase complex.
At1g09560	7156	P	14009	P	2.0	Germin-like protein. GLP5.

Table 2.1.d. Down-regulated genes in roots. 23 genes decreasing their expression in roots at least 2X under -Fe shown.

	WT roots under +Fe		WT roots under -Fe		Fold[3]	
AGI	Signal[1]	Call[2]	Signal[1]	Call[2]	under -Fe	Basic annotation
At5g15960	3314	P	753	P	-4.4	Cold and ABA inducible protein kin1.
At3g49960	1560	P	413	P	-3.8	Peroxidase ATP21a.
At5g01600	5117	P	1894	P	-2.7	Ferritin 1 precursor. AtFer1.
At4g25100	5141	P	1977	P	-2.6	FSD1; Fe-Superoxide dismutase.
At1g21140	1876	P	749	P	-2.5	Putative Nodulin N-21.
At4g08160	563	P	246	P	-2.3	Glycosyl hydrolase.
At4g38770	805	P	353	P	-2.3	Proline-rich gene. PRP4. Extensin - like protein.
At1g49660	1598	P	705	P	-2.3	Unknown protein.
At5g34940	1024	P	455	P	-2.3	Mitochondrion, beta-glucuronidase activity.
At4g37800	687	P	308	P	-2.2	Endo-xyloglucan transferase.
At3g55360	2255	P	1024	P	-2.2	Enoyl-CoA reductase. Targeted to the ER.
At2g40300	611	P	286	P	-2.1	Putative ferritin. AtFer4.
At4g28530	768	P	362	P	-2.1	NAM / CUC2 -like protein. Transcription factor-like.
At2g02120	477	P	226	P	-2.1	Protease inhibitor II. Plant defensin.
At4g09550	916	P	437	P	-2.1	Putative protein.
At1g65680	875	P	419	P	-2.1	AtEXPB2, Beta expansin.
At5g54700	469	P	227	P	-2.1	Unknown protein. Contains ankyrin repeat.
At3g16560	779	P	378	P	-2.1	Protein phosphatase 2C-like.
At5g14650	2819	P	1382	P	-2.0	Polygalacturonase - like protein.
At5g49770	634	P	311	P	-2.0	Receptor protein kinase-like.
At1g76860	824	P	407	P	-2.0	SnRNP-like protein.
At5g55180	2609	P	1328	P	-2.0	Glycosyl hydrolase family 17 protein.
At4g18550	552	P	282	P	-2.0	Lipase-like protein Pn47p.

[1] Fluorescent signal given by the probes especific for the gene in the Affymetrix microarray.
[2] (P)resent or (A)bsent. Qualitative interpretation of the signal level. Present indicates that the signal is above the background or noise levels, Absent indicates that the computer cannot differentiate between the signal coming from the probes for a specific gene and the general background or noise in the microarray.
[3] Fold increase is the signal value of a gene in either roots or shoots that were under iron deficiency conditions divided by the signal of the same gene in the same tissue but under nutrient complete conditions.
[4] Fold increase is a meaningless number in these cases since the base count is a number that the computer considers (A)bsent or background.
[5] In most cases a signal value below 200 is considered to be background even when the computer assigns a call of (P)resent.

Table 2.2. Affymetrix dataset from iron-sufficient and –deficient WT shoots or roots.

Table 2.2.a. Shoot Affymetrix microarray results for 43 genes that are or are related to known iron-regulated genes.

		WT shoots +Fe		WT shoots -Fe		Fold[3]
AGI	Name	Signal[1]	Call[2]	Signal[1]	Call[2]	increase
At2g38460	Fpt1	203	M	355	P	n/a[4]
At5g03570	Fpt2	95	P[5]	146	P[5]	n/a[4]
At5g26820	Fpt3	761	P	787	P	1.0
At5g01600	AtFer1	7533	P	1642	P	-4.6
At3g11050	AtFer2	22	A	81	A	n/a[4]
At3g61000	AtFer3	467	P	311	P	-1.5
At2g40300	AtFer4	2403	P	843	P	-2.8
At3g56090	Another ferritin	1570	P	472	P	-3.3
At1g23020	FRO3	1062	P	1486	P	1.4
At5g49730	FRO6	5294	P	6148	P	1.2
At5g50160	FRO8	586	P	653	P	1.1
At5g04950	AtNAS1	216	P	201	P[5]	-1.1
At5g56080	AtNAS2	104	A	79	A	n/a[4]
At1g09240	AtNAS3	1070	P	623	P	-1.7
At1g56430	AtNAS4	206	M	454	P	2.2
At4g24120	YSL1	1189	P	481	P	-2.5
At5g24380	YSL2	359	M	359	A	n/a[4]
At5g53550	YSL3	2648	P	2342	P	-1.1
At5g41000	YSL4	320	A	314	A	n/a[4]
At3g17650	YSL5	725	P	726	P	1.0
At3g27020	YSL6	1631	P	1680	P	1.0
At1g65730	YSL7	56	A	58	A	n/a[4]
At1g48370	YSL8	435	P	402	P	-1.1
At2g38170	CAX1	4413	P	5884	P	1.3
At3g13320	CAX2	627	P	636	P	1.0
At1g80830	AtNRAMP1	1053	P	1087	P	1.0
At1g47240	AtNRAMP2	512	P	425	P	-1.2
At2g23150	AtNRAMP3	400	P	392	P	1.0
At5g67330	AtNRAMP4	1139	P	1561	P	1.4
At4g18790	AtNRAMP5	38	A	59	A	n/a[4]
At1g15960	AtNRAMP6	177	A	229	A	n/a[4]
At4g19690	IRT1	32	A	49	A	n/a[4]
At4g19680	IRT2	22	A	47	A	n/a[4]
At1g60960	IRT3	1418	P	867	P	-1.6
At3g12750	ZIP1	283	P	289	P	1.0
At5g59520	ZIP2	75	P[5]	155	P[5]	n/a[4]
At2g32270	ZIP3	132	A	168	A	n/a[4]
At1g10970	ZIP4	395	P	378	P	1.0
At1g05300	ZIP5	694	P	485	P	-1.4
At2g30080	ZIP6	206	A	215	A	n/a[4]
At4g33020	ZIP9	76	A	69	A	n/a[4]
At1g31260	ZIP10	3	A	3	A	n/a[4]
At1g55910	ZIP11	1076	P	995	P	-1.1

Table 2.2.b. Root Affymetrix microarray results for 43 genes that are or are related to known iron-regulated genes.

		WT roots +Fe		WT roots -Fe		Fold[3]
AGI	Name	Signal[1]	Call[2]	Signal[1]	Call[2]	increase
At2g38460	Fpt1	236	P	358	P	1.5
At5g03570	Fpt2	1231	P	3976	P	3.2
At5g26820	Fpt3	356	P	636	P	1.8
At5g01600	AtFer1	5117	P	1894	P	-2.7
At3g11050	AtFer2	107	A	76	A	n/a[4]
At3g61000	AtFer3	595	P	570	P	1.0
At2g40300	AtFer4	611	P	286	P	-2.1
At3g56090	Another ferritin	1000	P	531	P	-1.9
At1g23020	FRO3	747	P	2182	P	2.9
At5g49730	FRO6	15	A	10	A	n/a[4]
At5g50160	FRO8	101	A	123	A	n/a[4]
At5g04950	AtNAS1	1622	P	2790	P	1.7
At5g56080	AtNAS2	1426	P	1219	P	-1.2
At1g09240	AtNAS3	91	A	119	A	n/a[4]
At1g56430	AtNAS4	392	P	466	P	1.2
At4g24120	YSL1	52	A	69	M	n/a[4]
At5g24380	YSL2	795	P	608	P	-1.3
At5g53550	YSL3	1327	P	1258	P	-1.1
At5g41000	YSL4	304	M	293	M	n/a[4]
At3g17650	YSL5	417	M	338	P	n/a[4]
At3g27020	YSL6	845	P	950	P	1.1
At1g65730	YSL7	142	A	149	A	n/a[4]
At1g48370	YSL8	421	P	429	P	1.0
At2g38170	CAX1	841	P	693	P	-1.2
At3g13320	CAX2	807	P	834	P	1.0
At1g80830	AtNRAMP1	2005	P	2335	P	1.2
At1g47240	AtNRAMP2	580	P	586	P	1.0
At2g23150	AtNRAMP3	353	P	411	P	1.2
At5g67330	AtNRAMP4	1330	P	2041	P	1.5
At4g18790	AtNRAMP5	25	A	62	A	n/a[4]
At1g15960	AtNRAMP6	96	A	59	A	n/a[4]
At4g19690	IRT1	591	P	7126	P	12.1
At4g19680	IRT2	378	P	2008	P	5.3
At1g60960	IRT3	4813	P	3086	P	-1.6
At3g12750	ZIP1	549	P	423	P	-1.3
At5g59520	ZIP2	2537	P	2036	P	-1.3
At2g32270	ZIP3	6608	P	6279	P	1.0
At1g10970	ZIP4	1388	P	906	P	-1.5
At1g05300	ZIP5	2279	P	1603	P	-1.4
At2g30080	ZIP6	389	P	397	P	1.0
At4g33020	ZIP9	588	P	680	P	1.2
At1g31260	ZIP10	3	A	7	A	n/a[4]
At1g55910	ZIP11	262	P	239	P	-1.1

[1] Fluorescent signal given by the probes especific for the gene in the Affymetrix microarray.
[2] (P)resent, (M)arginal, or (A)bsent. Qualitative interpretation of the signal level. Present indicates that the signal is above the background or noise levels, Absent indicates that the computer cannot differentiate between the signal coming from the probes for a specific gene and the general background or noise in the microarray. Marginal indicates a borderline value.
[3] p-value indicates how statistically certain the signal number is. A high p-value would indicate that the signal is not relevant, even though the signal may be high.
[4] Fold increase is the signal value of a gene in either roots or shoots that were under iron deficiency conditions divided by the signal of the same gene in the same tissue but under nutrient complete conditions.
[5] Fold increase is a meaningless number in these cases since the base count is a number that the computer considers (A)bsent or background.
[6] Minimal annotation as found in the Affymterix microarray.
[7] In most cases a signal value below 200 is considered to be background even when the computer assigns a call of (P)resent.
[8] More than one probe in the microarray may be directed towards one gene. Results for all probes in one gene presented.
[9] Some genes are not represented in the Affymetrix ATH-1 22k microarray. They are shown in tables anyway because they are closely related to the gene of interest being investigated.

Table 2.3. Individual T-DNA lines ordered from ABRC for each of the selected genes.

AGI	Annotation	T-DNA[1]	KO[2]	Visual[3]	Element[4]
At1g07600	Metallothionein-like protein. MT1A.	SALK_076355	Yes	No	Yes
		SALK_069220	Yes	No	Yes
At2g19110	Putative cadmium-transporting ATPase.	SALK_132258	Yes	No	Yes
	HMA4	SALK_050924	Yes	No	Yes
		SALK_093482	Yes	No	Yes
		SALK_042906	Yes	No	Yes
At4g30110	Cadmium-transporting ATPase-like protein.	SALK_034393	Yes	No	Yes
	HMA2	SALK_109431	Yes	No	Yes
At4g30120	Cadmium-transporting ATPase-like protein.	SALK_088015	Yes	No	Yes
	HMA3	SALK_073511	Yes	No	Yes
At5g13740	Sugar transporter-like protein.	SALK_112210	Yes	No	Yes
		SALK_011451	Yes	No	Yes
		SALK_094014	Yes	No	Yes
		SALK_058666	Yes	No	Yes
At4g31940	Cytochrome P450 CYP82C4.	SALK_001585	Yes	No	
At4g31950	Cytochrome P450 CYP82C3.	SALK_016715	Yes	No	
At4g31970	Cytochrome P450 CYP82C2.	SALK_024364	Yes	No	
		SALK_128974	Yes	No	
		SALK_047577	Yes	No	

[1] SALK T-DNA lines ordered from SiGNAL through ABRC.
[2] Shows wether an homozygous T-DNA insertion was found for each T-DNA line.
[3] Shows wether any homozygous or heterozygous T-DNA insertion line showed any visual phenotype.
[4] Indicates which T-DNA insertion lines were analyzed for their elemental profiles.

Table 2.4. Results of the Affymetrix microarray for selected genes.

Table 2.4.a. Results for eight selected genes in shoots.

		WT shoots +Fe		WT shoots -Fe		Fold[3]
AGI	Name	Signal[1]	Call[2]	Signal[1]	Call[2]	increase
At1g07600	MT1a metallothionein.	13789	P	18512	P	1.3
At5g13740	Sugar transp. MSH12.21	1028	P	1871	P	1.8
At4g30110	P-Type ATPase HMA2	116	A	141	A	n/a[4]
At4g30120	P-Type ATPase HMA3	5	A	3	A	n/a[4]
At2g19110	P-Type ATPase HMA4	145	A	261	A	n/a[4]

Table 2.4.b. Results for eight selected genes in roots.

		WT roots +Fe		WT roots -Fe		Fold[3]
AGI	Name	Signal[1]	Call[2]	Signal[1]	Call[2]	increase
At1g07600	MT1a metallothionein.	17352	P	19569	P	1.1
At5g13740	Sugar transp. MSH12.21	1487	P	2378	P	1.6
At4g30110	P-Type ATPase HMA2	1032	P	644	P	-1.6
At4g30120	P-Type ATPase HMA3	98	P[5]	383	P	Up
At2g19110	P-Type ATPase HMA4	1594	P	1191	P	-1.3

Table 2.4.c. Results for selected Cytochrome P450 genes in *frd3* roots.

		WT roots +Fe		WT roots -Fe		Fold[3]	*frd3* roots +Fe		*frd3* roots -Fe		Fold[3]
AGI	Name	Signal[1]	Call[2]	Signal[1]	Call[2]	increase	Signal[1]	Call[2]	Signal[1]	Call[2]	increase
At4g31940	Cyt. P450 CYP82C4.	4	A	238	P	Up	4564	P	3119	P	-1.5
At4g31950	Cyt. P450 CYP82C3.	3	A	4	A	n/a[4]	282	P	231	P	-1.2
At4g31970	Cyt. P450 CYP82C2.	20	A	1	A	n/a[4]	450	P	641	P	1.4

[1] Fluorescent signal given by the probes especific for the gene in the Affymetrix microarray.
[2] (P)resent or (A)bsent. Qualitative interpretation of the signal level. Present indicates that the signal is above the background or noise levels, Absent indicates that the computer cannot differentiate between the signal coming from the probes for a specific gene and the general background or noise in the microarray.
[3] Fold increase is the signal value of a gene in either roots or shoots that were under iron deficiency conditions divided by the signal of the same gene in the same tissue but under nutrient complete conditions.
[4] Fold increase is a meaningless number in these cases since the base count is a number that the computer considers (A)bsent or background.
[5] In most cases a signal value below 200 is considered to be background even when the computer assigns a call of (P)resent.

Table 2.5. Elemental analysis of selected T-DNA insertion lines compared with A*rabidopsis thalinana* Col-0 *(shaded column).*

				At2g19110 *HMA4*							
		A. t. Col-0		SALK_132258[3]		SALK_042906[3]		SALK_093482[3]		SALK_050924[3]	
Element	Unit	Average[1]	StDev[2]	Average[1]	StDev[2]	Average[1]	StDev[2]	Average[1]	StDev[2]	Average[1]	StDev[2]
Lithium	ppm	**4.42**	**1.43**	4.32	1.00	4.33	1.06	3.67	0.88	4.27	1.43
Sodium	ppm	**781.09**	**101.97**	794.69	91.02	720.20	51.48	671.68	82.25	767.32	157.02
Magnesium	ppm	**18787.44**	**1144.34**	19360.29	1130.24	19308.58	1540.59	18954.26	1066.14	18577.54	1071.20
Phosphorous	ppm	**9069.37**	**833.23**	9755.17	640.54	9690.69	628.09	9746.00	503.75	9300.70	828.16
Potassium	ppm	**46154.43**	**5349.81**	47200.05	4934.27	48782.48	3886.57	48678.36	3474.15	48178.43	5128.24
Calcium	ppm	**35684.96**	**2907.90**	37767.75	3788.25	37833.55	5322.44	38769.80	4668.44	37291.67	2917.07
Manganese	ppm	**278.12**	**26.49**	302.13	38.93	305.88	50.46	328.39	76.52	300.42	39.65
Iron	ppm	**70.79**	**8.21**	73.59	3.60	76.29	6.53	73.65	7.42	72.67	5.50
Cobalt	ppm	**1.56**	**0.33**	1.39	0.38	1.45	0.33	1.35	0.27	1.51	0.39
Nickel	ppm	**0.39**	**0.06**	0.38	0.09	0.40	0.09	0.41	0.07	0.36	0.07
Copper	ppm	**2.54**	**0.75**	2.59	0.55	2.72	0.66	2.81	0.70	2.77	0.46
Zinc[4]	ppm	**94.44**	**13.09**	42.98	3.38	43.56	4.53	44.63	4.77	41.88	6.06
Arsenic	ppm	**1.66**	**0.68**	1.62	0.65	1.56	0.59	1.47	0.61	1.51	0.71
Selenium	ppm	**8.99**	**1.01**	8.13	1.42	8.14	1.00	8.40	1.06	8.40	0.75
Molibdenum	ppm	**1.23**	**0.57**	1.32	0.50	1.42	0.53	1.54	0.44	1.46	0.46
Cadmium	ppm	**3.12**	**0.88**	2.88	0.88	2.89	0.68	2.49	0.59	2.80	0.86

[1] Average of one leaf from each of 25 plants grown on soil. Shaded results for the WT control.
[2] Standard deviation taking into account each of the 25 individual measurements.
[3] Code of each T-DNA insertion line.
[4] Shaded row shows data at least one standard deviation away from the control.

Table 2.6. 29 common sequences to all three selected P450s and four selection criteria to be selected for RNAi.

Table 2.6.a. Initial screening of 29 common sequences. Shaded squares indicate non-compliance with the selection rules.

Sequence[1]	Length[2]	100 bp away[3]	Stretch of four[4]	% GC[5]	Chosen[6]
CGTGTTTCTGAGATC	15	no	0	47	
GAGGATTCAGACATA	15	yes	0	40	
CCCTGGCTTAACCATT	16	yes	0	50	
CTACCTGCCTGGCACT	16	yes	0	63	
AAGATTTGTATTCCTT	16	yes	0	25	
CTTCATTGGCCATGCAA	17	yes	0	47	
GAAGATTGCACGGTCGC	17	yes	0	59	
ACAGGAGAAGCAAAAGA	17	yes	1	41	
ATTCTTGGAGGAAGTGA	17	yes	0	41	
GCAAAGCACATGGGTTAC	18	yes	0	50	
GTGGCAAGGAACAGCTTCT	19	yes	0	53	
GAGATGCGTAAAATCGCAA	19	yes	1	42	
GGAAGAAGATCATGCCCAGGC	21	yes	0	57	
AAGAAATCAAAGAAACCAAAA	21	no	0	24	
TACGGTCCAGCCATGTCGCTAC	22	yes	0	50	
CAATCCTTGTTTTCGTTTTTAT	22	no	2	27	
ATGGATACTTCCCTCTTTTCTTT	23	no	1	35	
GTATGGAAAATCCAAAGAGATCCGA	25	yes	1	40	
CAAGGACATGAGAAGGAGATGAAGCA	26	yes	0	46	YES
ATGTAAAAGCTCCTGCACCAAGTGGTGC	28	no	1	50	
TACCGAACCTTAGGAAAAATGGCTGACCA	29	yes	1	45	
GACATCCACGTCGGCAGAGACAGGAACGT	29	yes	0	59	YES
TGCTTCATTTAGGTCTTGCTCGTTTCCTTCA	31	yes	0	42	YES
ATTATCAAAGAAACATTGAGATTGTATCCAGCTG	34	yes	0	32	YES
AGAGGACAAAACTTTGAGCTGATGCCATTTGGTTC	35	yes	1	43	
AACCAGTAATGGTTGATCTAAAGAGCTGGTTAGAGGA	37	yes	0	41	YES
CATCAACCCTTACATGGGCCATTTCTCTTCTTCTAAACAATAA	43	yes	0	37	YES
GAGCAGTTTTGAGGTGGCTAAAGATTGTTTTACTGTGAACGACAA	45	yes	2	59	
TTAGATGTGATCCTTGAAAGATGGATTGAAAACCATCGACAACAACG	47	yes	1	36	YES

[1] Stretch of nucleotides with 100% homology within the three P450s.
[2] The homologous sequence must be at least 21 nucleotides long.
[3] The sequence that is the target for RNAi must be at least 100 bp away from both the start and stop codons.
[4] The target sequence should not have a stretch of four or more identical bases.
[5] Choose target seqeunces with 30-60% GC content.
[6] Sequences that meet most of the selection criteria were used for further analysis.

Table 2.6.b. Final screening of seven shared sequences.

Sequence[1]	Length	30-50%GC[2]	A/U@15-19[3]	A@3[4]	A@19[5]	G@13[6]	G/C@19[7]	Total	Selected?
AAG GAC ATG AGA AGG AGA TGA AG	23	**1**	**0**	**1**	**0**	**0**	**0**	**2**	
AAC CAG TAA TGG TTG ATC TAA AG	23	**1**	**0**	**1**	**0**	**0**	**0**	**2**	
GAC ATC CAC GTC GGC AGA GAC AG	23	**0**	**0**	**0**	**0**	**-1**	**-1**	**-2**	
CAT TTA GGT CTT GCT CGT TTC CT	23	**1**	**0**	**0**	**0**	**-1**	**0**	**0**	
AAC CCT TAC ATG GGC CAT TTC TC	23	**1**	**0**	**0**	**0**	**-1**	**0**	**0**	
TAG ATG TGA TCC TTG AAA GAT GG	23	**1**	**3**	**0**	**0**	**0**	**-1**	**3**	YES
AAC ATT GAG ATT GTA TCC AGC TG	23	**1**	**0**	**0**	**1**	**-1**	**0**	**1**	

[1] All seven sequences were selected and trimmed to be 23 bp long.
[2] Since sequences were trimmed the GC% was recalculated. One point given if GC% is between 30 and 50%.
[3] Any adenine in positions 15-19 gives one point.
[4] An adenine in position 3 gives one point.
[5] An adenine in position 19 gives one point.
[6] A guanine in position 13 takes one point out.
[7] A guanine or a citosine in position 19 takes one point out.

MATERIALS AND METHODS

GeneChip Microarray Experiment

Experiment design and execution were done in the lab of Dr. Mary Lou Guerinot at Dartmouth College (Hanover, NH) by Dr. Elizabeth E. Rogers as a post-doctoral fellow. The DNA Array Core Facility of the University of California–Irvine (Irvine, CA) hybridized the Affymetrix ATH-1 Microarrays (Affymetrix Inc., Santa Clara, CA). Data analysis was performed using Excel (Microsoft, Seattle, WA).

Affymetrix data filtering and analysis

Gene transcript levels between iron-complete and iron-deficient shoots or roots were compared using Excel (Microsoft Seattle, WA). For Table 2.1, all genes that showed signals with a call of (A) for Absent, (M) for Marginal, or (P) for present but with a signal value equal or below 200 were eliminated. All genes that modified their transcript levels under iron-deficiency conditions more than two-fold were shown. This filtering procedure was only used in Table 2.1. In Table 2.2 the cutoff was set arbitrarily at +/- 1.3-fold change in transcript level.

Gene annotation

We improved the basic functional annotation of the eight chosen genes by mining data from The Arabidopsis Information Resource – TAIR (http://www.arabidopsis.org),

the Arabidopsis thaliana Genome Data Base – AtGBD (http://www.plantgdb.org/AtGDB/), the Munich Information Center for Protein Sequences – MIPS (http://mips.gsf.de/proj/thal/db/index.html), and The Institute for Genomic Research – TIGR (http://www.tigr.org).

Similarity searches

To identify the most closely related genes to each one of the eight selected genes in our research, their protein sequences were downloaded from The Arabidopsis Information Resource (www.arabidopsis.org) and either the WU-BLAST2 algorithm (Washington University, St. Louis, MO) at www.ebi.ac.uk/blast2/ or the Blast algorithm (National Library of Medicine Bethesda, MD) at www.ncbi.nih.gov (Altschul et al., 1997) used to find similar genes present in the *Arabidpsis thaliana* genome. All databases were accessed on March 10, 2006.

Plant growth conditions

Arabidopsis thaliana var. Columbia *gl-1* plants were used in all experiments unless otherwise noted. For iron-sufficient or iron-deficient conditions, seed was surface sterilized, stratified for three days at 4^{o}C in 0.1% agar, planted on B5 plates, and allowed to grow at 22^{o}C under constant light in a growth chamber (Percival Scientific, Perry, IA). 14 day-old plants were transferred for three days to iron-sufficient or iron-deficient media (Yi and Guerinot, 1996). Iron-deficient media was supplemented with the iron chelator

ferrozine to reduce the availability of contaminant iron to the plants as described (Yi and Guerinot, 1996). All plates were covered with yellow Plexiglas at all times to avoid photo-degradation of Fe(III)-EDTA (Hangarter and Stasinopoulos, 1991).

Plant material and transformations

The Arabidopsis Biological Resources Center (ABRC) at Ohio State University (Columbus, OH) provided the T-DNA insertion lines (Alonso et al., 2003). Genomic DNA was extracted from the T-DNA insertion lines (Edwards et al., 1991) and the genomic area of the insertion was amplified using primers designed to span the region. For transformation, flowering *Arabidopsis thaliana gl-1* plants were dipped into a solution containing *Agrobacterium tumefasciens* GV3101 as described (Clough and Bent, 1998).

RNA blots

Shoots and roots of plants grown under iron-deficient or iron-sufficient conditions were harvested separately, and frozen in liquid nitrogen. Total RNA was extracted from each sample using the LiCl method (Verwoerd et al., 1989). *IRT1* probe was prepared as described (Rogers and Guerinot, 2002). The probe for the sugar transporter-like gene At5g13740 was a 1061 bp PCR product from genomic DNA amplified using the following primers: Forward: 5'-CATGAATCATCTCCTTCTACCGGG-3' and reverse 5'-CAGAACAGGTCCTAGCAGTTTCTC-3'. The probe for the *bHLH039* transcription

factor (At3g56980) was an 842 bp PCR product from genomic DNA amplified using the following primers: Forward: 5'-CATCCTCTGACTTAACTCTTCGC-3' and reverse: 5'-GTGTGCATTAGTACCTCCATTGT-3'. RNA blots were performed according to standard methods (Sambrook and Russell, 2001) using Osmonics membranes (Westborough, MA). Quantification of the signal was done using a Molecular Dynamics Storm 860 PhosphorImager (Amersham Biosciences, Piscataway, NJ). *UBQ5* probe was amplified as described previously (Rogers and Ausubel, 1997) and used to normalize the data to reduce the slight variation resulting from differences in RNA loading.

RNAi design

All three P450 cDNA sequences were aligned using the ClustalW algorithm from the European Bioinformatics Institute (EBI, Cambridge, UK) at www.ebi.ac.uk/clustalw. Homologous regions of at least 15 bases were selected and compared for characteristics to design RNAi targets as explained in (Elbashir et al., 2001b; Elbashir et al., 2001a; Reynolds et al., 2004). Briefly, the target region should be 23 bases long, be at least 100 bases away from both start and stop codons, GC content should be between 30-50%. Ideally, the sequence would have an adenine in positions one or two, in position three, and in positions 15 through 18. Additionally, a good RNAi target sequence would have an adenine or a guanine in position 19, and a guanine in positions 13. One sequence was selected, oligos representing the sense and antisense sequence with inserted restriction sites were ordered from IDT DNA (Coralville, IA). The sense and antisense oligos were mixed, heated to 95^{o}C, and cooled down slowly (1^{o}C/minute) until the solution reached

4^{o}C to anneal them. Newly double stranded oligos were phosphorylated using T4 Polynucleotide Kinase (New England Biolabs, Beverly, MA) and ligated into the vector pFGC5941 (The Plant Chromatin Data Base at www.chromdb.org, The University of Arizona, AZ).

ACKNOWLEDGEMENTS

I would like to thank Timothy Pouland and Lorena Da Ponte for their assistance with lab work. Juan Jose Gutierrez screened the T-DNA lines of the three P450 genes and Kareema Smith screened RNAi oligo candidates to silence them. We thank Dr. Christopher Todd for the generous gift of the vector pFGC5941. Special thanks to Timothy Durrett and Drs. Laura Green and Dirk Charlson who provided invaluable advice, kind patience, and support while conducting the research. Microarray experiments were carried out in collaboration with Dr. Mary Lou Guerinot at Dartmouth College. All T-DNA lines were obtained from the ABRC. This work was supported by grant USDA CREES 2002-35100-12331 and MU's Food for the 21st Century to EER, by the Life Sciences Undergraduate Research Opportunity Program (LSUROP), Plant Genomics Internship (PGI) held at the University of Missouri-Columbia for KS. A special thanks to the Interdisciplinary Plant Group at University of Missouri-Columbia for their continuous support to AM.

REFERENCES

Aharoni, A., and Vorst, O. (2002). DNA microarrays for functional plant genomics. Plant Molecular Biology **48,** 99-118.

Alonso, J.M., Stepanova, A.N., Leisse, T.J., Kim, C.J., Chen, H., Shinn, P., Stevenson, D.K., Zimmerman, J., Barajas, P., Cheuk, R., Gadrinab, C., Heller, C., Jeske, A., Koesema, E., Meyers, C.C., Parker, H., Prednis, L., Ansari, Y., Choy, N., Deen, H., Geralt, M., Hazari, N., Hom, E., Karnes, M., Mulholland, C., Ndubaku, R., Schmidt, I., Guzman, P., Aguilar-Henonin, L., Schmid, M., Weigel, D., Carter, D.E., Marchand, T., Risseeuw, E., Brogden, D., Zeko, A., Crosby, W.L., Berry, C.C., and Ecker, J.R. (2003). Genome-wide insertional mutagenesis of *Arabidopsis thaliana*. Science **301,** 653-657.

Altschul, S., Madden, T., Schaffer, A., Zhang, J., Zhang, Z., Miller, W., and Lipman, D. (1997). Gapped BLAST and PSI-BLAST: a new generation of protein database search programs. Nucleic Acids Research **25,** 3389-3402.

Axelsen, K.B., and Palmgren, M.G. (2001). Inventory of the superfamily of P-Type ion pumps in Arabidopsis. Plant Physiology **126,** 696-706.

Buckhout, T.J., and Thimm, O. (2003). Insights into metabolism obtained from microarray analysis. Current Opinion in Plant Biology **6,** 288-296.

Clough, S.J., and Bent, A.F. (1998). Floral dip: a simplified method for Agrobacterium-mediated transformation of *Arabidopsis thaliana*. Plant Journal **16,** 735-743.

Cobbett, C., and Goldsbrough, P. (2002). Phytochelatins and metallothioneins: roles in heavy metal detoxification and homeostasis. Annual Review of Plant Biology **53,** 159-182.

Colangelo, E.P., and Guerinot, M.L. (2004). The essential basic helix-loop-helix protein FIT1 is required for the iron deficiency response. Plant Cell **16,** 3400-3412.

Connolly, E.L., Fett, J.P., and Guerinot, M.L. (2002). Expression of the IRT1 metal transporter is controlled by metals at the levels of transcript and protein accumulation. Plant Cell **14,** 1347-1357.

Connolly, E.L., Campbell, N.H., Grotz, N., Prichard, C.L., and Guerinot, M.L. (2003). Overexpression of the FRO2 ferric chelate reductase confers tolerance to growth on low iron and uncovers posttranscriptional control. Plant Physiology **133,** 1102-1110.

Coughlan, S.J., Agrawal, V., and Meyers, B. (2004). A comparison of global gene expression measurement technologies in *Arabidopsis thaliana*. Comparative and Functional Genomics **5,** 245-252.

Donovan, A., Brownlie, A., Zhou, Y., Shepard, J., Pratt, S.J., Moynihan, J., Paw, B.H., Drejer, A., Barut, B., Zapata, A., Law, T.C., Brugnara, C., Lux, S.E., Pinkus, G.S., Pinkus, J.L., Kingsley, P.D., Palis, J., Fleming, M.D., Andrews, N.C., and Zon, L.I. (2000). Positional cloning of zebrafish ferroportin1 identifies a conserved vertebrate iron exporter. Nature **403,** 776-781.

Edwards, K., Johnstone, C., and C., T. (1991). A simple and rapid method for the preparation of plant genomic DNA for PCR analysis. Nucleic Acids Research **19,** 1349.

Elbashir, S.M., Martinez, J., Patkaniowska, A., Lendeckel, W., and Tuschl, T. (2001a). Functional anatomy of siRNAs for mediating efficient RNAi in *Drosophila melanogaster* embryo lysate. EMBO Journal **20,** 6877-6888.

Elbashir, S.M., Harborth, J., Lendeckel, W., Yalcin, A., Weber, K., and Tuschl, T. (2001b). Duplexes of 21-nucleotide RNAs mediate RNA interference in cultured mammalian cells. Nature **411,** 494-498.

Eren, E., and Arguello, J.M. (2004). Arabidopsis HMA2, a divalent heavy metal-transporting PIB-Type ATPase, is involved in cytoplasmic Zn^{2+} homeostasis. Plant Physiology **136,** 3712-3723.

Garcia-Hernandez, M., Murphy, A., and Taiz, L. (1998). Metallothioneins 1 and 2 have distinct but overlapping expression patterns in Arabidopsis. Plant Physiology **118,** 387-397.

Gravot, A., Lieutaud, A., Verret, F., Auroy, P., Vavasseur, A., and Richaud, P. (2004). AtHMA3, a plant P1B-ATPase, functions as a Cd/Pb transporter in yeast. FEBS Letters **561,** 22-28.

Grotz, N., Fox, T., Connolly, E., Park, W., Guerinot, M.L., and Eide, D. (1998). Identification of a family of zinc transporter genes from Arabidopsis that respond to zinc deficiency. Proceedings of the National Academy of Sciences of the United States of America **95,** 7220-7224.

Guan, Y., and Nothnagel, E.A. (2004). Binding of arabinogalactan proteins by yariv phenylglycoside triggers wound-like responses in Arabidopsis cell cultures. Plant Physiology **135,** 1346-1366.

Guerinot, M.L. (2000). The ZIP family of metal transporters. Biochimica et Biophysica Acta (BBA) - Biomembranes **1465,** 190-198.

Guo, W.-J., Bundithya, W., and Goldsbrough, P.B. (2003). Characterization of the Arabidopsis metallothionein gene family: tissue-specific expression and induction during senescence and in response to copper. New Phytologist **159,** 369-381.

Haas, B., Wortman, J., Ronning, C., Hannick, L., Smith, R., Maiti, R., Chan, A., Yu, C., Farzad, M., Wu, D., White, O., and Town, C. (2005). Complete reannotation of the Arabidopsis genome: methods, tools, protocols and the final release. BMC Biology **3,** 1-55.

Hangarter, R.P., and Stasinopoulos, T.C. (1991). Effect of Fe-catalyzed photooxidation of EDTA on root growth in plant culture media. Plant Physiology **96,** 843-847.

Harmer, S.L., Hogenesch, J.B., Straume, M., Chang, H.-S., Han, B., Zhu, T., Wang, X., Kreps, J.A., and Kay, S.A. (2000). Orchestrated transcription of key pathways in Arabidopsis by the circadian clock. Science **290,** 2110-2113.

Henriques, R., Jasik, J., Klein, M., Martinoia, E., Feller, U., Schell, J., Pais, M.S., and Koncz, C. (2002). Knock-out of Arabidopsis metal transporter gene *IRT1* results in iron deficiency accompanied by cell differentiation defects. Plant Molecular Biology **50,** 587-597.

Hirschi, K.D., Zhen, R.-G., Cunningham, K.W., Rea, P.A., and Fink, G.R. (1996). CAX1, an H+/Ca2+ antiporter from Arabidopsis. Proceedings of the National Academy of Sciences of the United States of America **93,** 8782-8786.

Hsieh, H.-M., Liu, W.-K., and Huang, P.C. (1995). A novel stress-inducible metallothionein-like gene from rice. Plant Molecular Biology **28,** 381-389.

Hussain, D., Haydon, M.J., Wang, Y., Wong, E., Sherson, S.M., Young, J., Camakaris, J., Harper, J.F., and Cobbett, C.S. (2004). P-Type ATPase heavy metal transporters with roles in essential zinc homeostasis in Arabidopsis. Plant Cell **16,** 1327-1339.

Ishii, M., Hashimoto, S.-i., Tsutsumi, S., Wada, Y., Matsushima, K., Kodama, T., and Aburatani, H. (2000). Direct comparison of GeneChip and SAGE on the quantitative accuracy in transcript profiling analysis. Genomics **68,** 136-143.

Kennedy, G.C., and Wilson, I.W. (2004). Plant functional genomics: opportunities in microarray databases and data mining. Functional Plant Biology **31,** 295-314.

Korshunova, Y.O., Eide, D., Gregg Clark, W., Lou Guerinot, M., and Pakrasi, H.B. (1999). The IRT1 protein from *Arabidopsis thaliana* is a metal transporter with a broad substrate range. Plant Molecular Biology **40,** 37-44.

Lanquar, V., Lelievre, F., Barbier-Brygoo, H., and Thomine, S. (2004). Regulation and function of AtNRAMP4 metal transporter protein. Soil Science and Plant Nutrition **50,** 1141–1150.

Lanquar, V., Lelièvre, F., Bolte, S., Hamès, C., Alcon, C., Neumann, D., Vansuyt, G., Curie, C., Schröder, A., Krämer, U., Barbier-Brygoo, H., and Thomine, S. (2005). Mobilization of vacuolar iron by AtNRAMP3 and AtNRAMP4 is essential for seed germination on low iron. EMBO Journal **24,** 4041-4051.

Lee, J., Donghwan, S., Won-yong, S., Inhwan, H., and Youngsook, L. (2004). Arabidopsis metallothioneins 2a and 3 enhance resistance to cadmium when expressed in *Vicia faba* guard cells. Plant Molecular Biology **54,** 805-815.

LeJean, M., Schikora, A., Mari, S., Briat, J.-F., and Curie, C. (2005). A loss-of-function mutation in AtYSL1 reveals its role in iron and nicotianamine seed loading. Plant Journal **44,** 769-782.

Marschner, H. (1995). Mineral nutrition of higher plants, second edition. Academic Press, London.

Maser, P., Thomine, S., Schroeder, J.I., Ward, J.M., Hirshi, K., Sze, H., Talke, I.N., Amtmann, A., Maathuis, F.J.M., Sanders, D., Harper, J.F., Tchieu, J., Gribskov, M., Persans, M.W., Salt, D.E., Kim, S.A., and Guerinot, M.L. (2001). Phylogenetic relationships within cation transporter families of Arabidopsis. Plant Physiology **126,** 1646-1667.

Meyers, B.C., Galbraith, D.W., Nelson, T., and Agrawal, V. (2004). Methods for transcriptional profiling in plants. Be fruitful and replicate. Plant Physiology **135,** 637-652.

Mills, R.F., Krijger, G.C., Baccarini, P.J., Hall, J.L., and Williams, L.E. (2003). Functional expression of AtHMA4, a P1B-type ATPase of the Zn/Co/Cd/Pb subclass. Plant Journal **35,** 164-176.

Mills, R.F., Francini, A., Ferreira da Rocha, P.S.C., Baccarini, P.J., Aylett, M., Krijger, G.C., and Williams, L.E. (2005). The plant P1B-type ATPase AtHMA4 transports Zn and Cd and plays a role in detoxification of transition metals supplied at elevated levels. FEBS Letters **579,** 783-791.

Murphy, A., and Taiz, L. (1995). Comparison of metallothionein gene expression and nonprotein thiols in ten Arabidopsis ecotypes (correlation with copper tolerance). Plant Physiology **109,** 945-954.

Narusaka, Y., Narusaka, M., Seki, M., Umezawa, T., Ishida, J., Nakajima, M., Enju, A., and Shinozaki, K. (2004). Crosstalk in the responses to abiotic and biotic stresses in Arabidopsis: Analysis of gene expression in cytochrome P450 gene superfamily by cDNA microarray. Plant Molecular Biology **55,** 327-342.

Nelson, D.R., Schuler, M.A., Paquette, S.M., Werck-Reichhart, D., and Bak, S. (2004). Comparative genomics of rice and Arabidopsis. Analysis of 727 cytochrome P450 genes and pseudogenes from a monocot and a dicot. Plant Physiology **135,** 756-772.

Paquette, S.M., Bak, S., and Feyereisen, R. (2000). Intron-exon organization and phylogeny in a large superfamily, the paralogous cytochrome P450 genes of *Arabidopsis thaliana*. DNA and Cell Biology **19,** 307-317.

Petit, J.-M., Briat, J.-F., and Lobreaux, S. (2001). Structure and differential expression of the four members of the *Arabidopsis thaliana* ferritin gene family. Biochemical Journal **359,** 575-582.

Reynolds, A., Leake, D., Boese, Q., Scaringe, S., Marshall, W.S., and Khvorova, A. (2004). Rational siRNA design for RNA interference. Nature Biotechnology **22,** 326-330.

Robinson, N.J., Procter, C.M., Connolly, E.L., and Guerinot, M.L. (1999). A ferric-chelate reductase for iron uptake from soils. Nature **397,** 694-697.

Rogers, E.E., and Ausubel, F.M. (1997). Arabidopsis enhanced disease susceptibility mutants exhibit enhanced susceptibility to several bacterial pathogens and alterations in PR-1 gene expression. Plant Cell **9,** 305-316.

Rogers, E.E., and Guerinot, M.L. (2002). FRD3, a member of the multidrug and toxin efflux family, controls iron deficiency responses in Arabidopsis. Plant Cell **14,** 1787-1799.

Rolland, F., Moore, B., and Sheen, J. (2002). Sugar sensing and signaling in plants. Plant Cell **14,** S185-205.

Sambrook, J., and Russell, D.W. (2001). Molecular cloning: a laboratory manual. (Cold Spring Harbor, NY: Cold Spring Harbor Laboratory Press).

Schikora, A., and Schmidt, W. (2001). Iron stress-induced changes in root epidermal cell fate are regulated independently from physiological responses to low iron availability. Plant Physiology **125,** 1679-1687.

Schmidt, W. (2003). Iron solutions: acquisition strategies and signaling pathways in plants. Trends in Plant Science **8,** 188-193.

Shaul, O. (2002). Magnesium transport and function in plants: the tip of the iceberg. BioMetals **15,** 307-321.

Snowden, K.C., Richards, K.D., and Gardner, R.C. (1995). Aluminum-induced genes (induction by toxic metals, low calcium, and wounding and pattern of expression in root tips). Plant Physiology **107,** 341-348.

The Arabidopsis Genome Initiative. (2000). Analysis of the genome sequence of the flowering plant *Arabidopsis thaliana*. Nature **408,** 796-815.

Thimm, O., Essigmann, B., Kloska, S., Altmann, T., and Buckhout, T.J. (2001). Response of Arabidopsis to iron deficiency stress as revealed by microarray analysis. Plant Physiology **127,** 1030-1043.

Truernit, E. (2001). Plant physiology: the importance of sucrose transporters. Current Biology **11,** R169-R171.

Varotto, C., Maiwald, D., Pesaresi, P., Jahns, P., Salamini, F., and Leister, D. (2002). The metal ion transporter IRT1 is necessary for iron homeostasis and efficient photosynthesis in *Arabidopsis thaliana*. Plant Journal **31,** 589-599.

Verret, F., Gravot, A., Auroy, P., Leonhardt, N., David, P., Nussaume, L., Vavasseur, A., and Richaud, P. (2004). Overexpression of AtHMA4 enhances root-to-shoot translocation of zinc and cadmium and plant metal tolerance. FEBS Letters **576,** 306-312.

Vert, G., Grotz, N., Dedaldechamp, F., Gaymard, F., Guerinot, M.L., Briat, J.-F., and Curie, C. (2002). IRT1, an Arabidopsis transporter essential for iron uptake from the soil and for plant growth. Plant Cell **14,** 1223-1233.

Vert, G.A., Briat, J.-F., and Curie, C. (2003). Dual regulation of the Arabidopsis high-affinity root iron uptake system by local and long-distance signals. Plant Physiology **132,** 796-804.

Verwoerd, T.C., Dekker, B.M., and Hoekema, A. (1989). A small-scale procedure for the rapid isolation of plant RNAs. Nucleic Acids Research **17,** 2362.

Walker, E.L. (2002). Functional analysis of the Arabidopsis yellow stripe-like (YSL) family. Heavy metal transport and partitioning via metal-nicotanamine (NA) complexes. Plant Physiology **129,** 431-432.

Wang, Y.-H., Garvin, D.F., and Kochian, L.V. (2002). Rapid induction of regulatory and transporter genes in response to phosphorus, potassium, and iron deficiencies in tomato roots. Evidence for cross talk and root/rhizosphere-mediated signals. Plant Physiology **130,** 1361-1370.

Williams, L.E., and Mills, R.F. (2005). P1B-ATPases - an ancient family of transition metal pumps with diverse functions in plants. Trends in Plant Science **10,** 491-502.

Williams, L.E., Lemoine, R., and Sauer, N. (2000). Sugar transporters in higher plants - a diversity of roles and complex regulation. Trends in Plant Science **5,** 283-290.

Wintz, H., Fox, T., Wu, Y.-Y., Feng, V., Chen, W., Chang, H.-S., Zhu, T., and Vulpe, C. (2003). Expression profiles of *Arabidopsis thaliana* in mineral deficiencies reveal novel transporters involved in metal homeostasis. Journal of Biological Chemistry **278,** 47644-47653.

Wisman, E., and Ohlrogge, J. (2000). Arabidopsis microarray service facilities. Plant Physiology **124,** 1468-1471.

Wu, H., Li, L., Du, J., Yuan, Y., Cheng, X., and Ling, H.-Q. (2005). Molecular and biochemical characterization of the Fe(III) chelate reductase gene family in *Arabidopsis thaliana*. Plant Cell Physiology **46,** 1505-1514.

Xu, W., Bak, S., Decker, A., Paquette, S.M., Feyereisen, R., and Galbraith, D.W. (2001). Microarray-based analysis of gene expression in very large gene families: the cytochrome P450 gene superfamily of *Arabidopsis thaliana*. Gene **272,** 61-74.

Yi, Y., and Guerinot, M.L. (1996). Genetic evidence that induction of root Fe(III) chelate reductase activity is necessary for iron uptake under iron deficiency. Plant Journal **10,** 835-844.

CHAPTER 3

INITIAL CHARACTERIZATION OF FOUR bHLH TRANSCRIPTION FACTORS UP-REGULATED IN RESPONSE TO IRON-DEFICIENCY CONDITIONS IN *Arabidopsis thaliana*

ABSTRACT

To discover and characterize novel components of the iron homeostasis system in *Arabidopsis thaliana*, we hybridized Affymetrix ATH-1 microarrays with RNA extracted from shoots and roots of iron-starved or -sufficient wild-type plants. We found that two bHLH transcription factors, belonging to a small sub-family of four genes, were up-regulated under iron-deficiency conditions. Time-course experiments showed up-regulation of all four genes in shoots and roots of iron-deficient plants. Therefore, we decided to use them in subsequent experiments. Even though elemental content of individual T-DNA insertion lines for all four transcription factors indicated a few elements were different than controls, all four had normal iron levels. We decided to focus our research on bHLH101 for three reasons: a) its transcription is induced by iron-deficient conditions, b) it is present in the Affymetrix ATH-1 microarray, and c) the elemental analysis of the bHLH101 T-DNA insertion line showed a more complex effect on metal homeostasis than the other three T-DNA insertion lines. The bHLH101 T-DNA insertion line exhibited differences in the transcriptional regulation of *IRT1* and *FRO2*, but not *AtFer1*, when compared with WT controls. bHLH101::GUS transgenic plants

showed *bHLH101* activity in root and shoot meristems, in cotyledons, and in the root vasculature. It is possible that the four TFs provide redundancy to one another and possibly do so by homo- or hetero-dimerizing with one another.

INTRODUCTION

Transcriptional regulation of gene expression is of fundamental importance for biological functions (Pabo and Sauer, 1992; Zimmermann et al., 2004). Tightly regulated interactions between transcription factors (TFs) and DNA brings a genome to life (Gong et al., 2004). TFs can bind to DNA in a sequence-specific manner, regulate promoter strength, and can act as activators, repressors, or both (Stracke et al., 2001), to direct the temporal and spatial gene expression that leads to normal development and proper physiological responses to environmental stimuli (Zhang and Wang, 2005).

Most TFs are modular proteins containing two independent domains: a protein-protein interaction domain and a DNA-binding domain. These TFs use their protein-protein interaction domain to homo- or hetero-dimerize with other transcription factors and successfully bind to DNA (Pabo and Sauer, 1992; Wray et al., 2003; Shiu et al., 2005). The DNA binding domain interacts with specific nucleotide sequences present in the promoter of the target gene. The DNA binding domain has been well-conserved through evolution making it useful to group TFs into families (Wolberger, 1999; Riechmann and Ratcliffe, 2000; Stracke et al., 2001). The 1,826 TFs present in Arabidopsis belong to 56 families (Guo et al., 2005). Five of these families (Dof, ARF-Aux/IAA, WRKY, AP2, and NAC) appear unique to plants. An additional four TF

families (MYB, bHLH, bZIP, and MADS) are greatly expanded in Arabidopsis when compared with *D. melanogaster*, *S. cerevisiae*, and *C. elegans*. It is common to find functionally redundant TFs within families, indicating that, in some cases, TFs should be studied in the context of the entire family (Riechmann and Ratcliffe, 2000). With 162 members, the basic-helix-loop-helix (bHLH) is one of the largest TF families in Arabidopsis. bHLH TFs have a range of different roles in plant cell and tissue development as well as plant metabolism (Bailey et al., 2003; Heim et al., 2003).

The first TF with a role in plant iron nutrition was discovered in the *fer* mutant tomato line and was named *LeFER*. *LeFER* encodes a bHLH transcription factor that shows increased transcription under iron-deficiency conditions, and high iron conditions reduce *LeFER* transcript and protein levels (Brumbarova and Bauer, 2005). *fer* mutant plants are unable to activate their Strategy I responses under iron-deficient conditions (Ling et al., 2002).

The Arabidopsis ortholog of *LeFER* is *FRU1* (FER-like Regulator of iron Uptake), also known as *FIT1* (Fe-deficiency Induced Transcription factor 1). *FRU/FIT1* is encoded by At2g28160 (*bHLH029*) and appears to be a mediator in the induction of iron-deficiency responses in Arabidopsis (Colangelo and Guerinot, 2004; Jakoby et al., 2004). It regulates *FRO2* at the transcriptional level and IRT1 protein accumulation (Colangelo and Guerinot, 2004; Jakoby et al., 2004). Additionally, 72 of 179 iron-regulated genes in Arabidopsis appear to be dependent on *FRU1/FIT1* (Colangelo and Guerinot, 2004). *FRU1/FIT1* complements *fer* tomato plants, suggesting that this bHLH transcription factor may be a universal iron-homeostasis regulator of Strategy I plants (Yuan et al., 2005).

In spite of all this research, we still know little about iron-regulation mechanisms and iron-regulated genes in *Arabidopsis thaliana*. In an effort to identify new genes involved in these processes, we took a transcriptome-wide approach by hybridizing Affymetrix ATH-1 microarrays with RNA extracted from roots and shoots of 14-day-old *A. thaliana* plants that were placed under iron-deficient or -sufficient conditions for three days (see Chapter 2 for more details). Analysis of the microarray data led us to two closely related bHLH transcription factors (*bHLH101* and *bHLH039*) that increase their transcript levels in both roots and shoots under iron-deficient conditions. Both TFs belong to a small sub-family of four bHLH TFs, but the other two were not present on the microarray.

Here we report initial efforts towards the characterization of these four bHLH TFs. T-DNA insertion lines for all four were obtained and used in various experiments aimed at identifying unique phenotypes. We characterized *bHLH101* further by analyzing gene expression levels of certain iron-regulated genes in its T-DNA insertion line, and by creating GUS and over-expressing transgenic lines. We are now in the process of obtaining double T-DNA insertions to eliminate possible functional redundancy within this small family. At the same time, we are building bait and prey constructs to investigate possible protein-protein interactions within the genes.

RESULTS

Microarray data mining and protein alignment

As part of her previous work, Dr. Elizabeth Rogers (University of Missouri-Columbia, Columbia, MO) in collaboration with Dr. Mary Lou Guerinot (Dartmouth College, Hanover, NH) examined gene expression using Affymetrix ATH-1 microarrays. These microarrays were hybridized with RNA from shoots and roots of WT *A. thaliana* plants grown under iron-complete and -deficient conditions. Growth under iron-deficient conditions depletes the plants of iron, causing them to up-regulate their iron-deficiency responses (Yi and Guerinot, 1996). Two closely related bHLH transcription factors, *bHLH039* and *bHLH101* (At3g56980 and At5g04150, respectively), were up-regulated in both roots and shoots of iron-deficient plants (Table 3.1). The predicted protein sequences of 18 closely related genes to bHLH039 and bHLH101 (Bailey et al., 2003; Toledo-Ortiz et al., 2003) were obtained from The Arabidopsis Information Resource (TAIR) website and aligned using the ClustalW algorithm (Figure 3.1). Of the 18 genes, nine were not present on the microarray and nine others did not show differential expression under iron-deficiency conditions. According to our ClustalW analysis, the two iron-regulated genes, *bHLH039* and *bHLH101*, are grouped in a small sub-family of four transcription factors that includes genes *bHLH038* and *bHLH100* (At3g56970 and At2g41240, respectively). All four protein sequences share ~30-40% identity and ~60% similarity (Figure 3.2 and Table 3.2) indicating that all four are

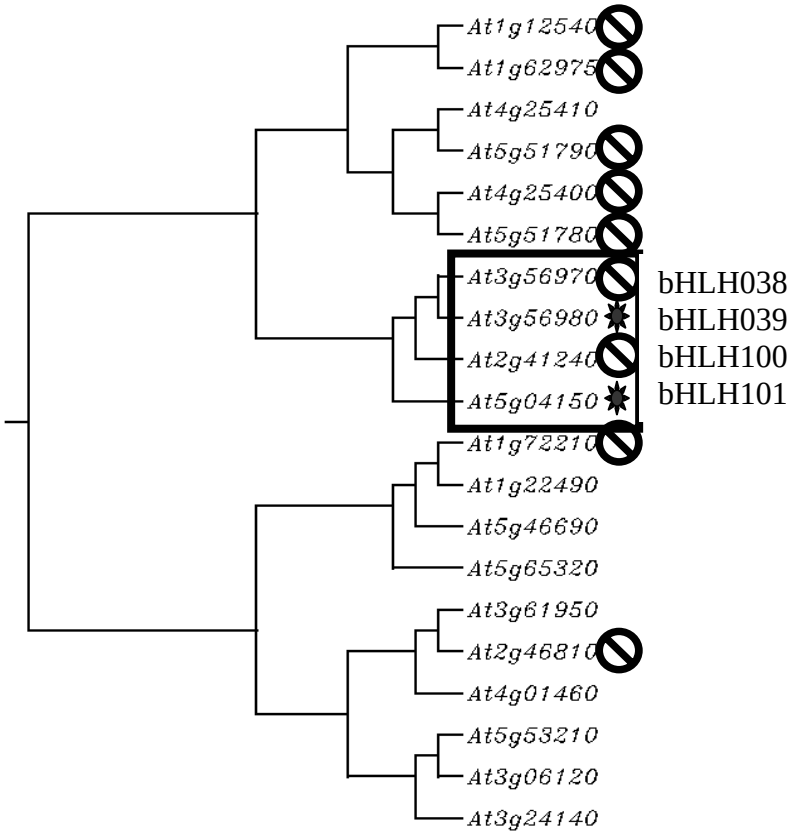

Figure 3.1.
ClustalW tree of 20 closely–related bHLH transcription factors.
The tree shows the relationship between 20 bHLH proteins. The 19 closest proteins to bHLH101 were selected from (Bailey et al., 2003). Protein sequences were obtained from www.arabidopsis.org. Alignment was done in http://align.genome.jp/. Crossed black circles show genes absent on the microarray. The clade of four transcription factors is boxed. Grey stars show genes up-regulated under iron-deficiency on the microarray.

```
CLUSTAL W (1.82) multiple sequence alignment

At3g56970   M-CALVPSFFTNFGWPSTNQYESYYGAGDNLNNGTFLELTVP-QTY----EVTHHQNSLG 54
At3g56980   M-CALVPPLFPNFGWPSTGEYDSYYLAGDILNNGGFLDFPVPEETYGAVTAVTQHQNSFG 59
At2g41240   M-CALVPPLYPNFGWPC-GDH-SFYETDD-VSN-TFLDFPLPDLT------VT-HEN--- 45
At5g04150   MEYPWLQSQVHSFS-PT-LHFPSFLHP---LDDSKSHNINLHHMS------LS-HSNN-  46
            *  . : .   .*. * : .. *:  ... :.:.   :: :   :      :: *.*. .

At3g56970   VSVSSEGNE---IDNNPVVV-KKLNHNASERDRRKKINTLFSSLRSCLPASDQSKKLSIP 110
At3g56980   VSVSSEGNE---IDNNPVVV-KKLNHNASERDRRRKINSLFSSLRSCLPASGQSKKLSIP 115
At2g41240   --VSSENNRTL-LDN-PVVM-KKLNHNASERERRKKINTMFSSLRSCLPPTNQTKKLSVS 100
At5g04150   --TNSNNNNYQEEDRGAVVLEKKLNHNASERDRRRKLNALYSSLRALLPLSDQKRKLSIP 104
             :..*:.*.    *...**: **********:**:*:*:::****: ** :.*.:***:.

At3g56970   ETVSKSLKYIPELQQQVKRLIQKKEEILVRVSGQRDFE-LYDKQQPKA---VASYLST-V 165
At3g56980   ATVSRSLKYIPELQEQVKKLIKKKEELLVQISGQRNTE-CYVKQPPKA---VANYIST-V 170
At2g41240   ATVSQALKYIPELQEQVKKLMKKKEELSFQISGQRDL--VYTDQNSKSEEGVTSYAST-V 157
At5g04150   MTVARVVKYIPEQKQELQRLSRRKEELLKRISRKTHQEQLRNKAMMDS---IDSSSSQRI 161
             **:: :***** ::::::* ::***:  ::* : . .    .   .:   : .  *  :

At3g56970   SATRLGDNEVMVQVSSSKIHNFSISNVLGGIEEDGFVLVDVSSSRSQGERLFYTLHLQVE 225
At3g56980   SATRLGDNEVMVQISSSKIHNFSISNVLSGLEEDRFVLVDMSSSRSQGERLFYTLHLQVE 230
At2g41240   SSTRLSETEVMVQISSLQTEKCSFGNVLSGVEEDGLVLVGASSSRSHGERLFYSMHLQIK 217
At5g04150   AANWLTDTEIAVQIATSKWT--SVSDMLLRLEENGLNVISVSSSVSSTARIFYTLHLQMR 219
            ::. * :.*: **::: :  . *.::*  :**: : ::. *** *   *:**::***:.

At3g56970   NMDDYKINCEELSERMLYLYEKCENSFN 253
At3g56980   KIENYKLNCEELSQRMLYLYEECGNSYI 258
At2g41240   N--G-QVNSEELGDRLLYLYEKCGHSFT 242
At5g04150   G--DCKVRLEELINGML-LGLR--QS- 240
              .. ::. *** : :* *  .. :*
```

Figure 3.2.
ClustalW aligment of four closely related bHLH transcription factors.
ClustalW aligment using the amino acid sequence of all the members of the small family of four genes. ★represent 100% identity; (:) represent a conserved amino acid; (.) represent semi-conserved amino acids.

closely related to each other. In addition, genes *bHLH038* and *bHLH039* are tightly linked, being ~1.5 kb apart in the genome (see later), making them likely to be the result of a recent duplication event. Even though *bHLH038* and *bHLH100* were not present on the microarray, due to their close identity to *bHLH101* and *bHLH039*, we decided to include all four in our studies to characterize their responses to iron-deficient conditions.

Timeline of transcriptional activity

To observe the transcriptional activity of the four TF's through time, RNA was extracted from shoots and roots of 14-day-old WT plants (time point zero). In addition, RNA was collected at one-half, one, two, and six days, after transfer to iron-sufficient or -deficient conditions (Figure 3.3). The well-characterized root ferric-chelate reductase gene *FRO2* was used as a positive control. In Figure 3.3 we can see that the up-regulation of *FRO2* was similar to previously published reports (Connolly et al., 2002; Vert et al., 2003; Wu et al., 2005). The transcript levels of all four transcription factors were up-regulated in both shoots and roots starting one day after iron withdrawal. Both *bHLH039* and *bHLH101* show high expression levels in shoots and roots after three days of iron-withdrawal, as seen in the microarray results. All four bHLH TFs continued increasing their transcript levels until day six in both shoots and roots (as seen after quantifying the signals and adjusting for loading controls; data not shown). These results, showing all four being up-regulated under iron-deficiency conditions, convinced us to investigate them further.

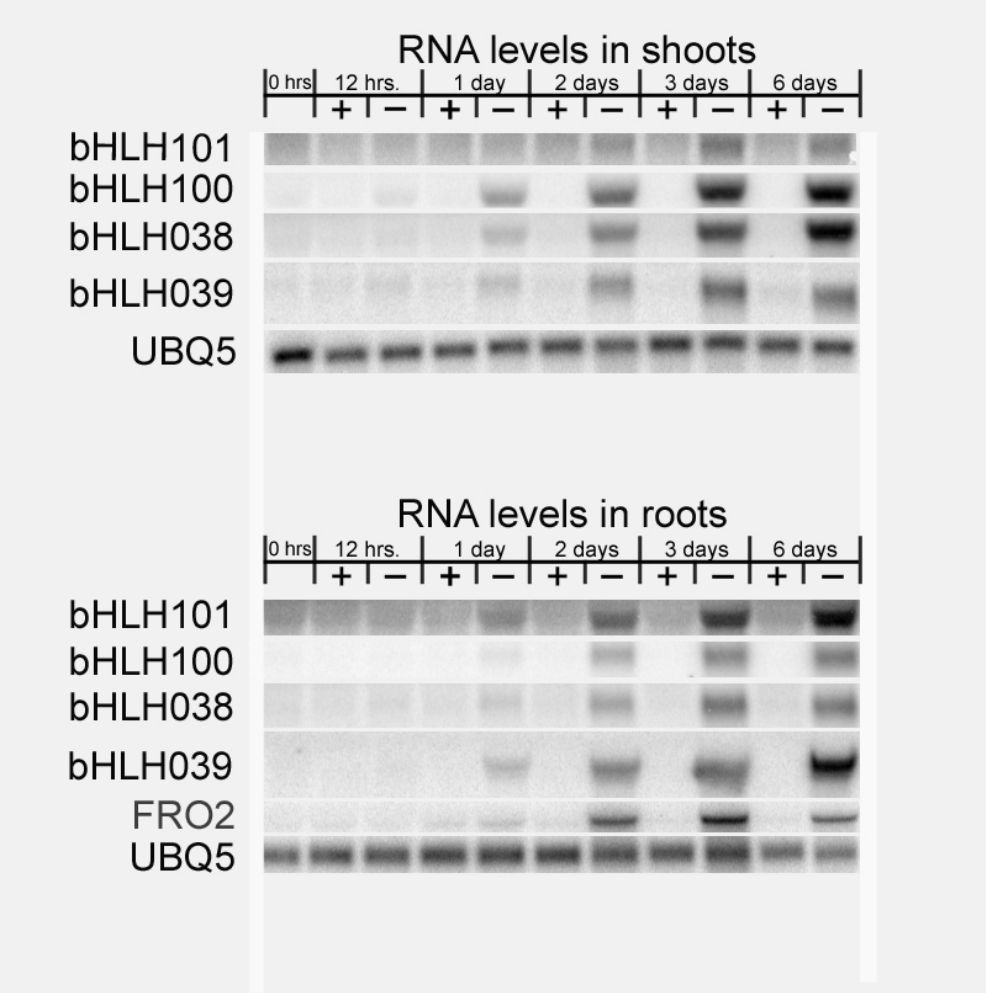

Figure 3.3. Timeline of expression of selected bHLH transcription factors under iron-deficiency and control conditions in shoots and roots.
WT Arabidopsis plants were planted and after 14 days (time point 0) transferred to media with (+) or without (-) iron and left in the new media for time point zero, and one-half, one, two, three, and six days after iron withdrawal. Ubiquitin5 (*UBQ5*) was used as a loading control. Experiment was done in duplicate with similar results.

Physiological characterization of individual T-DNA insertion lines

Individual T-DNA insertion lines did not show an obvious visual phenotype.

T-DNA insertion lines for the four transcription factors were obtained from the Arabidopsis Biological Resources Center (ABRC) (Figure 3.4). Homozygous insertions were confirmed by PCR. We confirmed the absence of *bHLH101* transcripts in the bHLH101 T-DNA line by RT-PCR (data not shown). All four T-DNA lines, three over-expressing (OX) lines (see later), and wild-type (WT) controls were subjected to a subset of the environmental conditions known as The Gauntlet (http://thale.biol.wwu.edu), with the goal of identifying a set of environmental conditions that caused a unique visual phenotype. None of the conditions included in the experiment (Table 3.3) revealed a visible phenotype associated with any T-DNA line.

Ferric-chelate reductase activity, fresh weight, and chlorophyll content

We measured the ferric-chelate reductase activity of all four T-DNA insertion lines to assess their iron-nutrition status indirectly. All four lines showed ferric-chelate reductase levels similar to WT controls (data not shown). We further analyzed the *bHLH101* T-DNA line for alterations in iron status: no differences were observed in shoot fresh weight or chlorophyll content between WT controls and the T-DNA line (data not shown).

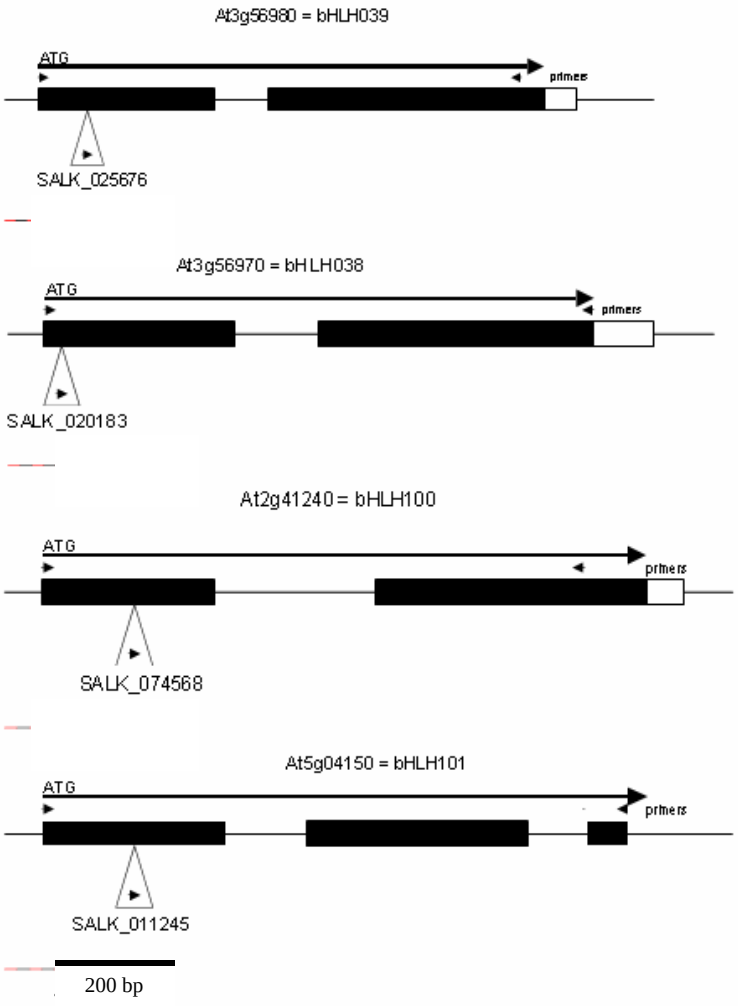

Figure 3.4. Diagrams of the four transcription factors and their T-DNA insertions. Filled boxes represent exons. Open boxes represent 3'- or 5'- UTRs. Lines represent intergenic regions or introns. The location of the ATG starting codon is given and the long filled arrow indicates the direction of transcription. Open triangles represent the location of the T-DNA insertion with the direction of the left border of the T-DNA indicated with a small arrow inside the open triangle. The T-DNA identifier is given under the open triangle. Small arrows indicate the location and direction of the primers used to identify homozygous T-DNA insertions.

Elemental analysis of the four T-DNA lines

Elemental analysis was done for the four homozygous T-DNA lines by Dr. David Salt's lab at Purdue University (Table 3.4). The elemental profile of the bHLH038 T-DNA insertion line was not significantly different from controls. The bHLH039 T-DNA insertion line had a 20% higher copper level than the control, and the bHLH100 T-DNA insertion line had 20% more copper and 6% less sodium than the control. On the other hand, the bHLH101 T-DNA insertion line had a more complex elemental profile with cobalt levels 11% higher, manganese levels 11% higher, molybdenum levels 10% lower, and zinc levels 2% lower than the control. All the elements mentioned showed significant ($p<0.05$) differences between individual T-DNA lines and the controls. There was no difference in iron levels for any of the four bHLH T-DNA lines. The analysis was conducted once.

RNA blots for *IRT1*, *FRO2* and *AtFer1* in the bHLH101 T-DNA background

We selected *bHLH101* for further characterization based on three reasons: 1) it showed high levels of up-regulation in roots of iron-deficient plants, 2) it was present on the Affymetrix microarray, and 3) it showed a unique metal profile when mutated. As a first step, we analyzed the transcriptional activity of the three well known iron-regulated genes *IRT1*, *FRO2*, and *AtFer1* in *bHLH101* T-DNA plants (Table 3.5). We extracted RNA from shoots and roots of iron-sufficient and -deficient WT and *bHLH101* T-DNA plants. RNA blots were done three times independently and as shown in Table 3.5, iron-deficient *bHLH101* T-DNA roots had lower expression levels of *IRT1* and *FRO2* than

WT controls (Student's T-Tests are p=0.024 and 0.051, respectively). On the other hand, *AtFer1* showed similar expression levels in iron-sufficient shoots of WT controls and the mutant line (Student's T-Test is p=0.296).

Microarray of bHLH101 T-DNA insertion line

RNA from the three different and independent extractions mentioned before were pooled together and used to hybridize Affymetrix ATH-1 microarrays. Comparisons were conducted for the transcriptional activity of four iron-regulated genes (*IRT1*, *FRO3*, *AtFer1*, and *FRU1/FIT*) between WT controls and *bHLH101* T-DNA insertion lines. Since *FRO2* is absent from the Affymetrix ATH-1, *FRO3* was used as a suitable replacement of *FRO2* (Wu et al., 2005; Mukherjee et al., 2006). In general, *IRT1*, *AtFer1*, and *FRU1/FIT1* had similar transcript levels in both mutant and control sets of microarrays, in all tissues and conditions. However, *FRO3* showed a complex reaction to the absence of expression of *bHLH101*: under iron-deficiency conditions, and when *bHLH101* was absent, *FRO3* had 15% and 60% higher expression level in roots and shoots, respectively. Under iron-sufficient conditions, *FRO3* showed ~40% lower expression levels in both roots and shoots of bHLH101 T-DNA line than WT controls (data not shown).

As a second step, we examined the list of the 25 most up-regulated genes in iron-deficient *bHLH101* T-DNA and WT roots. Both lists, although not identical, were similar with 60% of the genes shared by both lists (data not shown).

Using the microarray data we were able to compare *bHLH101* T-DNA and WT transcriptomes of shoots or roots under both iron-nutritional statuses (Table 3.6). 502 genes in the *bHLH101* T-DNA background showed at least a three-fold modification of their expression when compared with the WT control. 200 of the 502 are present in shoots and the other 302 are present in roots. 81 of the genes with differential expression in shoots (~40%) and 136 of the genes present in roots (~45%) do not have an assigned function.

Table 3.6.a shows the genes up-regulated in iron-deficient shoots when *bHLH101* was absent. Three of them are cold-inducible proteins (6.7-, 4.7-, and 3.6-fold increase in expression). One of the most up-regulated genes in iron-deficient shoots is *bHLH039* (5.7-fold) as compared with WT controls grown under the same conditions. This same gene showed transcript up-regulation in mutant iron-deficient roots by 70% when compared with WT controls. In iron-sufficient shoots and roots, its expression level is below the detection limits of the technique (data not shown). Finally, another interesting gene was the putative transporter *ZIP9* (At4g33020), which is down-regulated in iron-deficient roots of mutant plants 3.1-fold.

We found 21 common genes in Tables 3.6.a, 3.6.b, 3.6.c, and 3.6.d. These genes modified their expression in all iron-sufficient and -deficient shoots and roots of mutant plants when compared with WT controls. Out of the 21, only one showed up-regulation whereas the other 20 were down-regulated in the absence of a functional *bHLH101*, pointing to a possible positive regulation of these genes by *bHLH101*. It is interesting to note that most of them showed transcript level down-regulation to ~20% of WT levels, regardless of tissue or nutritional status. Sixteen of the 21 genes were

unknown, three were putative TFs, one was a cytochrome P450, and one was a putative ACC synthase. In summary, the absence of a functional *bHLH101* produces a complex change in the mRNA levels of several genes, but nonetheless a visual phenotype was not obtained.

Localization of bHLH101 expression

To further characterize bHLH101, we fused 2,182 bases of the sequence upstream of the ATG start codon and the first 20 bases of the coding region to a GUS reporter gene (Figure 3.6). WT Arabidopsis plants were transformed with the construct and eight lines carrying single, homozygous insertions were grown under standard conditions, harvested before and after iron-deficiency induction, and stained with X-GUS. GUS staining was observed in the shoot and root meristems, root vascular tissue, young leaf veins, cotyledons, root hairs, and parts of immature siliques (Figure 3.5). We did not detect staining in mature stems, flowers, ovaries, or pollen sacs. Iron-sufficient bHLH101::GUS lines showed minimal root staining in the vasculature and meristem, whereas iron-deficient roots showed more extensive staining. In contrast with roots, shoots of bHLH101::GUS transgenic plants showed a similar localization in staining pattern regardless of growth conditions. It is possible that the shoot meristem had increased staining intensity, but this was difficult to quantify (see discussion).

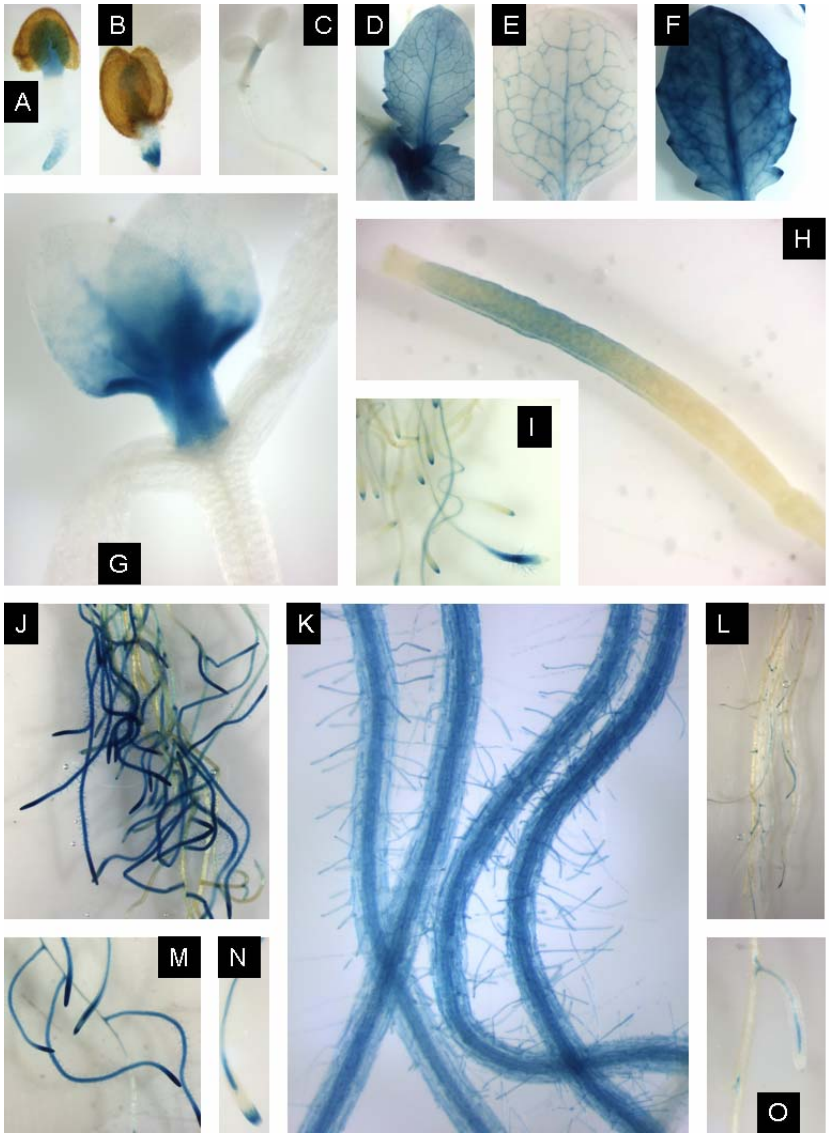

Figure 3.5. Staining of bHLH101::GUS transgenic Arabidopsis plants. All were stained for three days.
A) and B) Two-day old seedlings grown under iron-sufficient conditions. Root meristem and cotyledons show GUS expression. C) Three-day old seedling plant grown under iron-sufficient conditions. Note that the cotyledons are not expressing GUS anymore while the stem has low expression levels. D) 14-day old shoot meristem from plants grown under iron-sufficient conditions. E) Old leaf and F) young leaf, both taken from a 14-day old plant grown under iron-deficient conditions. G) Shoot meristem in a six-day old plant. H) One-week old silique. Note that GUS staining is superficial and present in the top third of the silique only. I), L), and O) show 17-day old roots from plants grown under iron-sufficient conditions. O) Detail of a secondary root. N) Secondary root grown for 14 days under iron-sufficient conditions. J) and M) 17-day old roots grown under iron-deficient conditions. Note the more extensive GUS staining under these conditions. M) Detail of secondary roots. K) Detail of 17-day old roots grown under iron-deficient conditions. Note the intense staining in the numerous root hairs present.

3.6.a.

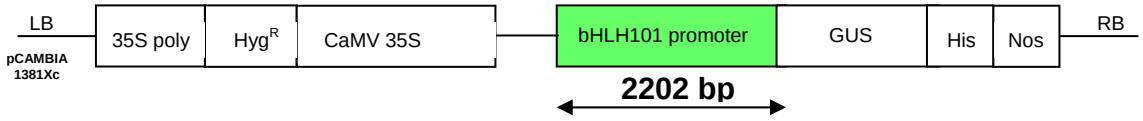

3.6.b.

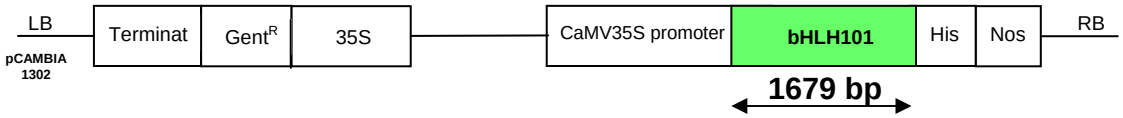

Figure 3.6. Diagram of the constructs used in our research.
3.6.a. Construct used to create transgenic bHLH101::GUS plants.
2.2 kbs of upstream region from bHLH101 was cloned in front of the GUS gene present in pCAMBIA1381Xc (see Materials and Methods).
3.6.b. Construct used to create transgenic CaMV35S::bHLH101 plants.
1.6 kbs of the genomic region containing the whole bHLH101 gene was cloned after the CaMV35S constitutive promoter.

Characterization of lines over-expressing bHLH101

To investigate further the role of bHLH101, a 35SCaMV::bHLH101 over-expression (OX) construct was made (Figure 3.6). Fourteen single-insertion, homozygous lines were selected and *bHLH01* expression levels examined using RNA blots. This experiment was done twice and all results are shown in Figure 3.7. Lines OX-(6), OX-(7), and OX-(12) were selected for further experiments based on the induction of *bHLH101* transcripts. OX lines were grown next to WT controls under standard conditions but an obvious phenotype was not detected. Ferric-chelate reductase activity in the three OX lines was similar to controls (data not shown), and the subset of Gauntlet experiments used for the T-DNA homozygous lines failed to induce an obvious phenotype in any of the three OX lines (Table 3.3) except for line OX-(12) whose roots grew slightly faster than controls. Since this phenotype was not present in the other two OX lines, we cannot rule out a positional effect of the OX insert in neighboring genes, as opposed to an effect of the high expression levels of *bHLH101* on the physiology of the plant.

DISCUSSION

In this chapter, we describe the initial characterization of four closely related bHLH transcription factors that are transcriptionally up-regulated under iron deficiency. The four TFs were identified using a combination of microarray data analysis and protein alignments. Due to the four TFs being closely related and the four of them being induced

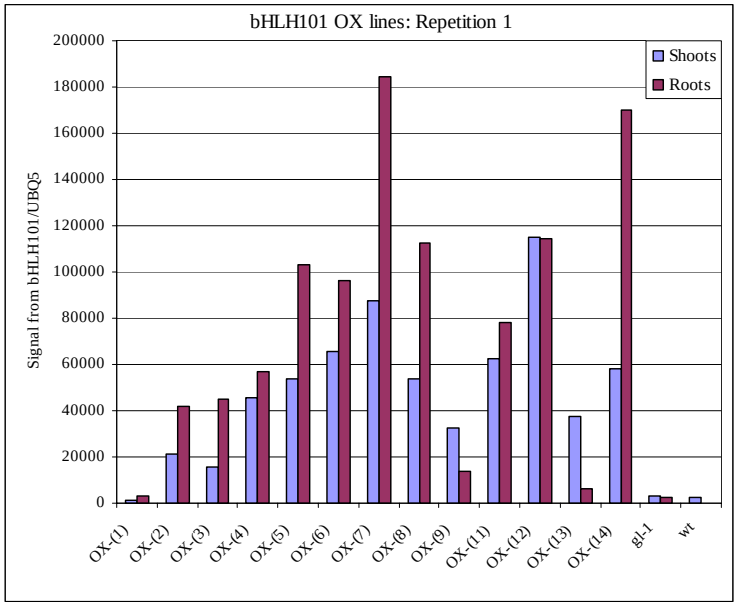

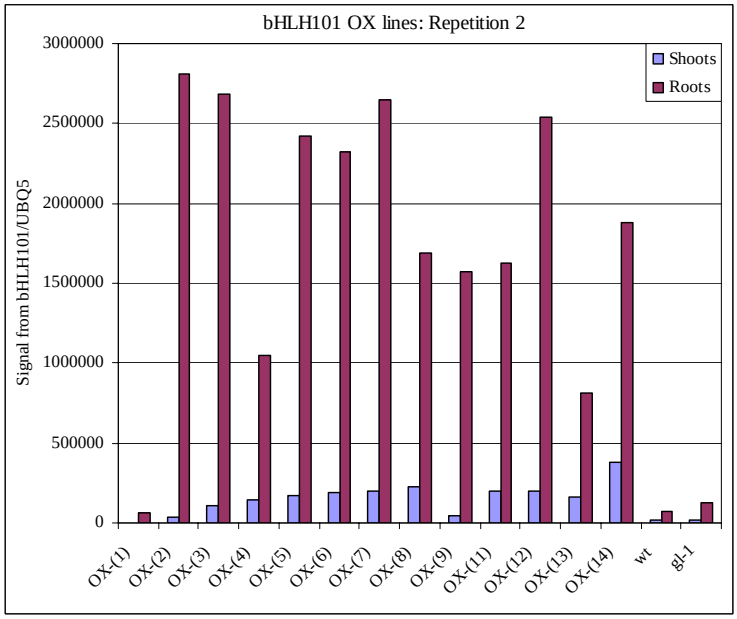

Figure 3.7. bHLH101 transcript levels in the over-expressor transgenic lines. Transgenic plants were grown under standard conditions, RNA extracted and probed for bHLH101 transcript levels using *UBQ5* levels as a loading control. Lines 6, 7 and 12 were chosen for further experiments.

under iron-deficient conditions, we decided to include all four in future studies.

A timeline of gene expression during iron-deficiency conditions showed the induction of *bHLH039* and *bHLH101* confirming results shown in the WT microarray dataset. The timeline also showed *bHLH038* and *bHLH100* induction under iron-deficiency conditions (Figure 3.3). All four genes demonstrated continuing increase in transcript levels for at least six days after iron withdrawal. Taking both repeats into consideration, *bHLH100* and *bHLH101* show higher expression level in shoots of iron-deficient plants than roots, whereas *bHLH038* and *bHLH039* show transcript induction to similar levels in both roots and shoots. This expression pattern reveals differences for each pair and may suggest co-regulation and possible interactions and/or redundancy in function.

When plants were grown in iron-sufficient media, *bHLH101* and *bHLH039* transcript levels were below the detection limit of both RNA blots and microarrays. These results seem to indicate that there is a minimal demand for them when plants are under complete conditions, or that they may be iron-deficiency specific.

bHLH038, *bHLH039*, and *bHLH101* have been previously mentioned in the literature. Both *bHLH038* and *bHLH039* seem to be directly regulated by another transcription factor called *OBP3* (At3g55370), which is present mainly in roots. Plants over-expressing *OBP3* show chlorosis, fewer leaves, smaller and denser root hairs, and a longer lifespan (Kang and Singh, 2000). *OBP3*, *bHLH038*, and *bHLH039* transcripts were induced when exposed to salicylic acid (SA), and down-regulated upon exposure to jasmonic acid (JA). An RNAi construct against *OBP3* reduced the expression levels of

OBP3, *bHLH038*, and *bHLH039*, suggesting that the expression of both bHLH TFs is *OBP3*-dependent (Kang et al., 2003).

bHLH039 appeared as part of a study of SHL, which is a TF and a chromatin-modifying enzyme. SHL (SHort Life of plants) over-expressing lines show early flowering, early senescence, and fewer flowers and seed whereas plants down-regulating SHL show compact rosettes, late flowering, and delayed senescence. Microarray data from SHL over-expressing plants showed 3.5-fold up-regulation of *bHLH039* (Muessig and Altmann, 2003). *bHLH039* appeared in a study of another TF called *Zat12* (At5g59820). Plants without a functional copy of *Zat12* are sensitive to H_2O_2 whereas over-expression causes tolerance to H_2O_2. Microarray analysis of 35S::Zat12 transgenic plants revealed that *bHLH039* is up-regulated 2.4-fold when compared with controls (Rizhsky et al., 2004). bHLH039 was again found in a study of the thylakoid-attached copper/zinc superoxide dismutase (*KD-SOD*; At2g28190), which is the key enzyme in the water-water cycle against the photo-oxidative damage of chloroplasts. When *KD-SOD* is disrupted, plants show reduced growth and development, smaller chloroplasts, less chlorophyll, and reduced photosynthetic activity, while up-regulating their oxidative stress defense responses. Microarray analysis of *KD-SOD* mutant plants revealed *bHLH039* being down-regulated 6.1-fold (Rizhsky et al., 2003). Finally, *bHLH101* and *bHLH039* show high transcript levels in phloem-cambium enriched tissue that had been taken from eight week-old *A. thaliana* stems (Zhao et al., 2005). It is interesting to note that all previous reports on any of the four TFs are related to oxidative stress, including the report about *OBP3* (Kang and Singh, 2000; Muessig and Altmann, 2003), SHL (Muessig and Altmann, 2003), *KD-SOD* (Rizhsky et al., 2003), and *ZAT12* (Rizhsky et

al., 2004). It is known that roots and root hairs need to create ROS to grow (Foreman et al., 2003; Rentel et al., 2004). It is possible that the four TFs mentioned in this study are involved in iron-deficiency regulation of oxidative stress, which in turn may be related to root growth.

T-DNA insertion lines for each of the TFs did not show an obvious, visual phenotype when grown under standard conditions, when starved for iron, or subjected to a subset of the Gauntlet environmental conditions. Elemental analysis showed that the four T-DNA lines had normal iron levels and only minor differences in other elements when compared with controls. This lack of a phenotype in any T-DNA insertion line may suggest that none of the four individual TFs is necessary to overcome the environmental conditions used in these experiments (Table 3.3). This raises the possibility that the contribution of each TF to general plant development or iron homeostasis may be too small to be identified using our regular set of experiments. It is also possible that the TFs are redundant. We have seen that homozygous T-DNA insertion lines for each of the four TFs did not show a visible phenotype; all had normal ferric-chelate reductase activity, and showed only minor differences in elemental content when compared to WT controls. *bHLH039* with *bHLH101* and *bHLH038* with *bHLH100* show similar tissue and expression activity under iron-deficiency conditions (Figure 3.3), suggesting co-localization of expression. This co-localization is supported for *bHLH101* and *bHLH039* in the vasculature as previously reported (Zhao et al., 2005). Finally, microarray results from the *bHLH101* T-DNA line show an up-regulation of *bHLH039* in iron-deficient roots and shoots, which may imply functional compensation in the absence of *bHLH101*. From the literature, we know that bHLH TFs form dimers to bind to DNA (Pabo and

Sauer, 1992; Wray et al., 2003; Shiu et al., 2005) and it is common for them to be redundant (Riechmann and Ratcliffe, 2000). All this leads to the hypothesis that the four transcription factors homo- or hetero-dimerize while at the same providing redundancy to each other, thus masking the appearance of phenotypes in the single T-DNA insertion lines.

bHLH101 was selected for further studies based on several factors (see Results). To establish a relationship between *bHLH101* and iron regulation, *FRO2*, *IRT1*, and *AtFer1* transcript levels in iron-starved and iron-complete *bHLH101* T-DNA and WT plants were studied. These experiments were done in triplicate and although general trends were present in all three (Table 3.5 and see later), only *IRT1* and *FRO2* levels are different from WT, whereas *AtFer1* levels were not significantly different from WT. If we include in our analysis the trends shown for *AtFer1*, RNA levels for these three iron-regulated genes reflect conditions commonly found in plants grown under iron-excess, where ferritin is up-regulated to store excess iron and when placed under iron-deficient conditions, the presence of extra stored iron delays the induction of *FRO2* and *IRT1*. This simple explanation contradicts both the elemental analysis, where iron levels are similar to the control, and the microarray data, where *IRT1* levels in the bHLH101 T-DNA line are similar to WT controls (Table 3.6, see later). It is possible that the RNA blot and microarray data, for which we pooled the RNA described here, may be skewed and not necessarily reflect normal conditions since after the experiments were done, we realized that plants for the second set had been grown in 1/10 of the normal micronutrient concentration, possibly invalidating that RNA blot and the bHLH101 T-DNA line microarray experiments. Also, the ~50% lower *FRO2* transcript levels do not correlate

with the WT levels of ferric-chelate reductase activity seen in the *bHLH101* T-DNA line, although it is known that *FRO2* is regulated at both the transcriptional and post-transcriptional levels (Connolly et al., 2003). These discrepancies will be studied further (see Future Research).

Affymetrix ATH-1 microarrays were used to identify the transcriptome of the *bHLH101* T-DNA line (Table 3.6). Results showed the complex transcriptome of the bHLH101 T-DNA line when compared with WT controls. Of all the genes with at least a three-fold differential expression in iron-sufficient and -deficient roots and shoots of *bHLH101* compared with WT controls, 21 genes were common to all lists (Table 3.6). Since 20 of them down-regulated their expression, we may speculate that the presence of *bHLH101* induces the expression of the majority of genes it regulates. Most of the 21 genes are unknown, suggesting that *bHLH101* regulates new and not-yet characterized regulatory pathways.

A GUS fusion construct was made to localize the expression of *bHLH101*. Transgenic GUS shoots stained the location of expression of *bHLH101* under iron-deficient or -sufficient conditions (Figure 3.6) in roots and shoots. In contrast with GUS expression in the root, where GUS transcription increased and the difference was visible; shoot GUS expression remained fairly similar under either iron-nutrition condition. This stands in contrast with *bHLH101* shoot expression levels as detected by microarrays and RNA blots. This can be due to an increase of transcriptional activity within the meristem and not due to an increase in area of expression, or also due to the difficulty of quantifying transcription activity using GUS as a reporter. GUS expression in roots, where under normal conditions it is minimal and localized to the vasculature and

meristem, extends to all the layers of the root and root hairs when placed under iron-deficiency conditions.

The GUS staining results and the RNA blot timeline suggested that all four TFs are highly expressed in roots of iron-deficient plants. It is known that iron-deficient roots dramatically increase the number of secondary roots and root hairs (Schikora and Schmidt, 2001; Schmidt, 2003). This led us to speculate that *bHLH101*, and by extension the other three TFs, may be involved in iron regulation through the modification of root architecture under iron stress. It is possible that the TFs will have this theoretical effect on root architecture until iron is re-supplied to the media. As seen in Table 3.3, we analyzed the root length, secondary root formation, and root gravitropism for all four T-DNA and three over-expressing lines without positive results, possibly due to gene redundancy.

WT Arabidopsis plants were transformed with a CaMV35S::bHLH101 construct. Three over-expressing (OX) lines were selected due to the high expression of the transgene. As noted in Figure 3.7, all 14 lines expressed the transgene in higher levels than WT controls. It is curious to note that even though both RNA blots were loaded with similar amounts of RNA, hybridized, washed, and exposed together; the signal levels for over-expression RNA blot 1 are much lower than for over-expression RNA blot 2. It may be possible that transgene expression levels in the shoot remained similar in both blots, but the higher expression level in roots of RNA blot 2 masks the signal from shoots. It is important to note that in spite of the signal differences, lines with highest transgene expression were ranked similarly in both blots, which are the ones used in subsequent experiments. *bHLH101* transcript levels are much higher in roots than in shoots of the

over-expressing lines. It is tempting to speculate that the over-expression RNA blots (Figure 3.7) show effects of a post-transcriptional mechanism that impedes the accumulation of *bHLH101* transcripts in shoots to the same levels as in roots.

In this chapter, we presented an initial effort to characterize transcription factors that up-regulate their transcriptional activity under iron-deficiency conditions. The experiments conducted shed light on the behavior of the four TF members of the small subfamily, but we lack enough data to infer a conclusive function for each one. All four are up-regulated under iron-deficiency conditions in both shoots and roots. One of them (*bHLH101*) is expressed in the vasculature of roots, young leaves, and meristem. It is possible that this TF is regulated at the transcriptional and post-transcriptional levels.

FUTURE RESEARCH

As seen in Figure 3.3, the highest expression levels of the four TFs are tissue-dependent and are obtained six days after iron withdrawal. On the other hand, whenever plants are under iron-sufficient conditions, the expression of all four is below RNA blot and microarray detection levels. Most of our experiments with the T-DNA insertion lines were done under iron-complete conditions, which is when the transcriptional activity of all four TFs is minimal or non-existent. We would like to repeat some experiments (see below) after plants have been iron-starved for six days. This may increase the likelihood of finding a phenotype since plants will be unable to up-regulate the genes with the T-DNA insertion. In particular we would like to repeat, under this new condition, the

elemental analysis, root growth experiments, and *FRO2*, *IRT1* and *AtFer1* expression and protein levels.

We also would like to test the hypothesis that all four TFs not only interact with each other, but also provide functional redundancy. There are four possible complementary approaches to test the hypothesis that we would like to pursue: 1) a yeast two-hybrid assays for all four TFs to detect possible protein-protein interactions, 2) obtain double and triple T-DNA insertions by crossing individual TF T-DNA insertion lines, which may eliminate redundancy and help us uncover novel phenotypes, 3) localize the expression of each TF under normal and iron-deficient conditions, using a reporter gene, indicating areas of transcriptional activity overlap that will serve as an indication of possible hetero-dimerizations, and 4) observe, in each individual T-DNA line, the transcriptional activity of the other three TFs, possibly indicating which ones show modified transcriptional activity as a way to compensate for one absence.

It would be interesting to obtain *OBP3* mutant plants to investigate the possible contribution of this TF to iron homeostasis. It has been reported that *OBP3* directly regulates both *bHLH038* and *bHLH039*, and an RNAi construct directed to *OBP3* down-regulates *bHLH038* and *bHLH039* as well. Since both are close to each other in the genome (~1.5 kb) it would be difficult to find recombinants starting with individual T-DNA lines, making the *OBP3* RNAi line useful, although it is possible that the phenotypes observed in the *OBP3* RNAi line are due to the activity of this TF on other targets and not necessarily an effect of the reduction in transcription of *bHLH038* and *bHLH039*. Another goal would be to establish the transcriptional activity of *bHLH100* and *bHLH101* in the *OBP3* RNAi background since it would be interesting to see if they

are *OBP3*-regulated as well. Another interesting approach would be to assay for ferric-chelate reductase and for elemental content in the *OBP3* mutant background.

Table 3.1. Transcript levels for genes At5g04150 and At3g56980. Microarrays were hybridized with RNA extracted from WT plants placed on either iron-complete or iron-deficient media. Shoots and roots were harvested independently.

Table 3.1.a. Shoots

		WT shoots +Fe		WT shoots -Fe		Fold
AGI[1]	**Name[2]**	**Signal[3]**	**Call[4]**	**Signal[3]**	**Call[4]**	**increase**
At5g04150	bHLH101	26	A	271	P	**Up[6]**
At3g56980	bHLH039	45	A	213	P	**Up[6]**

Table 3.1.b. Roots

		WT roots +Fe		WT roots -Fe		Fold
AGI[1]	**Name[2]**	**Signal[3]**	**Call[4]**	**Signal[3]**	**Call[4]**	**increase**
At5g04150	bHLH101	34	A	468	P	**Up[6]**
At3g56980	bHLH039	160	P[5]	1690	P	**Up[6]**

[1] AGI code as found in TAIR (www.arabidopsis.org).
[2] Name of the gene.
[3] Fluorescent signal given by the probes specific for the gene in the Affymetrix microarray.
[4] (P)resent or (A)bsent. Qualitative interpretation of the signal level. Present indicates that the signal is above the background or noise levels, Absent indicates that the computer could not differentiate between the signal coming from the probes for a specific gene and the general background on the microarray.
[5] In most cases a signal value below 200 was considered to be background even when the computer assigned a call of (P)resent.
[6] An actual number cannot be given since the base number is in the background level.

Table 3.2. Identity in amino acid sequences between the four TFs.

	Length (aa)	bHLH101	bHLH100	bHLH038	bHLH039
bHLH101	198	100.0			
bHLH100	174	39.4	100.0		
bHLH038	221	43.9	47.7	100.0	
bHLH039	237	48.0	46.0	49.8	100.0

Table 3.3. Gauntlet conditions used in the T-DNA and over-expressor lines. Grey boxes indicate reproducible differences between the line and the control. Controls used were *Arabidopsis thaliana gl-1* and *Arabidopsis thaliana* Col-0.

Gauntlet Assay	bHLH101 T-DNA line	bHLH100 T-DNA line	bHLH038 T-DNA line	bHLH039 T-DNA line	OX-(6)	OX-(7)	OX-(12)
Germination	No	No	No	No	No	No	No
Salt tolerance	No	No	No	No	No	No	No
UV tolerance	No	No	No	No	No	No	No
pH tolerance	No	No	No	No	No	No	Slight
Aluminum toxicity	No	No	No	No	No	No	No
Freezing tolerance	No	No	No	No	No	No	No
Root gravitropism	No	No	No	No	No	No	No
Lateral Roots	No	No	No	No	No	No	No
Heat	No	No	No	No	No	No	No
Chill	No	No	No	No	No	No	No
Etiolated growth	No	No	No	No	No	No	No
Root length	No	No	No	No	No	No	Yes
Buffer conditions	No	No	No	No	No	No	No
Phototropism	No	No	No	No	No	No	No
Fresh weight	No	n/a	n/a	n/a	n/a	n/a	n/a
Chlorophyll content	No	n/a	n/a	n/a	n/a	n/a	n/a

No = No statistical difference with the control.
Slight = Control and line are different but within one standard deviation.
Yes = The difference between the control and the line is bigger than one standard deviation.
n/a = Experiment not conducted.

Table 3.4. Elemental analysis of the TFs T-DNA lines. Experiment with bHLH101 T-DNA line was done independently than the experiment with the other three lines.

Table 3.4.a. Elemental analysis of bHLH101 T-DNA line compared with *Arabidopsis thaliana* Col-0 control plants.

	WT	bHLH101 T-DNA line		
Element	Average[1]	Average[1]	% diff.[2]	p-value[3]
Lithium	**18.30**	17.83	-2.63	0.28
Sodium	**784.74**	731.33	-7.30	0.10
Magnesium	**11799.26**	11655.65	-1.23	0.11
Phosphorous	**7925.02**	7623.63	-3.95	0.24
Potassium	**40019.71**	37725.24	-6.08	0.34
Calcium	**39090.37**	39820.86	1.83	0.19
Manganese	**34.83**	38.57	9.68	<0.01
Iron	**78.02**	76.93	-1.40	0.06
Cobalt	**1.96**	2.19	10.55	<0.01
Nickel	**1.60**	1.64	2.37	0.33
Copper	**3.87**	2.50	-54.79	0.25
Zinc	**53.45**	52.19	-2.41	0.03
Arsenic	**0.65**	0.55	-18.83	<0.01
Selenium	**23.81**	21.84	-9.02	0.02
Molibdenum	**9.16**	8.21	-11.50	<0.01
Cadmium	**1.65**	1.76	6.01	0.11

Table 3.4.b. Elemental analysis of bHLH038, bHLH039, and bHLH100 T-DNA lines compared with *Arabidopsis thaliana* Col-0 plants.

	WT	bHLH038 T-DNA line			bHLH039 T-DNA line			bHLH100 T-DNA line		
Element	Average[1]	Average[1]	% diff.[2]	p-value[3]	Average[1]	% diff.[2]	p-value[3]	Average[1]	% diff.[2]	p-value[3]
Lithium	**7.78**	7.80	0.15	0.97	8.04	3.24	0.55	8.08	3.63	0.48
Sodium	**1217.18**	1169.06	-4.12	0.24	1170.35	-4.00	0.23	1150.26	-5.82	0.08
Magnesium	**21827.88**	21506.65	-1.49	0.48	21402.70	-1.99	0.32	21467.76	-1.68	0.31
Phosphorous	**9890.29**	10107.23	2.15	0.47	10021.70	1.31	0.68	10130.58	2.37	0.36
Potassium	**45188.50**	45965.26	1.69	0.73	46662.81	3.16	0.44	45646.19	1.00	0.85
Calcium	**43369.85**	43472.16	0.24	0.93	43058.19	-0.72	0.78	42454.69	-2.16	0.36
Manganese	**122.07**	132.90	8.15	0.33	137.44	11.18	0.11	135.34	9.81	0.18
Iron	**75.38**	77.25	2.42	0.59	74.60	-1.04	0.81	72.55	-3.90	0.22
Cobalt	**2.03**	2.01	-1.12	0.93	1.77	-14.53	0.11	1.82	-11.43	0.34
Nickel	**1.10**	0.87	-26.56	0.41	0.79	-39.57	0.27	0.95	-15.90	0.63
Copper	**4.50**	5.79	22.26	0.06	5.56	19.05	0.04	5.58	19.36	0.04
Zinc	**129.04**	127.14	-1.49	0.75	132.57	2.67	0.46	128.60	-0.34	0.95
Arsenic	**1.64**	1.55	-6.31	0.52	1.54	-6.97	0.56	1.45	-13.07	0.27
Selenium	**26.98**	27.36	1.41	0.65	27.77	2.85	0.31	28.03	3.76	0.14
Molibdenum	**1.84**	2.07	10.89	0.49	2.08	11.55	0.33	2.14	14.01	0.19
Cadmium	**4.37**	4.32	-1.27	0.88	4.09	-6.83	0.27	4.47	2.23	0.72

[1] Average elemental content of one leaf from 25 individual plants.
[2] % difference with WT control plants.
[3] p-value of the two-tailed T-Test. Highlighting shows those values of $p<0.05$

Table 3.5. Expression of three iron-regulated genes in roots of iron-deficient WT and bHLH101 T-DNA plants shown. WT levels set at 1.

Experiment repetition	Known iron-regulated genes		
	IRT1	**FRO2**	**AtFer1**
1st set	0.38	0.38	5.00
2nd set	0.13	0.16	1.25
3rd set	0.71	0.83	1.25
Average	0.41	0.46	2.50
Standard dev.	0.29	0.34	2.17
Student's T-Test	p=0.024	p=0.051	p=0.296

Table 3.6. Affymetrix microarray results analysis. Shown all genes with at least a three-fold variation in transcript levels in the bHLH101 T-DNA microarray compared with WT microarrays hybridized with tissue from plants grown under the same conditions.

Table 3.6.a. Genes up-regulated in iron-sufficient shoots of the bHLH101 T-DNA line as compared to WT iron-sufficient shoots.

	WT shoots +Fe		bHLH101 T-DNA shoots +Fe		Fold[4] increase in bHLH101 T-DNA	
AGI[1]	Signal[2]	Call[3]	Signal[2]	Call[3]		Annotation summary[5]
At4g30650	345	P	2315	P	6.7	Low temperature and salt responsive protein.
At1g15270	637	P	3360	P	5.3	Unknown protein.
At2g43550	272	P	1337	P	4.9	Putative trypsin inhibitor.
At5g15960	1894	P	8944	P	4.7	Cold and ABA inducible protein.
At2g21210	500	P	2318	P	4.6	Putative auxin-regulated protein.
At5g01870	458	P	1677	P	3.7	Lipid-transfer protein.
At2g42530	375	P	1338	P	3.6	Cold-regulated protein.
At2g43590	480	P	1700	P	3.5	Putative endochitinase.
At5g39210	412	P	1439	P	3.5	Hypothetical protein.
At4g13770	653	P	2159	P	3.3	Cytochrome P450.
At3g63160	1501	P	4935	P	3.3	Putative outer envelope chloroplast membrane.
At2g30150	204	P	657	P	3.2	Putative glucosyltransferase.
At1g31180	621	P	1988	P	3.2	DNA glycosylase.
At4g24340	484	P	1516	P	3.1	Putative storage protein.
At2g28740	259	P	808	P	3.1	Histone H4.
At3g05730	3602	P	11146	P	3.1	Unknown protein.
At5g18660	304	P	931	P	3.1	Putative protein 2 -hydroxyisoflavone reductase.
At3g10840	233	P	709	P	3.0	Putative alpha/beta hydrolase.

Table 3.6.b. Genes down-regulated in iron-sufficient shoots of the bHLH101 T-DNA line as compared to WT iron-sufficient shoots.

	WT shoots +Fe		bHLH101 T-DNA shoots +Fe		Fold[4] decrease in bHLH101 T-DNA	
AGI[1]	Signal[2]	Call[3]	Signal[2]	Call[3]		Annotation summary[5]
At4g27652	3600	P	210	P	-17.1	Expressed protein.
At4g29780	5146	P	314	P	-16.4	Hypothetical protein.
At5g59820	3373	P	232	P	-14.5	Zinc finger protein Zat12.
At5g22250	3095	P	224	P	-13.8	CCR4-associated factor-like protein.
At1g73540	4329	P	331	P	-13.1	Unknown protein.
At3g44260	3894	P	350	P	-11.1	CCR4-associated factor 1-like protein.
At4g24570	6845	P	621	P	-11.0	Putative mitochondrial uncoupling protein.
At1g28370	2579	P	265	P	-9.7	Ethylene-responsive element binding factor.
At5g45340	2500	P	271	P	-9.2	Cytochrome P450.
At3g10930	2631	P	315	P	-8.4	Hypothetical protein.
At1g74450	4100	P	515	P	-8.0	Unknown protein.
At1g15010	1758	P	236	P	-7.4	Hypothetical protein.
At3g48650	1595	P	217	P	-7.4	Hypothetical protein.
At2g27080	2531	P	363	P	-7.0	Unknown protein.
At3g04640	5015	P	726	P	-6.9	Hypothetical protein.

At1g76650	1957	P	310	P	-6.3	Putative calmodulin.
At4g11280	2522	P	411	P	-6.1	ACC synthase (AtACS-6).
At5g51190	1623	P	286	P	-5.7	Similar to ethylene responsive binding factor.
At1g80840	4262	P	756	P	-5.6	Transcription factor similar to WRKY.
At3g28340	1515	P	281	P	-5.4	Unknown protein.
At1g27730	8638	P	1635	P	-5.3	Salt-tolerance zinc finger protein.
At2g46400	2454	P	473	P	-5.2	Putative WRKY-type DNA binding protein.
At1g18740	4017	P	783	P	-5.1	Unknown protein.
At3g50930	1657	P	335	P	-5.0	BCS1 protein-like protein.
At2g25250	2166	P	442	P	-4.9	Unknown protein.
At3g46620	4867	P	993	P	-4.9	Putative protein.
At5g59550	3824	P	784	P	-4.9	Putative protein COP1.
At2g41640	1275	P	265	P	-4.8	Unknown protein.
At1g61890	1368	P	291	P	-4.7	Hypothetical protein.
At3g19580	1398	P	300	P	-4.7	Zinc finger protein.
At1g44830	1564	P	351	P	-4.5	Transcription factor.
At5g66070	910	P	205	P	-4.4	Putative protein.
At5g04340	2724	P	622	P	-4.4	Putative c2h2 zinc finger transcription factor
At1g66090	1286	P	298	P	-4.3	Disease resistance protein similar to RPP1-WsA.
At3g12830	1645	P	393	P	-4.2	Unknown protein similar to auxin-induced protein.
At5g47230	946	P	230	P	-4.1	Ethylene responsive element binding factor 5.
At4g17490	849	P	206	P	-4.1	Ethylene responsive element binding factor.
At4g13340	2941	P	714	P	-4.1	Extensin-like protein.
At5g64310	4228	P	1072	P	-3.9	Arabinogalactan-protein.
At2g41010	1456	P	369	P	-3.9	Unknown protein.
At1g77640	1329	P	340	P	-3.9	Hypothetical protein.
At4g33920	1081	P	278	P	-3.9	Putative protein phosphatase Wip1.
At1g23710	1151	P	300	P	-3.8	Unknown protein.
At1g01560	1064	P	277	P	-3.8	Putative MAP kinase.
At2g22500	4371	P	1172	P	-3.7	Putative mitochondrial dicarboxylate carrier protein.
At1g30970	775	P	208	P	-3.7	Putative zinc finger protein.
At1g66400	862	P	234	P	-3.7	Calmodulin-related protein.
At5g41080	993	P	270	P	-3.7	Putative protein.
At3g52400	3745	P	1021	P	-3.7	Syntaxin-like protein synt4.
At1g34310	5331	P	1457	P	-3.7	Auxin response factor 1.
At1g25400	1902	P	523	P	-3.6	Unknown protein.
At4g32020	5188	P	1450	P	-3.6	Putative protein.
At5g62470	744	P	209	P	-3.6	MYB96 transcription factor-like protein.
At5g06320	8302	P	2338	P	-3.6	Harpin-induced protein-like.
At1g22190	2625	P	744	P	-3.5	AP2 domain containing protein RAP2.
At1g05575	1227	P	349	P	-3.5	Expressed protein.
At4g24380	1070	P	308	P	-3.5	Putative protein dihydrofolate reductase.
At1g76600	3804	P	1135	P	-3.4	Unknown protein.
At5g64660	711	P	217	P	-3.3	Putative protein.
At1g10340	2477	P	756	P	-3.3	Hypothetical protein.
At4g19420	4243	P	1302	P	-3.3	Putative pectinacetylesterase precursor.
At3g54810	2021	P	621	P	-3.3	Putative protein GATA transcription factor 3.
At1g08900	923	P	284	P	-3.3	Putative sugar transport protein.
At3g01830	1212	P	373	P	-3.3	Similar to calmodulin.

At4g22470	814	P	252	P	-3.2	Extensin - like protein.
At5g24590	980	P	307	P	-3.2	NAC2-like protein.
At1g57990	5399	P	1696	P	-3.2	Unknown protein.
At4g01250	1141	P	358	P	-3.2	Putative DNA-binding protein.
At2g40140	2781	P	874	P	-3.2	Putative CCCH-type zinc finger protein.
At5g05410	669	P	216	P	-3.1	DREB2A.
At3g50060	1923	P	629	P	-3.1	R2R3-MYB transcription factor.
At3g55980	4053	P	1326	P	-3.1	Putative zinc finger transcription factor (PEI1).
At3g01130	793	P	264	P	-3.0	Unknown protein.
At2g46620	1013	P	337	P	-3.0	Hypothetical protein.
At1g19250	640	P	214	P	-3.0	Similar to dimethylaniline monooxygenase.
At1g35710	2394	P	802	P	-3.0	Protein kinase.

Table 3.6.c. Genes up-regulated in iron-deficient shoots of the bHLH101 T-DNA line as compared to WT iron-deficient shoots.

	WT shoots -Fe		**bHLH101 T-DNA shoots -Fe**		**Fold[4] increase in bHLH101 T-DNA**	
AGI[1]	**Signal[2]**	**Call[3]**	**Signal[2]**	**Call[3]**		**Annotation summary[5]**
At1g15270	455	P	3125	P	6.9	Unknown protein.
At3g56980	213	P	1210	P	5.7	bHLH039.
At5g50335	286	P	1332	P	4.7	Expressed protein.
At3g45930	289	P	1121	P	3.9	Histone H4 - like protein.
At3g25760	1024	P	3962	P	3.9	Hypothetical protein.
At2g43550	341	P	1275	P	3.7	Putative trypsin inhibitor.
At4g16146	312	P	1163	P	3.7	Expressed protein.
At2g46100	680	P	2481	P	3.7	Unknown protein.
At5g15960	1822	P	6621	P	3.6	Cold and ABA inducible protein kin1.
At3g06680	747	P	2664	P	3.6	Ribosomal protein L29.
At5g10400	254	P	894	P	3.5	Histone H3 - like protein.
At3g02790	419	P	1442	P	3.4	Unknown protein.
At3g50900	201	P	685	P	3.4	Hypothetical protein.
At1g29500	393	P	1329	P	3.4	Auxin-induced protein.
At3g06700	1153	P	3838	P	3.3	Ribosomal protein L29.
At5g01870	475	P	1526	P	3.2	Lipid-transfer protein.
At3g10840	208	P	657	P	3.2	Putative alpha/beta hydrolase.
At2g21210	673	P	2121	P	3.2	Putative auxin-regulated protein.
At5g39210	397	P	1222	P	3.1	Hypothetical protein.
At4g30650	421	P	1290	P	3.1	Low temperature and salt responsive protein.
At3g63160	1551	P	4743	P	3.1	Outer envelope chloroplast membrane protein.
At4g26530	1490	P	4554	P	3.1	Fructose-bisphosphate aldolase.
At3g05730	4220	P	12849	P	3.0	Unknown protein.
At4g14320	2247	P	6774	P	3.0	Ribosomal protein.
At2g34860	1775	P	5289	P	3.0	Unknown protein.
At4g30330	223	P	664	P	3.0	Small nuclear ribonucleoprotein homolog.

Table 3.6.d. Genes down-regulated in iron-deficient shoots of the bHLH101 T-DNA line as compared to WT iron-deficient shoots.

	WT shoots -Fe		bHLH101 T-DNA shoots -Fe		Fold[4] decrease in bHLH101 T-DNA	
AGI[1]	Signal[2]	Call[3]	Signal[2]	Call[3]		Annotation summary[5]
At4g29780	5308	P	254	P	-20.9	Hypothetical protein.
At1g21310	3975	P	271	P	-14.7	Hypothetical protein.
At4g24570	7263	P	538	P	-13.5	Putative mitochondrial uncoupling protein.
At1g73540	4227	P	326	P	-13.0	Unknown protein.
At3g44260	3904	P	326	P	-12.0	CCR4-associated factor 1-like protein.
At5g59820	2889	P	249	P	-11.6	Zinc finger protein Zat12.
At5g22250	2537	P	247	P	-10.3	CCR4-associated factor-like protein.
At3g61190	1564	P	211	P	-7.4	Putative protein.
At2g27080	2340	P	322	P	-7.3	Unknown protein.
At4g11280	2507	P	348	P	-7.2	ACC synthase (AtACS-6).
At3g04640	5100	P	728	P	-7.0	Hypothetical protein.
At5g45340	2344	P	339	P	-6.9	Cytochrome P450.
At3g48650	1490	P	220	P	-6.8	Hypothetical protein.
At1g27730	8758	P	1300	P	-6.7	Salt-tolerance zinc finger protein.
At1g34310	6500	P	972	P	-6.7	Auxin response factor 1.
At5g51190	1307	P	203	P	-6.4	Similar to ethylene responsive binding factor.
At1g28370	2039	P	322	P	-6.3	Similar to ethylene responsive binding factor.
At1g74450	3702	P	627	P	-5.9	Unknown protein.
At2g46400	2767	P	485	P	-5.7	Putative WRKY-type DNA binding protein.
At1g61890	1781	P	328	P	-5.4	Hypothetical protein.
At1g18740	3727	P	692	P	-5.4	Unknown protein.
At2g25250	2425	P	456	P	-5.3	Unknown protein.
At1g15010	1938	P	370	P	-5.2	Hypothetical protein.
At1g35210	1021	P	201	P	-5.1	Hypothetical protein.
At3g28340	1528	P	302	P	-5.1	Unknown protein.
At2g22500	4323	P	873	P	-5.0	Putative mitochondrial dicarboxylate carrier protein.
At3g10930	1780	P	367	P	-4.9	Hypothetical protein.
At5g59550	3876	P	802	P	-4.8	Putative protein similar to COPT1.
At4g32020	5445	P	1128	P	-4.8	Putative protein.
At1g66090	1156	P	241	P	-4.8	Disease resistance protein.
At1g80840	4633	P	968	P	-4.8	Putative transcription factor similar to WRKY.
At5g66070	1079	P	227	P	-4.7	Putative protein.
At1g57990	5514	P	1179	P	-4.7	Unknown protein.
At1g30970	924	P	205	P	-4.5	Putative zinc finger protein.
At5g04340	2279	P	515	P	-4.4	Putative c2h2 zinc finger transcription factor.
At1g77640	1330	P	308	P	-4.3	Hypothetical protein.
At3g12830	1610	P	381	P	-4.2	Unknown protein.
At3g46620	4195	P	999	P	-4.2	Putative protein.
At4g33920	1187	P	287	P	-4.1	Putative protein phosphatase Wip1.
At5g64310	4412	P	1091	P	-4.0	Arabinogalactan-protein.
At3g55980	4062	P	1023	P	-4.0	Putative zinc finger transcription factor (PEI1).
At1g63890	1035	P	261	P	-4.0	Unknown protein.
At3g19580	1225	P	310	P	-4.0	Zinc finger protein.
At2g41640	1063	P	270	P	-3.9	Unknown protein.
At1g57760	794	P	202	P	-3.9	Hypothetical protein.

At5g06320	9890	P	2560	P	-3.9	Harpin-induced protein-like.
At2g33580	865	P	226	P	-3.8	Putative protein kinase.
At5g24590	1136	P	298	P	-3.8	NAC2-like protein
At4g39670	804	P	213	P	-3.8	Putative protein.
At3g50930	1363	P	361	P	-3.8	Mitochondrial ubiquinol-cytochrome c complex.
At3g54810	2322	P	619	P	-3.8	Putative protein GATA transcription factor 3.
At4g01950	1222	P	327	P	-3.7	Predicted protein.
At2g41010	1535	P	412	P	-3.7	Unknown protein.
At3g10760	883	P	240	P	-3.7	Unknown protein.
At3g52400	3642	P	1002	P	-3.6	Syntaxin-like protein synt4.
At1g05575	1066	P	294	P	-3.6	Expressed protein.
At4g13340	3232	P	909	P	-3.6	Extensin-like protein.
At4g34150	6341	P	1790	P	-3.5	Putative hydroxyproline-rich glycoprotein.
At2g45220	905	P	259	P	-3.5	Putative pectinesterase.
At2g24850	1516	P	435	P	-3.5	Putative tyrosine aminotransferase.
At1g73805	710	P	204	P	-3.5	Putative calmodulin-binding protein.
At1g19180	2511	P	726	P	-3.5	Unknown protein.
At5g62470	782	P	228	P	-3.4	MYB96 transcription factor-like protein.
At4g18020	891	P	265	P	-3.4	Putative protein.
At4g19420	4564	P	1357	P	-3.4	Putative pectinacetylesterase precursor.
At5g01460	1138	P	341	P	-3.3	Putative protein.
At2g38470	3239	P	975	P	-3.3	Putative WRKY-type DNA binding protein.
At2g40140	2891	P	872	P	-3.3	Putative CCCH-type zinc finger protein.
At5g49280	1176	P	355	P	-3.3	Unknown protein.
At3g63460	810	P	247	P	-3.3	Putative protein.
At4g24380	913	P	290	P	-3.1	Putative protein dihydrofolate reductase.
At3g10300	1048	P	335	P	-3.1	Unknown protein.
At5g64660	691	P	223	P	-3.1	Putative protein.
At5g26920	1522	P	495	P	-3.1	Calmodulin-binding - like.
At5g62000	1435	P	467	P	-3.1	Auxin response factor - like.
At4g40050	615	P	201	P	-3.1	Hypothetical protein.
At1g69450	671	P	220	P	-3.1	Unknown protein.
At1g24190	758	P	255	P	-3.0	Hypothetical protein.
At5g61600	3598	P	1212	P	-3.0	DNA binding protein - like EREBP-4.
At5g26030	2153	P	728	P	-3.0	Ferrochelatase-I.

Table 3.6.e. Genes up-regulated in iron-sufficient roots of the bHLH101 T-DNA line as compared to WT iron-sufficient roots.

	WT roots +Fe		**bHLH101 T-DNA roots +Fe**		**Fold[4] increase in bHLH101 T-DNA**	
AGI[1]	**Signal[2]**	**Call[3]**	**Signal[2]**	**Call[3]**		**Annotation summary[5]**
At3g22840	211	P	1056	P	5.0	Early light-induced protein.
At5g10130	475	P	2332	P	4.9	Pollen allergen.
At5g10400	244	P	1194	P	4.9	Histone H3 - like protein.
At2g33790	277	P	1278	P	4.6	Putative proline-rich protein.
At4g10270	444	P	1935	P	4.4	Probable wound-induced protein.
At3g50900	211	P	880	P	4.2	Hypothetical protein.
At3g06680	1121	P	4577	P	4.1	Ribosomal protein L29.
At3g06700	2177	P	8830	P	4.1	Ribosomal protein L29.

At2g05510	1432	P	5710	P	4.0	Putative glycine-rich protein.
At3g07050	302	P	1202	P	4.0	Putative GTPase.
At3g11120	1684	P	6619	P	3.9	Ribosomal protein L41.
At3g49100	238	P	936	P	3.9	Signal recognition particle subunit 9.
At5g62340	778	P	3042	P	3.9	Putative protein.
At2g39390	1049	P	3841	P	3.7	60S ribosomal protein.
At1g15270	1077	P	3929	P	3.6	Unknown protein.
At3g62810	315	P	1129	P	3.6	Hypothetical protein.
At2g35190	208	P	728	P	3.5	Unknown protein.
At4g23700	571	P	1998	P	3.5	Putative Na+/H+-exchanging protein.
At3g55120	365	P	1274	P	3.5	Chalcone isomerase.
At5g59910	1276	P	4404	P	3.5	Histone H2B - like protein.
At5g62440	261	P	898	P	3.4	Putative protein.
At3g25940	229	P	786	P	3.4	Hypothetical protein.
At4g30330	287	P	986	P	3.4	Small nuclear ribonucleoprotein homolog.
At1g57590	201	P	689	P	3.4	Pectinacetylesterase precursor.
At5g49210	313	P	1068	P	3.4	Unknown protein.
At4g14320	3103	P	10488	P	3.4	Ribosomal protein.
At1g17180	448	P	1505	P	3.4	Putative glutathione transferase.
At5g67510	1481	P	4929	P	3.3	60S ribosomal protein L26.
At2g29530	870	P	2886	P	3.3	Unknown protein.
At3g10610	1156	P	3793	P	3.3	Putative 40S ribosomal protein S17.
At3g45930	672	P	2173	P	3.2	Histone H4 - like protein.
At2g18140	435	P	1402	P	3.2	Putative peroxidase.
At1g74500	498	P	1600	P	3.2	Putative DNA-binding protein.
At5g48240	321	P	1029	P	3.2	Unknown protein.
At4g29520	289	P	920	P	3.2	Putative protein.
At4g10750	277	P	874	P	3.2	Putative aldolase.
At5g55915	245	P	771	P	3.1	Nucleolar protein-like.
At2g20515	494	P	1541	P	3.1	Expressed protein.
At1g09690	4262	P	13229	P	3.1	Putative 60S ribosomal protein L21.
At3g05000	319	P	989	P	3.1	Unknown protein.
At2g25210	2010	P	6162	P	3.1	60S ribosomal protein L39
At1g29250	1650	P	5051	P	3.1	Unknown protein.
At2g28740	303	P	923	P	3.1	Histone H4.
At1g08780	344	P	1044	P	3.0	Unknown protein.
At2g45860	203	P	615	P	3.0	Hypothetical protein.
At3g17160	450	P	1364	P	3.0	Unknown protein.
At5g52370	323	P	972	P	3.0	Unknown protein.

Table 3.6.f. Genes down-regulated in iron-sufficient roots of the bHLH101 T-DNA line as compared to WT iron-sufficient roots.

	WT roots +Fe		bHLH101 T-DNA roots +Fe		Fold[4] decrease in bHLH101 T-DNA	
AGI[1]	Signal[2]	Call[3]	Signal[2]	Call[3]		Annotation summary[5]
At4g24570	4526	P	233	P	-19.5	Mitochondrial uncoupling protein.
At1g27730	7045	P	519	P	-13.6	Salt-tolerance zinc finger protein.
At4g27652	4334	P	336	P	-12.9	Expressed protein.
At1g73540	2843	P	226	P	-12.6	Unknown protein.
At5g51190	2542	P	219	P	-11.6	Putative protein.
At4g11280	3223	P	318	P	-10.1	ACC synthase (AtACS-6).
At1g74450	2274	P	255	P	-8.9	Unknown protein.
At2g26530	2531	P	307	P	-8.2	AR781, similar to yeast pheromone receptor.
At5g57560	3565	P	440	P	-8.1	TCH4 protein.
At2g30020	2277	P	317	P	-7.2	Putative protein phosphatase 2C.
At5g59820	3804	P	538	P	-7.1	Zinc finger protein Zat12.
At3g55980	3439	P	525	P	-6.6	Putative zinc finger transcription factor (PEI1).
At4g27280	6067	P	928	P	-6.5	Putative protein centrin.
At4g22710	2346	P	363	P	-6.5	Cytochrome P450.
At3g04640	2527	P	409	P	-6.2	Hypothetical protein.
At1g18740	3135	P	511	P	-6.1	Unknown protein.
At2g27080	3368	P	561	P	-6.0	Unknown protein.
At2g41010	2283	P	388	P	-5.9	Unknown protein.
At3g28340	1181	P	208	P	-5.7	Unknown protein.
At4g17490	1433	P	260	P	-5.5	Ethylene responsive binding factor (AtERF6).
At4g08410	2783	P	507	P	-5.5	Extensin-like hydroxyproline-rich glycoprotein.
At5g06320	4715	P	890	P	-5.3	Harpin-induced protein-like.
At1g21310	8654	P	1637	P	-5.3	Hypothetical protein.
At1g19180	4535	P	859	P	-5.3	Unknown protein.
At5g66070	1339	P	265	P	-5.1	Putative protein.
At5g06640	5816	P	1158	P	-5.0	Putative protein.
At3g25780	1469	P	299	P	-4.9	Unknown protein.
At3g54580	3857	P	785	P	-4.9	Extensin precursor .
At3g22800	1464	P	303	P	-4.8	Hypothetical protein.
At5g11070	1657	P	349	P	-4.7	Putative protein.
At5g61600	4891	P	1052	P	-4.6	DNA binding protein.
At1g25400	1291	P	282	P	-4.6	Unknown protein.
At1g57990	1807	P	396	P	-4.6	Unknown protein.
At4g34150	2543	P	557	P	-4.6	Putative hydroxyproline-rich glycoprotein.
At1g05575	1948	P	440	P	-4.4	Expressed protein.
At5g59550	2871	P	657	P	-4.4	Putative protein COP1.
At1g10970	1388	P	326	P	-4.3	Putative zinc transporter ZIP4.
At2g41640	1464	P	354	P	-4.1	Unknown protein.
At5g35735	2512	P	613	P	-4.1	Expressed protein.
At2g36220	1209	P	295	P	-4.1	Unknown protein.
At5g43360	909	P	223	P	-4.1	Inorganic phosphate transporter.
At3g62260	981	P	241	P	-4.1	Putative phosphoprotein phosphatase.
At2g38470	2261	P	563	P	-4.0	Putative WRKY-type DNA binding protein.
At1g19380	1919	P	486	P	-3.9	Hypothetical protein.
At3g48520	1645	P	419	P	-3.9	Cytochrome P450-like protein.

At1g26250	6573	P	1673	P	-3.9	Unknown protein.
At3g52400	3234	P	826	P	-3.9	Syntaxin-like protein synt4.
At1g20380	1351	P	351	P	-3.8	Prolyl endopeptidase.
At3g16720	1024	P	272	P	-3.8	Putative RING zinc finger protein.
At1g21910	1076	P	287	P	-3.7	TINY-like protein.
At4g17500	1774	P	476	P	-3.7	Ethylene responsive element binding factor 1.
At1g66400	1167	P	315	P	-3.7	Calmodulin-related protein.
At3g60550	871	P	237	P	-3.7	Regulatory protein.
At2g42760	1911	P	520	P	-3.7	Unknown protein.
At1g30370	1751	P	479	P	-3.7	Putative lipase.
At5g45340	3016	P	841	P	-3.6	Cytochrome P450.
At5g50400	3315	P	925	P	-3.6	Putative protein.
At5g06630	5661	P	1586	P	-3.6	Putative protein.
At3g23400	1124	P	318	P	-3.5	Unknown protein.
At1g66180	3141	P	898	P	-3.5	Unknown protein.
At5g19890	3324	P	962	P	-3.5	Peroxidase ATP N.
At2g18210	1016	P	295	P	-3.4	Unknown protein.
At3g56400	825	P	245	P	-3.4	DNA-binding protein WRKY4.
At4g26750	788	P	235	P	-3.4	Putative protein extensin precursor.
At3g61850	1108	P	331	P	-3.3	Transcription factor BBFa.
At5g37770	1480	P	442	P	-3.3	Calmodulin-related protein 2.
At3g62720	1594	P	482	P	-3.3	Alpha galactosyltransferase-like protein.
At2g40000	2917	P	885	P	-3.3	Putative nematode-resistance protein.
At4g25390	887	P	270	P	-3.3	Receptor kinase-like protein RLK3.
At1g19770	5271	P	1607	P	-3.3	Unknown protein.
At2g16660	2368	P	725	P	-3.3	Nodulin-like protein.
At4g25810	1024	P	317	P	-3.2	Xyloglucan endo-1,4-beta-D-glucanase (XTR-6).
At3g59100	689	P	215	P	-3.2	Putative callose synthase catalytic subunit (CFL1).
At4g33920	1122	P	351	P	-3.2	Putative protein phosphatase Wip1.
At1g23850	1293	P	406	P	-3.2	Unknown protein.
At5g59490	717	P	225	P	-3.2	Putative ripening-related protein.
At3g52450	1619	P	510	P	-3.2	Putative protein arm repeat.
At2g35930	2156	P	681	P	-3.2	Unknown protein.
At1g49570	2873	P	909	P	-3.2	Putative peroxidase.
At1g23710	821	P	262	P	-3.1	Unknown protein.
At2g25250	1826	P	583	P	-3.1	Unknown protein.
At4g25100	5141	P	1648	P	-3.1	Superoxide dismutase.
At5g14540	1544	P	495	P	-3.1	Putative proline-rich protein M14 precursor.
At1g20510	1139	P	369	P	-3.1	Hypothetical protein.
At5g47230	1410	P	458	P	-3.1	Ethylene responsive element factor 5 (ATERF5).
At5g23840	986	P	321	P	-3.1	Putative protein.
At3g22120	785	P	257	P	-3.1	Unknown protein.
At5g64660	696	P	229	P	-3.0	Putative protein.
At5g35100	945	P	312	P	-3.0	Putative protein.
At3g25250	614	P	203	P	-3.0	Protein kinase.

Table 3.6.g. Genes up-regulated in iron-deficient roots of the bHLH101 T-DNA line as compared to WT iron-deficient roots.

	WT roots -Fe		bHLH101 T-DNA roots -Fe		Fold[4] increase in bHLH101 T-DNA	
AGI[1]	Signal[2]	Call[3]	Signal[2]	Call[3]		Annotation summary[5]
At4g31940	238	P	2247	P	9.5	Cytochrome P450-like protein.
At2g33790	251	P	1515	P	6.0	Putative proline-rich protein.
At3g22840	245	P	1345	P	5.5	Early light-induced protein.
At3g11120	1251	P	6371	P	5.1	Ribosomal protein L41.
At1g73120	327	P	1616	P	4.9	Hypothetical protein.
At3g45930	422	P	2006	P	4.7	Histone H4 - like protein.
At3g06700	1829	P	8621	P	4.7	Ribosomal protein L29.
At3g06680	1103	P	5069	P	4.6	Ribosomal protein L29.
At2g39390	871	P	3728	P	4.3	60S ribosomal protein L35.
At5g10130	310	P	1308	P	4.2	Pollen allergen -like protein.
At4g29520	242	P	993	P	4.1	Putative protein.
At1g15270	927	P	3706	P	4.0	Unknown protein.
At4g30330	249	P	959	P	3.9	Small nuclear ribonucleoprotein homolog.
At2g21580	1003	P	3867	P	3.9	40S ribosomal protein S25.
At1g64750	363	P	1360	P	3.8	Unknown protein.
At2g25210	1601	P	5897	P	3.7	60S ribosomal protein L39
At5g59910	1202	P	4413	P	3.7	Histone H2B - like protein.
At1g12080	1279	P	4678	P	3.7	Unknown protein.
At3g15357	241	P	882	P	3.7	Expressed protein.
At3g10610	1075	P	3874	P	3.6	Putative 40S ribosomal protein S17.
At1g29250	1521	P	5331	P	3.5	Unknown protein.
At4g26230	1674	P	5790	P	3.5	Putative ribosomal protein.
At5g15960	753	P	2561	P	3.4	Cold and ABA inducible protein kin1.
At2g44860	768	P	2602	P	3.4	60S ribosomal protein L30.
At5g60670	2235	P	7539	P	3.4	60S ribosomal protein L12.
At5g25460	586	P	1944	P	3.3	Putative protein.
At2g07350	420	P	1393	P	3.3	Hypothetical protein.
At2g29530	850	P	2817	P	3.3	Unknown protein.
At2g20515	402	P	1328	P	3.3	Expressed protein.
At2g41650	370	P	1220	P	3.3	Unknown protein.
At3g24500	256	P	842	P	3.3	Ethylene-responsive transcriptional coactivator.
At3g62810	395	P	1284	P	3.3	Hypothetical protein.
At3g46560	798	P	2586	P	3.2	Small zinc finger-like protein TIM9.
At2g31410	465	P	1502	P	3.2	Unknown protein.
At4g29160	254	P	816	P	3.2	Putative protein.
At3g05000	351	P	1123	P	3.2	Unknown protein.
At2g40590	1665	P	5272	P	3.2	40S ribosomal protein S26.
At4g07950	657	P	2073	P	3.2	Putative DNA-directed RNA polymerase subunit.
At5g05270	610	P	1920	P	3.1	Similar to chalcone-flavonone isomerase.
At2g39960	488	P	1533	P	3.1	Unknown protein.
At5g61310	341	P	1070	P	3.1	Cytochrome c oxidase subunit.
At2g38810	267	P	835	P	3.1	Histone H2A.
At5g43970	627	P	1959	P	3.1	Putative protein.
At5g62340	923	P	2874	P	3.1	Putative protein.
At3g27360	259	P	802	P	3.1	Histone H3.

At5g49210	348	P	1072	P	3.1	Unknown protein.
At4g10750	262	P	807	P	3.1	Putative aldolase.
At2g18400	589	P	1812	P	3.1	Putative protein.
At3g10090	1211	P	3716	P	3.1	Putative ribosomal protein S28.
At4g13050	232	P	711	P	3.1	Hydrolase-like protein.
At5g44710	541	P	1635	P	3.0	Putative protein.
At3g62840	989	P	2986	P	3.0	Small nuclear ribonucleoprotein chain D2.
At1g64880	512	P	1539	P	3.0	Similar 30S ribosomal protein S5.
At1g07070	564	P	1685	P	3.0	Ribosomal protein.
At4g15000	2924	P	8716	P	3.0	Ribosomal protein.
At5g02050	490	P	1452	P	3.0	Putative protein gene product of suAprgA1.
At1g23410	441	P	1306	P	3.0	Ubiquitin extension protein.
At1g23720	4110	P	12142	P	3.0	Putative 60S ribosomal protein L21.

Table 3.6.h. Genes down-regulated in iron-deficient roots of the bHLH101 T-DNA line as compared to WT iron-deficient roots.

	WT roots -Fe		**bHLH101 T-DNA roots -Fe**		**Fold[4] decrease in bHLH101 T-DNA**	
AGI[1]	**Signal[2]**	**Call[3]**	**Signal[2]**	**Call[3]**		**Annotation summary[5]**
At4g27652	4413	P	231	P	-19.1	Expressed protein.
At4g29780	4329	P	270	P	-16.0	Hypothetical protein.
At1g27730	7422	P	574	P	-12.9	Salt-tolerance zinc finger protein.
At1g73540	3225	P	277	P	-11.7	Unknown protein.
At4g11280	2866	P	259	P	-11.1	ACC synthase (AtACS-6).
At4g08410	3407	P	328	P	-10.4	Extensin-like protein.
At4g13340	2189	P	216	P	-10.1	Extensin-like protein.
At3g48520	2080	P	243	P	-8.6	Cytochrome P450-like protein.
At5g57560	3165	P	398	P	-8.0	TCH4 protein.
At1g74450	2213	P	280	P	-7.9	Unknown protein.
At1g76650	1590	P	201	P	-7.9	Putative calmodulin.
At2g26530	2647	P	342	P	-7.7	Similar to yeast pheromone receptor.
At1g18740	3492	P	455	P	-7.7	Unknown protein.
At5g59820	3823	P	540	P	-7.1	Zinc finger protein Zat12.
At1g28480	1418	P	214	P	-6.6	Glutaredoxin.
At1g21310	10104	P	1553	P	-6.5	Hypothetical protein.
At3g54580	4559	P	716	P	-6.4	Extensin precursor -like protein.
At2g30020	1749	P	280	P	-6.3	Putative protein phosphatase 2C.
At3g04640	2504	P	413	P	-6.1	Hypothetical protein.
At3g55980	3194	P	530	P	-6.0	Putative zinc finger transcription factor (PEI1).
At4g27280	5964	P	992	P	-6.0	Putative protein centrin.
At1g49570	4116	P	685	P	-6.0	Peroxidase.
At5g06630	7410	P	1283	P	-5.8	Putative protein.
At1g26250	7557	P	1313	P	-5.8	Unknown protein.
At5g06640	6445	P	1143	P	-5.6	Putative protein.
At1g57990	2317	P	426	P	-5.4	Unknown protein.
At5g66070	1428	P	263	P	-5.4	Putative protein.
At1g21910	1098	P	203	P	-5.4	TINY-like protein.
At3g28340	1104	P	204	P	-5.4	Unknown protein.

At3g62260	1251	P	232	P	-5.4	Putative protein phosphoprotein phosphatase.
At2g43150	1451	P	270	P	-5.4	Putative extensin.
At2g27080	3380	P	636	P	-5.3	Unknown protein.
At5g65300	1205	P	229	P	-5.3	Unknown protein.
At5g11070	1861	P	358	P	-5.2	Putative protein.
At2g38470	2607	P	532	P	-4.9	Putative WRKY-type DNA binding protein.
At2g41640	1466	P	299	P	-4.9	Unknown protein.
At5g62340	1723	P	361	P	-4.8	Putative protein.
At2g41010	1498	P	320	P	-4.7	Unknown protein.
At5g59550	3307	P	726	P	-4.6	Putative protein COP1.
At3g23400	1260	P	277	P	-4.5	Unknown protein.
At5g35735	2575	P	567	P	-4.5	Expressed protein.
At2g25250	1989	P	443	P	-4.5	Unknown protein.
At4g22710	2009	P	449	P	-4.5	Cytochrome P450.
At5g19890	4564	P	1049	P	-4.4	Peroxidase ATP N.
At3g62720	1640	P	378	P	-4.3	Alpha galactosyltransferase-like protein.
At4g34150	2706	P	627	P	-4.3	Putative hydroxyproline-rich glycoprotein.
At2g36220	1413	P	329	P	-4.3	Unknown protein.
At1g25400	1011	P	241	P	-4.2	Unknown protein.
At5g42650	1094	P	267	P	-4.1	Allene oxide synthase.
At4g17490	1537	P	378	P	-4.1	Ethylene responsive element (AtERF6).
At1g28380	1387	P	347	P	-4.0	Unknown protein.
At5g61600	4531	P	1139	P	-4.0	DNA binding protein.
At1g12040	869	P	220	P	-4.0	Putative extensin.
At2g18210	1383	P	351	P	-3.9	Unknown protein.
At5g04730	1665	P	428	P	-3.9	Putative protein.
At1g10340	850	P	221	P	-3.9	Hypothetical protein.
At1g19180	5420	P	1408	P	-3.9	Unknown protein.
At1g19770	5434	P	1423	P	-3.8	Unknown protein.
At3g25780	1408	P	372	P	-3.8	Unknown protein.
At2g22500	2512	P	664	P	-3.8	Putative mitochondrial dicarboxylate carrier.
At1g10970	906	P	240	P	-3.8	Putative zinc transporter ZIP4.
At5g04340	2828	P	779	P	-3.6	Putative c2h2 zinc finger transcription factor.
At1g61890	2690	P	742	P	-3.6	Hypothetical protein.
At5g37770	1503	P	416	P	-3.6	Calmodulin-related protein.
At1g20510	1413	P	392	P	-3.6	Hypothetical protein.
At1g66400	986	P	274	P	-3.6	Calmodulin-related protein.
At5g43360	829	P	231	P	-3.6	Inorganic phosphate transporter.
At2g42760	2083	P	581	P	-3.6	Unknown protein.
At5g13200	1050	P	295	P	-3.6	ABA-responsive protein.
At4g17500	1668	P	472	P	-3.5	Ethylene responsive element binding factor 1.
At4g33920	1270	P	360	P	-3.5	Putative protein phosphatase Wip1.
At5g06320	5269	P	1495	P	-3.5	Harpin-induced protein.
At3g16720	899	P	255	P	-3.5	Putative RING zinc finger protein.
At1g23720	6762	P	1921	P	-3.5	Unknown protein.
At1g05575	1758	P	506	P	-3.5	Expressed protein.
At4g24380	1643	P	475	P	-3.5	Putative protein dihydrofolate reductase.
At2g33770	1349	P	395	P	-3.4	Ubiquitin-conjugating enzyme E2.
At3g52710	789	P	235	P	-3.4	Hypothetical protein.
At1g27100	2095	P	628	P	-3.3	Unknown protein.

At2g24980	7683	P	2330	P	-3.3	Unknown protein.
At3g54200	2329	P	709	P	-3.3	Putative hin1 protein.
At5g35100	943	P	288	P	-3.3	Putative protein.
At1g76600	1748	P	547	P	-3.2	Unknown protein.
At5g50400	3050	P	970	P	-3.1	Putative protein.
At5g24590	1219	P	388	P	-3.1	NAC2-like protein
At3g54590	9211	P	2948	P	-3.1	Extensin precursor.
At1g23710	1046	P	336	P	-3.1	Unknown protein.
At4g34950	1146	P	369	P	-3.1	Putative protein.
At1g21830	734	P	239	P	-3.1	Unknown protein.
At3g60550	737	P	241	P	-3.1	Regulatory protein.
At4g33020	680	P	223	P	-3.1	ZIP9.
At2g40000	3549	P	1168	P	-3.0	Putative nematode-resistance protein.
At2g38120	3013	P	995	P	-3.0	Unknown protein.
At5g35940	796	P	263	P	-3.0	Similar to jasmonate inducible protein.
At1g72450	1190	P	394	P	-3.0	Unknown protein.
At5g45340	2470	P	821	P	-3.0	Cytochrome P450.
At1g30370	1591	P	529	P	-3.0	Lipase.
At5g44350	608	P	202	P	-3.0	Ethylene-regulated nuclear protein ERT2.
At1g20823	1113	P	372	P	-3.0	Putative protein.
At2g25735	751	P	252	P	-3.0	Expressed protein.
At3g52450	1483	P	498	P	-3.0	Putative protein ARC1.
At5g12880	2256	P	760	P	-3.0	Putative hydroxyproline-rich glycoprotein.
At1g76410	923	P	311	P	-3.0	Putative RING zinc finger protein.
At1g57760	669	P	226	P	-3.0	Hypothetical protein.
At2g35930	3120	P	1054	P	-3.0	Unknown protein.
At3g19580	2360	P	798	P	-3.0	Zinc finger protein.
At3g10300	1831	P	621	P	-3.0	Unknown protein.

[1] AGI code as found in TAIR (www.arabidopsis.org).
[2] Fluorescent signal given by the probes especific for the gene in the Affymetrix microarray.
[3] (P)resent or (A)bsent. Qualitative interpretation of the signal level. Present indicates that the signal is above the background or noise levels, Absent indicates that the computer cannot differentiate between the signal coming from the probes for a specific gene and the general background or noise in the microarray.
[4] Fold difference in the expression level of a gene as detected by the microarray. WT expression level set to one in up-regulation or bHLH101 set to one in down-regulation.
[5] Annotation summary as found in NetAffx (www.affymetrix.com).

MATERIALS AND METHODS

Gene Names and T-DNA Insertion Lines

Gene At2g41240 is transcription factor *bHLH100*, and its T-DNA insertion line is SALK_074568. Gene At3g56970 is transcription factor *bHLH038*, and its T-DNA insertion line is SALK_020183. Gene At3g56980 is transcription factor *bHLH039*, and its T-DNA insertion line is SALK_025676. Gene At5g04150 is transcription factor *bHLH101* and its T-DNA insertion line is SALK_011245.

GeneChip Microarray Experiment

These experiments were explained in detail in Chapter 2. Briefly, RNA extraction was done by Dr. Elizabeth E. Rogers as a post-doctoral fellow in the lab of Dr. Mary Lou Guerinot at Dartmouth College (Hanover, NH). cRNA preparation, hybridization, and data preparation of the Affymetrix ATH-1 Microarray (Affymetrix Inc., Santa Clara, CA) was done at the DNA Array Core Facility of the University of California–Irvine (Irvine, CA). All data analysis was performed using Excel (Microsoft, Seattle, WA).

Bioinformatics Analysis Tools

Amino acid sequence for the 20 transcription factors was obtained from The Arabidopsis Information Resource (TAIR) website at www.arabidopsis.org. The protein tree alignment was done using the amino acid sequences of 20 TFs and aligned them at

the http://align.genome.jp website from Kyoto University Bioinformatics Center (Kyoto, Japan). The protein alignment analysis to detect similarity of the four transcription factors was done using the ClustalW algorithm from the European Bioinformatics Institute (Cambridge, UK) at www.ebi.ac.uk/clustalw.

Plant growth conditions

Unless otherwise noted all plants were treated as previously described (Yi and Guerinot, 1996). Briefly, plants were surface sterilized, stratified for three days at 4^{o}C in 0.1% agar, planted on Gamborg's B5 media (Phytotechnology Laboratories, Shawnee Mission, KS), and grown in a growth chamber (Percival Scientific, Perry, IA) for 14 days at 22^{o}C under constant light. 14-day old plants were used for experiments or transferred to iron-sufficient or iron-deficient media for three days under constant light at 22^{o}C (Yi and Guerinot, 1996). Iron-deficient plates were supplemented with ferrozine to chelate any possible iron contamination, making it unavailable to the plant. Plates were under yellow plexiglass at all times to inhibit Fe(III)-EDTA photodegradation (Hangarter and Stasinopoulos, 1991).

Plant materials and transformation

Unless otherwise noted, controls (WT) were *Arabidopsis thaliana Columbia gl-1* plants. T-DNA insertion lines (Alonso et al., 2003) were obtained from the Arabidopsis Biological Resources Center (ABRC) at Ohio State University (Columbus, OH). To

identify homozygous T-DNA insertions individual plants were sampled and genomic DNA extracted (Edwards et al., 1991) and used as template for PCR reactions with primers spanning the point of insertion. For plant transformations, we dipped flowering WT plants into a solution containing *Agrobacterium tumefasciens* GV3101 as described (Clough and Bent, 1998).

RNA blots

RNA was extracted from plants using the LiCl method (Verwoerd et al., 1989). For the expression timeline plants were grown as described previously and tissue sampled at 0, 12 hours, 24 hours, 1 day, 2 days, 3 days, and 6 days after transfer to iron-sufficient and iron-deficient medium. Due to the high similarity between the four transcription factors, the primers for the probe were designed to span areas of low similarity. This experiment was done twice, independently. Each time total RNA was aliquoted into four samples. RNA blots were run with each sample, and membranes probed with only one probe but for bHLH101, which had UBQ5 loading control probe as well. This loading control was used for the other blots run with the same aliquots. All blots were used only once. For the other RNA blots, plants were harvested 3 days after being transferred to iron-deficient or iron-sufficient medium. In each case, roots and shoots were harvested separately. Probes for *IRT1* and *FRO2* were prepared as described (Rogers and Guerinot, 2002), *AtFer1* was prepared as described (Petit et al., 2001), and *UBQ5* probe was prepared as described (Rogers and Ausubel, 1997). In all cases, RNA blots were conducted following standard protocols (Sambrook and Russell, 2001), RNA was

transferred onto Osmonics membranes (Westborough, MA), radioactive signals were quantified using a Molecular Dynamics Storm 860 Phosphoroimager (Amersham Biosciences, Piscataway, NJ), and *UBQ5* signals were used as loading controls.

Plant assays

Ferric-chelate reductase activity assays have been described previously (Yi and Guerinot, 1996). Gauntlet assays were done as described at http://thale.biol.wwu.edu. For shoot fresh weight assay plants were grown on B5 plates for a week before transfer to soil and grown at 22^{o}C at 16/8 hours of light/dark for three weeks with six plants for each replication and three experiments for each treatment. When plants were ready, they were decapitated, immediately weighted, and submerged in 20 ml of methanol overnight in sealed containers. The resulting solution was used to quantify chlorophyll as described (Porra et al., 1989).

Elemental analysis

ICP-MS analysis of shoots of the four homozygous T-DNA lines was done by Dr. David Salt as described in (Lahner et al., 2003).

bHLH101 T-DNA microarray

RNA from 14-day old plants was placed for three additional days on iron-sufficient or iron-deficient plates. Roots and shoots from plants grown under either condition were harvested and RNA extracted separately. This procedure was done three times independently. RNA from tissue grown under similar conditions was pooled. cRNA was generated, labeled, and hybridized to four Affymetrix ATH-1 Microarrays at the DNA Core Facility at the University of Missouri-Columbia (Columbia, MO). Datasets were analyzed using Excel (Microsoft, Seattle, WA).

GUS staining

A fragment of DNA containing 2182 bases upstream of the ATG start codon for *bHLH101* and its first 20 bases were amplified by PCR using Pfu polymerase (Stratagene, La Jolla, CA) and primers containing in-frame BglII and EcoRI restriction sites. Vector pCAMBIA1381Xc (CAMBIA, Black Mountain, Australia) and the PCR product were digested using both restriction enzymes. Both linear DNA fragments were ligated in-frame with the GUS open reading frame, creating vector pC-1381-101-GUS. The new vector was inserted into *Agrobacterium tumefasciens* GV3101 which was used to transform *Arabidopsis thaliana* Columbia *gl-1* plants. 13 T_3 single-insertion homozygous lines were selected for staining. Five of the 13 were discarded for having unusual staining patterns, ranging from complete staining of the plant to not being able to stain any tissue. The resulting eight T_3 bHLH101::GUS lines were grown on B5 plates

for 14 days, harvested, and stained; or grown for 14 days and transferred to iron-deficient or iron-sufficient plates for three days and then harvested and stained. Once harvested, plants were immediately submerged in 90% acetone for 1 hour at -20^{o}C. The acetone was replaced with the staining solution [50mM $NaPO_4$, pH7.0; 0.1% Triton X-100; 1mM EDTA; 1mM $K_4Fe(CN)_6$ $3H_2O$; 1mM $K_3Fe(CN)_6$; 0.01% (w/v) chloramphenicol; 0.1% (w/v) X-Gluc] and stored away from the light at 37^{o}C for three days. At the end of the three days, the staining solution was replaced with 70% ethanol twice in a 48 hour period. Pictures were taken using a Leica MZFLIII Stereoscope (Leica Microsystems GmbH, Wetzlar, Gemany) and an Optronics Magnafire digital camera (Optronics, Goleta, CA) at the Molecular Cytology Core Facility of the University of Missouri-Columbia (Columbia, MO).

Over-Expression

pCAMBIA1302 (CAMBIA, Black Mountain, Australia) was used to design the over-expressing construct for bHLH101. This vector contains the CaMV35S promoter driving mGFP5. We replaced mGFP5 with a 1679-base genomic DNA fragment containing the complete sequence of bHLH101 including the three exons, 366 bases upstream of the ATG and 371 bases downstream of the stop codon to assure that possible 5'- and 3'- untranslated regions were present. The genomic DNA fragment was amplified using Pfu polymerase (Strategene, La Jolla, CA) and primers containing BamHI sites. The linearized vector and digested PCR product were ligated to create the new vector pC-OX-101. pC-OX-101 was used to transform *Agrobacterium tumefasciens* GV3101. 14 T_3

independent lines containing a single, homozygous insertion event were screened twice, independently, using RNA blots. Three lines were selected for further experiments. Controls were *Arabidopsis thaliana* Col-0 and *gl-1*.

Gauntlet experiments

The Gauntlet is a set of 44 experiments. We chose 16 that were directly related to environmental conditions since the Affymetrix microarray data showed that most of the genes that changed expression levels under iron-deficiency conditions could be related to environmental stress. The complete list of Gauntlet experiments and their protocols can be found at http://thale.biol.wwu.edu. The sub-set of Gantlet conditions used in this report can be found in Table 3.

ACKNOWLEDGEMENTS

Support for this work came from grants USDA CREES 2002-35100-12331 and MU's Food for the 21st Century to EER. Special thanks to the Interdisciplinary Plant Group at University of Missouri-Columbia for their continuous support to AM. We thank Sandhya Thondapu, Jan Judy-March, Brandon Celaya, Ullas Pedmale, and Yan He for providing technical assistance during different stages of the project. Sandhya Thondapu was supported by the Life Sciences Undergraduate Research Opportunity Program (LSUROP) at MU. Thanks to Timothy Durrett and Dr. Dirk Charlson for critical reading

the manuscript and providing generous feedback. Dr. David Salt (Purdue Universtity) provided the ICP data for elemental content.

REFERENCES

Alonso, J.M., Stepanova, A.N., Leisse, T.J., Kim, C.J., Chen, H., Shinn, P., Stevenson, D.K., Zimmerman, J., Barajas, P., Cheuk, R., Gadrinab, C., Heller, C., Jeske, A., Koesema, E., Meyers, C.C., Parker, H., Prednis, L., Ansari, Y., Choy, N., Deen, H., Geralt, M., Hazari, N., Hom, E., Karnes, M., Mulholland, C., Ndubaku, R., Schmidt, I., Guzman, P., Aguilar-Henonin, L., Schmid, M., Weigel, D., Carter, D.E., Marchand, T., Risseeuw, E., Brogden, D., Zeko, A., Crosby, W.L., Berry, C.C., and Ecker, J.R. (2003). Genome-wide insertional mutagenesis of *Arabidopsis thaliana*. Science **301,** 653-657.

Bailey, P.C., Martin, C., Toledo-Ortiz, G., Quail, P.H., Huq, E., Heim, M.A., Jakoby, M., Werber, M., and Weisshaar, B. (2003). Update on the basic helix-loop-helix transcription factor gene family in *Arabidopsis thaliana*. Plant Cell **15,** 2497-2502.

Brumbarova, T., and Bauer, P. (2005). Iron-mediated control of the basic helix-loop-helix protein FER, a regulator of iron uptake in tomato. Plant Physiology **137,** 1018-1026.

Clough, S.J., and Bent, A.F. (1998). Floral dip: a simplified method for Agrobacterium-mediated transformation of *Arabidopsis thaliana*. Plant Journal **16,** 735-743.

Colangelo, E.P., and Guerinot, M.L. (2004). The essential basic helix-loop-helix protein FIT1 is required for the iron deficiency response. Plant Cell **16,** 3400-3412.

Connolly, E.L., Fett, J.P., and Guerinot, M.L. (2002). Expression of the IRT1 metal transporter is controlled by metals at the levels of transcript and protein accumulation. Plant Cell **14,** 1347-1357.

Connolly, E.L., Campbell, N.H., Grotz, N., Prichard, C.L., and Guerinot, M.L. (2003). Overexpression of the FRO2 ferric chelate reductase confers tolerance to growth on low iron and uncovers posttranscriptional control. Plant Physiology **133,** 1102-1110.

Edwards, K., Johnstone, C., and C., T. (1991). A simple and rapid method for the preparation of plant genomic DNA for PCR analysis. Nucleic Acids Research **19,** 1349.

Foreman, J., Demidchik, V., Bothwell, J.H.F., Mylona, P., Miedema, H., Torres, M.A., Linstead, P., Costa, S., Brownlee, C., Jones, J.D.G., Davies, J.M., and Dolan, L. (2003). Reactive oxygen species produced by NADPH oxidase regulate plant cell growth. Nature **422,** 442-446.

Gong, W., Shen, Y.-P., Ma, L.-G., Pan, Y., Du, Y.-L., Wang, D.-H., Yang, J.-Y., Hu, L.-D., Liu, X.-F., Dong, C.-X., Ma, L., Chen, Y.-H., Yang, X.-Y., Gao, Y., Zhu, D., Tan, X., Mu, J.-Y., Zhang, D.-B., Liu, Y.-L., Dinesh-Kumar, S.P., Li, Y., Wang, X.-P., Gu, H.-Y., Qu, L.-J., Bai, S.-N., Lu, Y.-T., Li, J.-Y., Zhao, J.-D., Zuo, J., Huang, H., Deng, X.W., and Zhu, Y.-X. (2004). Genome-wide ORFeome cloning and analysis of Arabidopsis transcription factor genes. Plant Physiology **135,** 773-782.

Guo, A., He, K., Liu, D., Bai, S., Gu, X., Wei, L., and Luo, J. (2005). DATF: a database of Arabidopsis transcription factors. Bioinformatics **21,** 2568-2569.

Hangarter, R.P., and Stasinopoulos, T.C. (1991). Effect of Fe-catalyzed photooxidation of EDTA on root growth in plant culture media. Plant Physiology **96,** 843-847.

Heim, M.A., Jakoby, M., Werber, M., Martin, C., Weisshaar, B., and Bailey, P.C. (2003). The basic helix-loop-helix transcription factor family in plants: A genome-wide study of protein structure and functional diversity. Molecular Biology and Evolution **20,** 735-747.

Jakoby, M., Wang, H.-Y., Reidt, W., Weisshaar, B., and Bauer, P. (2004). *FRU (BHLH029)* is required for induction of iron mobilization genes in *Arabidopsis thaliana*. FEBS Letters **577,** 528-534.

Kang, H.-G., and Singh, K.B. (2000). Characterization of salicylic acid-responsive, Arabidopsis Dof domain proteins: overexpression of OBP3 leads to growth defects. Plant Journal **21,** 329-339.

Kang, H.-G., Foley, R.C., Onate-Sanchez, L., Lin, C., and Singh, K.B. (2003). Target genes for OBP3, a Dof transcription factor, include novel basic helix-loop-helix domain proteins inducible by salicylic acid. Plant Journal **35,** 362-372.

Lahner, B., Gong, J., Mahmoudian, M., Smith, E.L., Abid, K.B., Rogers, E.E., Guerinot, M.L., Harper, J.F., Ward, J.M., McIntyre, L., Schroeder, J.I., and Salt, D.E. (2003). Genomic scale profiling of nutrient and trace elements in *Arabidopsis thaliana*. Nature Biotechnology **21,** 1215-1221.

Ling, H.-Q., Bauer, P., Bereczky, Z., Keller, B., and Ganal, M. (2002). The tomato *fer* gene encoding a bHLH protein controls iron-uptake responses in roots. Proceedings of the National Academy of Sciences of the United States of America **99,** 13938-13943.

Muessig, C., and Altmann, T. (2003). Changes in gene expression in response to altered SHL transcript levels. Plant Molecular Biology **53,** 805-820.

Mukherjee, I., Campbell, N., Ash, J., and Connolly, E. (2006). Expression profiling of the Arabidopsis ferric chelate reductase (*FRO*) gene family reveals differential regulation by iron and copper. Planta**,** in press.

Pabo, C.O., and Sauer, R.T. (1992). Transcription factors: structural families and principles of DNA recognition. Annual Review of Biochemistry **61,** 1053-1095.

Petit, J.-M., Briat, J.-F., and Lobreaux, S. (2001). Structure and differential expression of the four members of the *Arabidopsis thaliana* ferritin gene family. Biochemical Journal **359,** 575-582.

Porra, R.J., Thompson, W.A., and Kreidmann, P.E. (1989). Determination of accurate extinction coefficients and simultaneous equations for assaying chlorophylls a and b extracted with four different solvents: verification of the concentration of chlorophyll standards by atomic absortion spectroscopy. Biochimica et Biophysica Acta (BBA) **975,** 348-394.

Rentel, M.C., Lecourieux, D., Ouaked, F., Usher, S.L., Petersen, L., Okamoto, H., Knight, H., Peck, S.C., Grierson, C.S., Hirt, H., and Knight, M.R. (2004). OXI1 kinase is necessary for oxidative burst-mediated signaling in Arabidopsis. Nature **427,** 858-861.

Riechmann, J.L., and Ratcliffe, O.J. (2000). A genomic perspective on plant transcription factors. Current Opinion in Plant Biology **3,** 423-434.

Rizhsky, L., Liang, H., and Mittler, R. (2003). The water-water cycle is essential for chloroplast protection in the absence of stress. Journal of Biological Chemistry **278,** 38921-38925.

Rizhsky, L., Davletova, S., Liang, H., and Mittler, R. (2004). The zinc finger protein Zat12 is required for cytosolic ascorbate peroxidase 1 expression during oxidative stress in Arabidopsis. Journal of Biological Chemistry **279,** 11736-11743.

Rogers, E.E., and Ausubel, F.M. (1997). Arabidopsis enhanced disease susceptibility mutants exhibit enhanced susceptibility to several bacterial pathogens and alterations in PR-1 gene expression. Plant Cell **9,** 305-316.

Rogers, E.E., and Guerinot, M.L. (2002). FRD3, a member of the multidrug and toxin efflux family, controls iron deficiency responses in Arabidopsis. Plant Cell **14,** 1787-1799.

Sambrook, J., and Russell, D.W. (2001). Molecular cloning: a laboratory manual. (Cold Spring Harbor, NY: Cold Spring Harbor Laboratory Press).

Schikora, A., and Schmidt, W. (2001). Iron stress-induced changes in root epidermal cell fate are regulated independently from physiological responses to low iron availability. Plant Physiology **125,** 1679-1687.

Schmidt, W. (2003). Iron solutions: acquisition strategies and signaling pathways in plants. Trends in Plant Science **8,** 188-193.

Shiu, S.-H., Shih, M.-C., and Li, W.-H. (2005). Transcription factor families have much higher expansion rates in plants than in animals. Plant Physiology **139,** 18-26.

Stracke, R., Werber, M., and Weisshaar, B. (2001). The R2R3-MYB gene family in *Arabidopsis thaliana*. Current Opinion in Plant Biology **4,** 447-456.

Toledo-Ortiz, G., Huq, E., and Quail, P.H. (2003). The Arabidopsis basic-helix-loop-helix transcription factor family. Plant Cell **15,** 1749-1770.

Vert, G.A., Briat, J.-F., and Curie, C. (2003). Dual regulation of the Arabidopsis high-affinity root iron uptake system by local and long-distance signals. Plant Physiology **132,** 796-804.

Verwoerd, T.C., Dekker, B.M., and Hoekema, A. (1989). A small-scale procedure for the rapid isolation of plant RNAs. Nucleic Acids Research **17,** 2362.

Wolberger, C. (1999). Multiprotein-DNA complexes in transcriptional regulation. Annual Review of Biophysics and Biomolecular Structure **28,** 29-56.

Wray, G.A., Hahn, M.W., Abouheif, E., Balhoff, J.P., Pizer, M., Rockman, M.V., and Romano, L.A. (2003). The evolution of transcriptional regulation in eukaryotes. Molecular Biology and Evolution **20,** 1377-1419.

Wu, H., Li, L., Du, J., Yuan, Y., Cheng, X., and Ling, H.-Q. (2005). Molecular and biochemical characterization of the Fe(III) chelate reductase gene family in *Arabidopsis thaliana*. Plant and Cell Physiology **46,** 1505-1514.

Yi, Y., and Guerinot, M.L. (1996). Genetic evidence that induction of root Fe(III) chelate reductase activity is necessary for iron uptake under iron deficiency. Plant Journal **10,** 835-844.

Yuan, Y.X., Zhang, J., Wang, D.W., and Ling, H.Q. (2005). AtbHLH29 of *Arabidopsis thaliana* is a functional ortholog of tomato *FER* involved in controlling iron acquisition in strategy I plants. Cell Research **15,** 613-621.

Zhang, Y., and Wang, L. (2005). The WRKY transcription factor superfamily: its origin in eukaryotes and expansion in plants. BMC Evolutionary Biology **5,** 1-12.

Zhao, C., Craig, J.C., Petzold, H.E., Dickerman, A.W., and Beers, E.P. (2005). The xylem and phloem transcriptomes from secondary tissues of the Arabidopsis root-hypocotyl. Plant Physiology **138,** 803-818.

Zimmermann, I.M., Heim, M.A., Weisshaar, B., and Uhrig, J.F. (2004). Comprehensive identification of *Arabidopsis thaliana* MYB transcription factors interacting with R/B-like BHLH proteins. Plant Journal **40,** 22-34.

CHAPTER 4

DEFECTS IN CHLOROPLAST PURINE BIOSYNTHESIS ALTER METAL HOMEOSTASIS IN *Arabidopsis thaliana*

ABSTRACT

The chloroplast is a major site for metal use in plants and alterations in chloroplast metal levels are hypothesized to affect metal homeostasis throughout the plant. In screens for altered metal homeostasis in *Arabidopsis thaliana* we identified a role for AtATase2 (EC 2.4.2.14) which encodes a chloroplast-localized enzyme (phosphoribosyl amidotransferase) that catalyzes the first committed step in purine biosynthesis. This disruption in the chloroplast purine biosynthesis pathway appears to compromise normal functions of the chloroplast, including metal use and storage in the organelle. Both point and T-DNA disruption mutations in AtATase2 confer variegated chlorosis and stunted growth. Additionally, the mutants exhibit delayed induction of iron deficiency-inducible ferric chelate reductase activity. Mutant plants have significant decreases in potassium, zinc and copper levels, while over-accumulating manganese, cobalt and cadmium; however, iron levels in the mutants are unchanged. The mutant phenotype is partially overcome by supplementation with the purine inosine. While the link between purine metabolism and metal homeostasis is difficult to define, we have, to our knowledge, provided the first direct evidence linking disruption of chloroplast function with defects in general metal homeostasis in Arabidopsis.

INTRODUCTION

Mineral ions are required for the proper function and nutrition of all living organisms (Lahner et al., 2003). They are an integral part of the electrophysiology, signaling, hormone perception, enzyme activity, membrane transport, and osmoregulation and used as cofactors and catalysts through the organism (Salt, 2004). Plants acquire mineral ions from the s`oil through a complex and highly integrated network of genes that remains largely unknown (Lahner et al., 2003; Salt, 2004). Mineral ion homeostasis is also carefully regulated because these ions are toxic when present in excess or in free form.

In plants, the chloroplast is the general stress sensor (Biswal et al., 2003), and the main storage site of divalent metal cations in the plant, including iron and copper (Shikanai et al., 2003; Terry, 1983; Terry and Low, 1982). The regulation of different mineral ions in each organelle is subject to crosstalk between them (Li and Kaplan, 2004; Shaul, 2002), where deregulation of one ion affects ion levels in other organelles. For example it is known that a minor de-regulation of Mg^{2+} homeostasis in the vacuole strongly affects key enzymes in the chloroplast (Shaul, 2002). Additionally, in yeast the deletion of mitochondrial proteins altered vacuolar metal homeostasis (Li and Kaplan, 2004).

Most of the required purines in the plant are provided by the salvage pathway, but the extra demands imposed by actively growing plant parts are supplied with *de novo* purine synthesis in chloroplasts and mitochondria (Smith and Atkins, 2002). ATP and GTP are final products of the purine synthesis pathway and are essential for chloroplast

activity and survival (Allakhverdiev et al., 2005; Chen et al., 2005; Olsen et al., 1989; Theg et al., 1989; Young et al., 1999). The first link between purine availability and chloroplast function was reported in maize, where a gene knock-out (KO) mutation of a chloroplastic purine importer resulted in a mutant line that shows disrupted chloroplast ultrastructure, localized leaf chlorosis and photosensitivity (Schultes et al., 1996). Amido phosphoribosyl transferase or PPRT has been proposed to be the first committed step in, and general regulator of, purine biosynthesis in Arabidopsis (Boldt and Zrenner, 2003). There is a family of three PPRTs in Arabidopsis (Boldt and Zrenner, 2003; Ito et al., 1994) which are localized to the chloroplast (Hung et al., 2004) and have been named *AtATase1-3*.

AtATase2 has higher and wider expression levels than the two other members of the family (Boldt and Zrenner, 2003; Hung et al., 2004; Ito et al., 1994; van der Graaf et al., 2004). The expression of *AtATase1* is lower and more restricted than *AtATase2* (Boldt and Zrenner, 2003; Hung et al., 2004; Ito et al., 1994; van der Graaf et al., 2004). An *AtATase1* KO line did not show any visual phenotype, but overexpression of *AtATase1* complements an *AtATase2* KO line. *AtATase3* has the lowest expression level of the three but the gene is active enough to permit plant survival of an *AtATase1 AtATase2* double KO line. An RNAi construct for all three members was lethal; indicating that at least one member of the family has to be active to permit plant survival (Hung et al., 2004). There are two recently published reports linking mutations in *AtATase2* to defects in the chloroplast (Hung et al., 2004; van der Graaf et al., 2004). In the first, the disruption of *AtATase2* was accomplished using a T-DNA insertion. Chloroplast maturation was impaired in the knock-out line and plants showed photosensitivity and variegated leaves

(van der Graaf et al., 2004). The second report used forward genetics to screen for mutants defective in the chloroplast protein import system – the translocon. They found two new alleles of *AtATase2* which were named *cia1-1* and *cia1-2*. Both had C→T point mutations that converted Q114* in *cia1-1* and H187Y in *cia1-2*. The *cia1-2* allele was studied in more detail. It showed up to a 50% reduction in its capacity to import proteins into the chloroplast, was chlorotic under normal growing conditions, and was highly dependent on the environment (Hung et al., 2004).

In the process of screening mutagenized Arabidopsis seedlings for phenotypes linked to altered metal ion homeostasis, we identified two new alleles of *AtATase2*. Both mutants, named SP46 and CS557, show variegated chlorosis and stunted growth. SP46 shoots showed differences in the accumulation of several minerals when compared to wild type, suggesting alterations in metal and other ion homeostasis. We suggest that this major disruption in chloroplast integrity causes this altered mineral ion accumulation, and *AtATase2* does not play a direct role in mineral ion homeostasis. Here we are demonstrating for the first time a link between chloroplast function and general metal ion homeostasis in Arabidopsis.

RESULTS

Mutant identification

We used leaf chlorosis as our initial marker to screen for individual plants with altered iron homeostasis in a T-DNA-mutagenized population of *Arabidopsis thaliana*

Columbia gl-1 plants (Campisi et al., 1999). Of the approximately 5,000 individual plants screened, one putative mutant with a novel chlorotic pattern was identified: SP46 (Soil Putant #46). In this mutant, cotyledons are dark green and leaves are dark green upon first emergence. However, as the leaves expand a characteristic variegated pattern emerges (compare Figures 4.1.a and 4.1.b).

Individual chlorotic Arabidopsis lines were also ordered from the Arabidopsis Biological Resource Center (ABRC). One of these lines was *Arabidopsis thaliana* var Enkheim (En-2) CS557, which had a similar chlorotic phenotype to SP46. F_1 progeny from reciprocal crosses between CS557 and SP46 displayed the same chlorotic phenotype as the parental lines, indicating that the mutations were allelic.
Out of 814 F_2 progeny analyzed from an SP46 and *Arabidopsis thaliana* Col-0 cross, 210 individuals showed variegated chlorosis and the remaining 604 had a wild-type phenotype. The χ^2 analysis indicated that this ratio is consistent with the 3:1 segregation pattern expected for a single, recessive mutation in a nuclear-encoded gene (χ^2=0.14; 0.7<P<0.75 for 3:1 segregation).

Analysis of plant responses to iron deficiency

Ferric-chelate reductase activity was used as a secondary screening procedure to increase the probability of identifying plants with defects in iron nutrition and screening out those with defects in the regulation of other elements like Mg or S (Marschner, 1995) or with direct mutations in the photosynthetic apparatus. Reductase activity was measured in SP46 and CS557 mutant plants on transfer to iron-limiting conditions and at

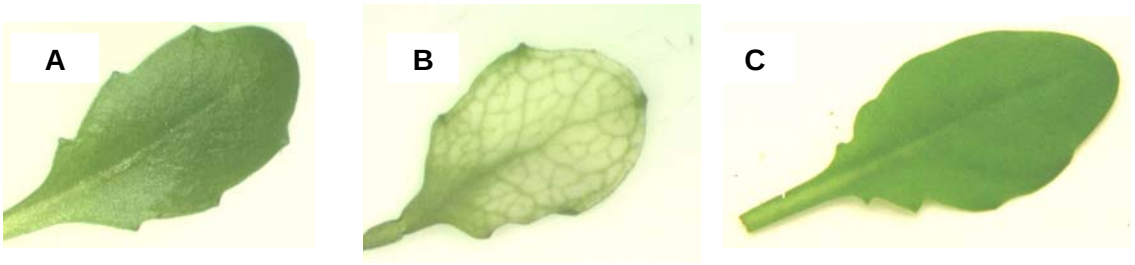

Figure 4.1. Phenotype of rosette leaves and 4-week-old plants.
a.) wild type leaf. b) SP46 leaf. c) leaf of SP46 transformed with a wild-type copy of AtATase2.

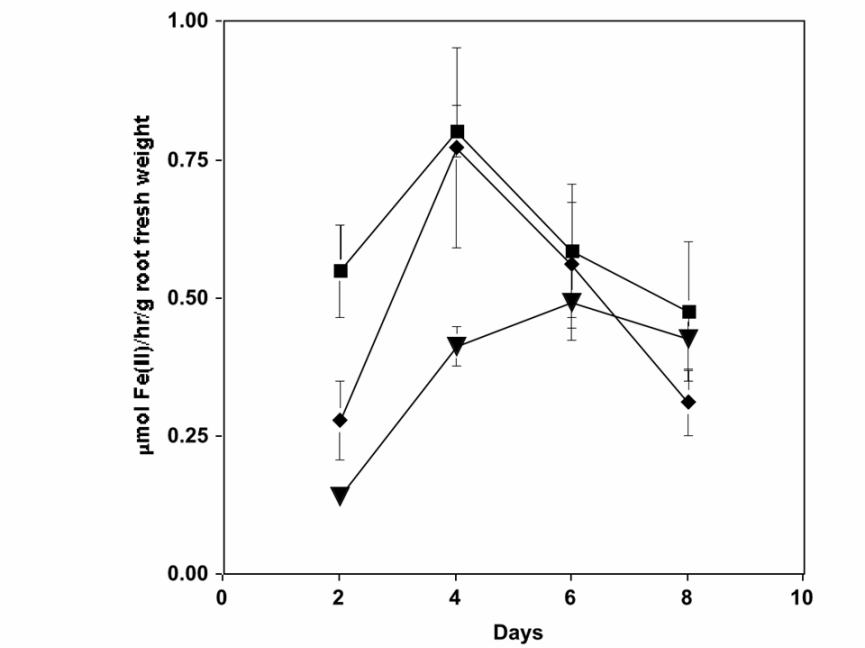

Figure 4.2. Time course of ferric chelate reductase activity.
Ferric chelate reductase activity was measured during an 8-day period after transfer to iron-deficient conditions for wild type (filled squares), SP46 (filled rhomboids), and CS557 (filled inverted triangles). The experiment was repeated three times and a representative data set is shown. Standard deviation is represented by error bars.

2-day intervals thereafter. Both SP46 and CS557 showed delayed induction of ferric-chelate reductase activity when compared to *Arabidopsis thaliana* Col-0 plants (Figure 4.2). SP46 plants reached wild-type ferric-chelate reductase activity levels at day 4. CS557 was able to induce reduction in a limited way and equaled wild-type activity at day 6 when wild-type levels were dropping due to the prolonged absence of iron in the media (Connolly et al., 2003; Vert et al., 2003).

To test whether the expression of iron-regulated genes was altered in SP46, 14-day-old wild type and SP46 plants were grown under iron-deficient conditions for three days to induce their iron-uptake responses, and total RNA from both roots and shoots was isolated. We examined mRNA levels of the main root iron uptake transporter *IRT1*, the root ferric chelate reductase *FRO2*, and the iron-responsive iron storage protein ferritin1 (*AtFer1*). No significant differences were observed in either root or shoot mRNA levels under either iron-sufficient or iron-deficient growth conditions for any of the three genes examined (data not shown).

To test further the effect of the mutation on iron homeostasis, elemental analysis was performed on shoots of mutant and wild-type plants grown on soil. SP46 plants showed significant over-accumulation of arsenic (+48.7%), cadmium (+20.7%), cobalt (+23.2%), lithium (+16.9%), and manganese (+30.1%). However, they showed significant under-accumulation of copper (-41.7%), potassium (-20.7%), selenium (-8.6%), and zinc (-10.3%). To our surprise, iron levels were not significantly different from wild type. The data suggests that SP46 plants show a general defect in their mineral ion homeostasis (Table 4.1).

Identification of the mutant gene in SP46

Phenotypic and PCR analysis of the F_2 progeny from a SP46 and *Arabidopsis thaliana* Col-0 cross demonstrated that no T-DNA was linked to the chlorotic phenotype (data not shown). Therefore SP46 (in the Col-0 background) was crossed to Landsberg *erecta* to create an F_2 mapping population. As a first step, bulked genomic DNA (Lukowitz et al., 2000) from 82 F_2-mutant plants was analyzed using both Cleaved Amplified Polymorphic Sequences (CAPS) and Simple Sequence Length Polymorphisms (SSLP) markers (Jander et al., 2002). The mutation was located on the bottom of Chromosome IV (Figure 4.3.a). Using a total of 967 F_2 mutant plants the mutant locus was mapped to a 75 kb or 0.3 cM region that contained 24 predicted Open Reading Frames (ORFs) (Figure 4.3.b) (The Arabidopsis Genome Initiative, 2000). T-DNA insertion lines (Alonso et al., 2003) for 19 of these ORFs were obtained from the ABRC. One of the 19 homozygous T-DNA lines, SALK_028034, showed a variegated chlorosis similar to SP46. This T-DNA insertion is estimated to be 29 bp upstream of the start codon of At4g34740 (Figure 4.3.c). We confirmed that At4g34740 is not expressed in T-DNA line SALK_028034 by RT-PCR (data not shown).

F_1 individuals from a cross between SP46 and SALK_028034 maintained the variegated chlorotic phenotype. This lack of complementation demonstrated that the mutation in SP46 and the T-DNA insertion in line SALK_029034 affected the same gene. We confirmed At4g34740 as the locus of the mutation by complementing mutant SP46 Arabidopsis plants with a wild-type genomic fragment containing the complete coding sequence of At4g34740 as predicted by publicly available EST information, and

approximately 1,000 bp of sequence upstream of the starting ATG to serve as the native promoter (Figure 4.1.c). Locus At4g34740 encodes the enzyme phosphoribosyl amidotransferase or PPRT (Boldt and Zrenner, 2003; Ito et al., 1994; van der Graaf et al., 2004).

Comparison of *AtATase2* sequences

We sequenced both mutant alleles of *AtATase2* and discovered that SP46 had a point mutation in position 723 where adenine replaced a guanine, which changes the amino acid in position 242 from a glycine to a serine. This glycine is highly conserved in both plant and bacterial PPRTs, which may explain why this serine substitution confers such a severe phenotype on the SP46 mutant.

The wild-type sequence of *AtATase2* from the ecotype Enkheim is not publicly available; therefore En-2 seeds were obtained from the ABRC and *AtATase2* was sequenced (GenBank Accession Number AY842241). As compared to *Arabidopsis thaliana* Col-0, the En-2 *AtATase2* has three polymorphisms. A CT nucleotide pair at positions 14 and 15 in the Arabidopsis thaliana Col-0 sequence is a GC in En-2; this changes the 5th amino acid from a serine to a cysteine. The first approximately 53 amino acids of *AtATase2* are predicted to encode a chloroplast localization sequence; the substitution of a cysteine for a serine at position 5 does not change this prediction (Emanuelsson et al., 2000). Also, nucleotide 213 is a G in the *Arabidopsis thaliana* Col-0 sequence and is replaced by a T in En-2; this polymorphism is silent and does not change the predicted polypeptide sequence.

The sequencing of *AtATase2* in CS557 revealed two nucleotide changes relative to both the *Arabidopsis thaliana* Col-0 and En-2 sequences, therefore they were considered mutations. The first one was a three bp in-frame deletion (Δ129-131) that resulted in the elimination of a serine in position 44. The second one was a point mutation in position 1090 that replaces a G with an A which in turn changes the amino acid in position 364 from a valine to a methionine (Figure 4.4). However, CS557 had the *Arabidopsis thaliana* Col-0 sequence at all three base pairs polymorphic between *Arabidopsis thaliana* Col-0 and En-2; thus calling into question the ecotype background of CS557. The serine deletion in CS557 is in the predicted chloroplast localization sequence, but does not change the predicted chloroplast localization of the mutant polypeptide (Emanuelsson et al., 2000). The V364M change occurs in an amino acid residue that is highly conserved in plant, animal and bacterial PPRTs; therefore it is likely this second mutation caused the phenotype observed in CS557. *AtATase2* mRNA levels in both mutant alleles remained comparable to wild type (data not shown).

As mentioned previously, mutant alleles of *AtATase2* have been described before. To provide a unified nomenclature system, we will use the *atd2* nomenclature of the first reported *AtATase2* mutants (van der Graaf et al., 2004) and name our new alleles as follows: SP46 as *atd2-2*, CS557 as *atd2-3*, and SALK_029034 as *atd2-4*.

Phenotypic complementation with inosine

Inosine is one of the downstream products of the purine biosynthetic pathway and it has been previously reported that inosine-5'-phosphate is able to complement the

chlorotic phenotype of *atd2* (van der Graaf et al., 2004). We grew *atd2-2* (SP46) mutant and wild-type plants in solid and liquid media with or without 10 mM inosine for 14 days and rated them for chlorosis. Inosine was able to complement the chlorotic phenotype of mutant plants grown in liquid media only, but not when grown on solid media (data not shown). Elemental analysis was performed to verify whether inosine complemented the alterations in metal accumulation. Under liquid growth conditions, only manganese and potassium levels in *atd2-2* were significantly different from wild type (Table 4.2). Neither of these metal accumulation differences were complemented by growth in 10 mM inosine.

DISCUSSION

This work outlines the isolation, characterization and cloning of an Arabidopsis mutant gene that causes defects in both chloroplast function and in maintenance of mineral ion homeostasis. We were able to identify both allelic mutants, called SP46 (*atd2-2*) and CS557 (*atd2-3*) using foliar chlorosis and abnormal ferric chelate reductase activity as phenotypic markers for mutations in iron homeostasis. In spite of both screens being directed to identify iron-related mutants, both iron levels and mRNA levels of several iron-deficiency regulated genes (*IRT1, FRO2,* and *AtFer1*) were similar to WT.

Using map-based cloning, we identified the gene responsible for the mutant phenotype at locus At4g34740, which was confirmed by genetic analysis, sequencing, and complementation. This locus encodes AtATase2, a phosphoribosyl amidotransferase or PPRT. PPRT is a Fe-S-dependent enzyme that has been proposed to be the first

Table 4.1. Average leaf elemental content[a] of wild-type (WT) and SP46 Arabidopsis plants.

Element	Units[b]	WT	SP46	% difference	p-value[c]	Significance[d]
Metals						
Cadmium	ppm	1.82	2.19	20.7	0.0003	*
Calcium	%	4.24	4.15	-2.1	0.6100	
Cobalt	ppm	1.52	1.87	23.2	<0.0001	*
Copper	ppm	1.19	0.69	-41.7	0.0027	*
Iron	ppm	87.69	87.86	0.2	0.9800	
Lithium	ppm	14.81	17.31	16.9	0.0170	*
Sodium	ppm	595.15	715.11	20.2	0.0510	
Potassium	%	3.17	2.51	-20.7	0.0022	*
Magnesium	%	1.21	1.18	-2.7	0.3800	
Manganese	ppm	39.98	52.00	30.1	<0.0001	*
Molybdenum	ppm	5.90	6.34	7.5	0.2000	
Nickel	ppm	0.93	0.73	-21.2	0.4500	
Zinc	ppm	48.57	43.58	-10.3	0.0032	*
Non-metals						
Arsenic	ppm	1.42	2.11	48.7	<0.0001	*
Phosphorous	%	0.82	0.91	10.8	0.5500	
Selenium	ppm	9.90	9.05	-8.6	0.0500	*

[a] Average from one leaf from each of 25 individual plants for WT and for SP46.

[b] Units=ppm/gram or % dry weight.

[c] p-value from the ANOVA test.

[d] Significance level at $p \leq 0.05$.

Table 4.2. Elemental analysis in ppm/gram dry weight of Arabidopsis plants grown in liquid media with or without 10mM inosine.

	Average content in			p-value of 2-tailed t-test of difference	Average content in			p-value of 2-tailed t-test of difference
	WT	SP46			WT	SP46		
Element	- inosine	- inosine	% diff.		+ inosine	+ inosine	% diff.	
Potassium	73066	83245	13.9%	0.0039	75205	85390	13.5%	0.0140
Manganese	134	153	14.2%	0.0043	136	154	13.2%	0.0927

committed step in and a general regulator of the chloroplastic purine biosynthesis pathway. PPRT belongs to a small family of three genes in Arabidopsis (Boldt and Zrenner, 2003).

Even though *atd2-2* (SP46) was part of a T-DNA mutagenized population this mutation was not caused by a T-DNA insertion. The sequence changes in the *atd2-3* mutant are unique. *atd2-3* (CS557) has the *Arabidopsis thaliana* Col-0 sequence at the three nucleotides polymorphic between *Arabidopsis thaliana* Col-0 and En-2. Additionally, it has two sequence changes found in neither *Arabidopsis thaliana* Col-0 nor En-2, a G/C to A/T transition and a three base pair in-frame deletion. Both the occurrence of two separate mutations and a three base deletion are uncommon in EMS-derived mutants (Greene et al., 2003). It is possible that *atd2-3* is in another, different genetic background that contains the *Arabidopsis thaliana* Col-0 sequence and the in-frame three base deletion in its wild-type sequence. Therefore, the mutation responsible for the phenotypes would be the G/C to A/T transition, a change highly consistent with the mode of action of EMS (Greene *et al.*, 2003). However, more experiments will be necessary to determine both the ecotype background of CS557 and the exact cause of the mutant phenotype. The variegated chlorotic phenotype typical of *atd* mutant plants (Hung et al., 2004; van der Graaf et al., 2004; this work) is, on closer examination, an interveinal chlorosis surrounded by green vasculature and certain green parts close to the hydathodes of the leaves (Figure 4.1). Since *AtATase2* and *AtATase1* are expressed in leaves (Boldt and Zrenner, 2003; Hung et al., 2004; Ito et al., 1994), it is possible that *AtATase1* is expressed in the green areas, along the veins and in the borders of the leaves, whereas *AtATase2* might be expressed mostly in the interveinal areas, where chlorosis can be seen

Figure 4.3.

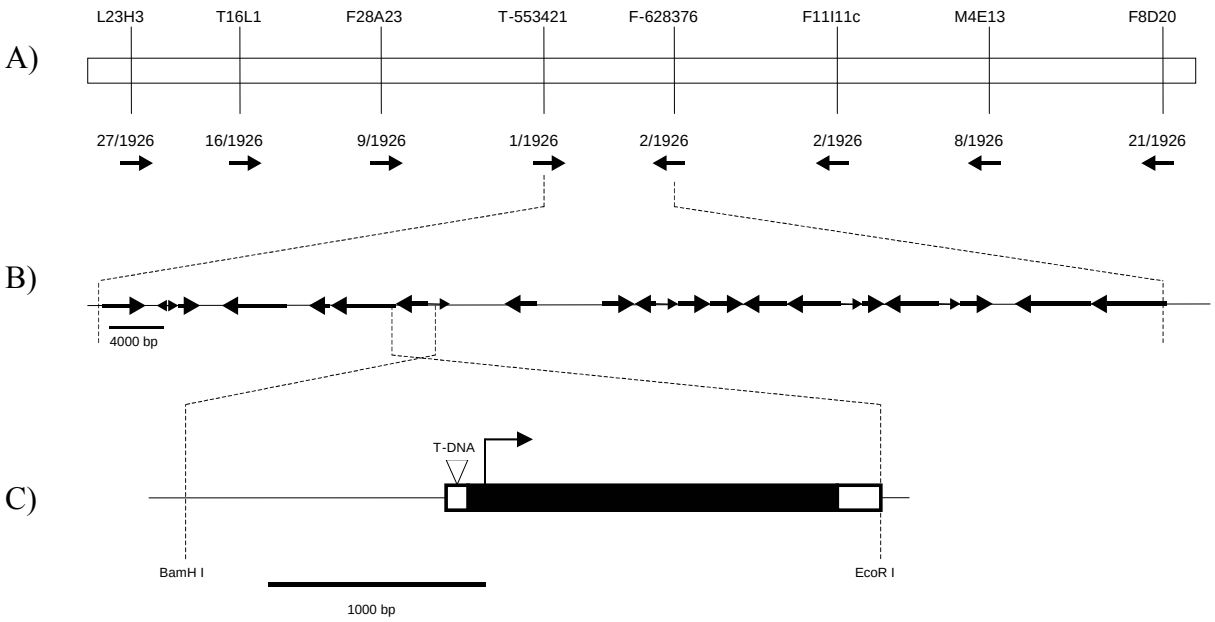

Figure 4.3. Map-based cloning of the SP46 locus.
a) PCR-based molecular markers used are shown by thin vertical lines. Number of recombination events for each marker/total number of mutant chromosomes tested are noted under the molecular markers. Arrows point towards the location of the mutant locus. b) The minimal map location contains 24 predicted ORFs and arrows show the predicted direction of translation for each ORF. c) Representation of AtATase2, locus of SP46. The thin line represents the promoter and the filled box represents the coding sequence of AtATase2. Empty boxes represent predicted 5'- and 3'- UTRs. The triangle marks the T-DNA insertion in line SALK_028034. The arrow represents the translation initiation site. BamHI and EcoRI restriction sites used for cloning and complementation are noted.

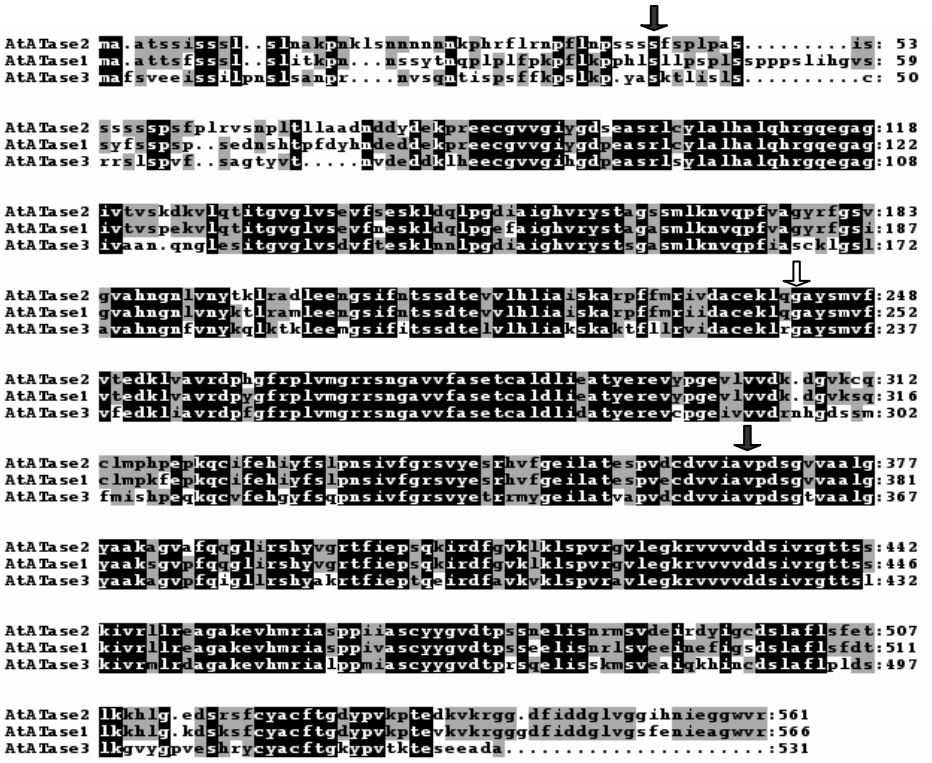

Figure 4.4. Amino acid sequence analysis of the AtATase family.
Protein alignment of the AtATase family in Arabidopsis thaliana was conducted using ClustalW. Residues shown in black letters on grey background represent conserved residues in at least two members of the family. Numbers indicate amino acid position. White arrow shows the location of the missense mutation in atd2-2 that results in G242S. Black arrows show the location of both mutations in atd2-3: a 3 bp deletion that causes S44Δ and a missense mutation that causes V364M.

in the mutants.

When grown on soil and compared to WT, *atd2-2* plants showed alterations in arsenic, cadmium, cobalt, copper, lithium, manganese, potassium, selenium, and zinc levels. When grown on liquid media the same mutant line showed alterations only in manganese and potassium content. It has been shown that mutant Arabidopsis plants often over- or under-accumulate a different set of metals under different growth conditions (Lahner et al., 2003). Therefore, it is not surprising that *atd2-2* exhibited a different pattern of metal accumulation on soil versus liquid culture (compare Tables 4.1 and 4.2).

It is not clear why inosine supplementation was unable to complement the metal accumulation defects of *atd2-2*. Most likely, external supplementation with inosine restores partial chloroplast function, which would be sufficient to reverse the chlorotic phenotype, but not sufficient to complement the aberrant metal accumulation. In our experiments, plants in liquid media were grown under approximately 55 μEinsteins constant light or about half the 100 μEinsteins used for seedlings grown on plates. Given the previously reported photosensitivity of *atd* mutants, it is possible that inosine supplementation was able to partially rescue the *atd2-2* chlorotic phenotype. The level of rescue was sufficient to restore a uniform green appearance to seedlings grown in liquid culture at low light levels but was not sufficient to fully complement the *atd2-2* phenotype, including its alteration in metal ion homeostasis. Since chloroplast function in the mutant supplemented with inosine has not been examined in detail, this remains a matter for further investigation.

The delay in the expression of iron-deficiency inducible ferric-chelate reductase

activity in *atd2-2* and *atd2-3* mutant plants were not related to deficiencies in iron homeostasis since iron levels in *atd2-2* were similar to WT (Table 4.1). It has been shown before that *FRO2* activity is regulated transcriptionally and post-transcriptionally, and may be regulated post-translationally as well. Iron, zinc, and cadmium affect transcription of *FRO2*, but the post-transcriptional or post-translational regulators remain unknown (Connolly et al., 2003). The fact that *FRO2* transcript levels are similar to WT in the presence of statistically different levels of zinc and cadmium in mutant plants (Table 4.1) indicates that at the transcript level, zinc and cadmium are minor regulators of *FRO2* transcription when compared to iron.

The WT levels of *FRO2* mRNA in *atd2-2* indicate that the *FRO2* gene is being appropriately regulated at the transcriptional level. The lower levels of ferric-chelate reductase activity in *atd2-2* point to defects in post-transcriptional regulation. It is possible that the over-accumulation of toxic cadmium ions or under-accumulation of zinc ions under iron-deficiency conditions in the mutant causes the down-regulation of the ferric-chelate reductase protein or activity. This might possibly be a way for the plant to adjust to or correct the alterations in zinc or cadmium accumulation. However, since neither zinc nor cadmium must be reduced prior to uptake, it is more likely an indirect effect. Neither the high cadmium nor the low zinc levels in the *atd2-2* mutant are ideal for plant growth. Therefore, the *atd2-2* mutants may simply not be able to perform the energy-intensive reduction of ferric iron to the same extent as wild-type plants. The delay in induction of ferric chelate reductase activity could be linked with the low copper levels. It has been shown that under iron-deficiency conditions, the reduction of Cu(II) to Cu(I) was induced in Arabidopsis plants (Yi and Guerinot, 1996). The *frd1* mutant plant

line lacks root epidermal ferric chelate reductase activity, and these plants, although incapable of reducing Cu(II) to Cu(I), increased their total copper content (Yi and Guerinot, 1996). This points to the absence of a direct link between copper reduction and copper acquisition in Arabidopsis plants.

We propose that the chloroplastic defects due to the *atd2-2* mutation have an indirect effect on mineral ion homeostasis in the leaves of the mutant plants. The chloroplast is a major site of metal use and storage in the plant (Shikanai et al., 2003; Terry, 1983; Terry and Low, 1982), and since many chloroplasts in *AtATase2* mutants are nonfunctional, the mutants have altered requirements for a variety of metal ions including copper, manganese and zinc (Table 4.1). While PPRT is a Fe-S cluster-containing enzyme, it is unlikely that simply the lack of this one Fe-S cluster protein would have a direct effect on mineral ion levels, especially since overall iron levels are not changed in the mutants. It has been shown previously that mutant Arabidopsis plants rarely have alterations in the levels of only one metal ion (Lahner et al., 2003). Therefore, it is not unexpected that the chloroplast defects in *AtATase2* mutants alter the levels of several elements.

From the literature a consensus starts to emerge that the chloroplast defects caused by mutations in *AtATase2* have a general pleiotropic effect on the plant. Mutations in *AtATase2* alter chloroplast development, eliminate the mesophyll layer of cells in the leaves, reduce chloroplast number, confer photosensitivity (van der Graaf et al., 2004), reduce protein import into the chloroplast by up to 50%, reduce leaf cell number and size (Hung et al., 2004), delay the activation of ferric-chelate reductase activity under iron deficiency conditions, and alter general ion homeostasis in Arabidopsis plants. The

combination of phenotypes observed in the *atd2* mutants points to the chloroplast as a key player in the complex processes that maintain metal ion homeostasis in plants.

FUTURE DIRECTIONS

This report raises new questions about different leads in iron- and metal-homeostasis systems in Arabidopsis.

Localized chlorosis

atd2-2 mutant plants show localized chlorosis in their leaves. It is possible that purine biosynthesis alone is responsible for this variegated phenotype, with different members of the AtATase family being expressed in different areas of the leaf and plant. It is also possible that chlorotic regions are not supplemented with exogenous purines as well as green areas. To differentiate between these two hypotheses we would like to localize the expression of all three members of the AtATase family of genes using reporter genes like GUS. This would confirm if areas of expression of *AtATase2* co-localizes with the chlorotic areas in the leaves and if the green areas show expression of the other members of the family.

Delay in ferric chelate reductase activity

Another phenotype shown by *atd2-2* mutant plants is a delay in the activation of ferric chelate reductase activity. It is known that *FRO2* is the main root ferric chelate reductase in Arabidopsis (Yi and Guerinot, 1996), is regulated at the transcriptional level by metals like iron, cadmium, and zinc, and at the post-transcriptional level by as-yet unknown factors (Connolly et al., 2003). Since *atd2-2* plants over-accumulate cadmium and under-accumulate zinc, we would like to reproduce the delay in ferric chelate reductase activity in WT plants under iron-deficient conditions and different levels of zinc and cadmium. Hopefully these experiments will help explain this one phenotype and at the same time give us more information about the interactions between different *FRO2* transcriptional regulators.

De-regulation of metal homeostasis

As we can see in Table 1, nine of the sixteen elements present in the analysis show levels that are statistically different between *atd2-2* plants and the control. This phenotype could be due to a chloroplast-specific defect or to a defect in the purine biosynthesis pathway. To confirm or eliminate the hypothesis of the chloroplast-specific defect we would like to analyze the elemental contents of different chloroplast-specific mutants. It is possible that the phenotype is related to only a specific step in the purine biosynthesis pathway, by way of a missing protein or the overaccumulation of intermediate synthates. To help us understand how the purine biosynthetic pathway and

the phenotype are related, we would like to analyze the elemental content of the individual T-DNA lines for all members of the purine biosynthesis pathway.

MATERIALS AND METHODS

Plant Growth Conditions

Unless specified otherwise, plants were grown under sterile conditions as described previously (Yi and Guerinot, 1996). Briefly, seeds were surface sterilized, planted on Gamborg's B5 medium (Caisson Labs, Rexburg, ID) and stratified in the dark for 4 days at 4°C. B5 medium for transgenic plants was supplemented with 50 μg mL^{-1} kanamycin or 25 μg mL^{-1} hygromycin. Plants were transferred to a growth chamber (Percival Scientific, Perry, IA), grown for 14 days at 21°C under approximately 100 μEinsteins constant light, and then transferred to plates with or without 50 mM Fe(III) EDTA for iron-sufficient or iron-deficient conditions, respectively (Yi and Guerinot, 1996).

Identification of Arabidopsis mutants with altered iron homeostasis

A pool ~5,000 T-DNA mutagenized Arabidopsis seed (Campisi et al., 1999) and line CS557 were obtained from the ABRC (The Arabidopsis Biological Resources Center, Columbus, OH), planted on MetroMix 200 (Hummert, St. Louis, MO), and grown under 16 hr days at 20°C. Approximately 3-week-old seedlings were visually

screened for chlorotic phenotypes. Seed was collected from chlorotic individuals and tested in the next generation for chlorosis and alterations in ferric chelate reductase activity as described before (Yi and Guerinot, 1996).

RNA Blots

Total RNA was isolated from plant tissue using the LiCl method (Verwoerd et al., 1989). *IRT1* and *FRO2* probes were prepared as described (Rogers and Guerinot, 2002). The UBQ5 probe was amplified as described previously (Rogers and Ausubel, 1997). The probe for ferritin1 (AtFer1) gene was the 3'-UTR as described (Petit et al., 2001). RNA blots were performed according to standard methods (Sambrook and Russell, 2001) using Osmonics membranes (Westborough, MA). Quantification of the signal was done using a Molecular Dynamics Storm 860 PhosphorImager (Amersham Biosciences, Piscataway, NJ) and normalized to UBQ5 mRNA levels.

Mapping and cloning of SP46

Genomic DNA was extracted as described previously (Edwards et al., 1991), and used for mapping. New molecular markers were designed using information from the complete *Arabidopsis thaliana* var. Columbia genomic sequence (The Arabidopsis Genome Initiative, 2000) and the draft genomic sequence of *Arabidopsis thaliana* var. *Landsberg erecta* (Jander et al., 2002). T-DNA insertion lines (Alonso et al., 2003) were obtained from the ABRC. DNA sequencing of PCR products was performed at the

University of Missouri DNA Sequencing Core Facility using an Applied Biosystems 377 automated DNA sequencer using Applied Biosystems Prism BigDye Terminator cycle sequencing chemistry (Foster City, CA). Protein alignments were performed with ClustalW (Thompson et al., 1994).

Complementation analysis

BAC clone F11I11, which contained a complete copy of the gene At4g34740, was ordered from the ABRC, isolated, and cut with EcoRI and BamHI restriction enzymes (Promega, Madison, WI) using standard molecular techniques (Sambrook and Russell, 2001). A single 2,926 bp fragment that contained the complete gene, 1,026 bp of upstream sequence, and 214 bases of downstream sequence, was cloned into the vector pCAMBIA 2200 (CAMBIA, Black Mountain, Australia). The fragment was inserted into mutant SP46 Arabidopsis plants via *Agrobacterium tumefascines* GV3101 using the dipping method (Clough and Bent, 1998). T_1 and T_2 seed were planted on selectable media. Only transformed lines segregating for the selectable marker in a 3:1 ratio in the T_2 generation were used for further experiments.

Elemental analysis

Shoots were analyzed by Inductively Coupled Plasma Mass Spectroscopy (ICP-MS) as described previously (Lahner et al., 2003).

Inosine complementation

Mutant and wild-type plants were grown on liquid B5 media or liquid B5 media supplemented with 10mM Inosine (Sigma-Aldrich, Saint Louis, MO). All plants were harvested after 14 days, visually analyzed for chlorosis, washed with ultra-pure water, and dried for 4 days at 65^{o}C on a conventional oven before being subjected to elemental analysis as described above.

ACKNOWLEDGEMENTS

We would like to thank Lorena DaPonte, Juan Jose Gutierrez, and Timothy Pouland for their technical support through different stages of the project. We thank Dr. David Salt and Brett Lahner for elemental analysis, Timothy Durrett for advice on the experiments, and Drs. Dirk Charlson, Walter Gassmann and Joe Polacco for critically reading the manuscript. We acknowledge the Arabidopsis Biological Resource Center (ABRC) for supplying seed. Funding was supplied by MU Mission Enhancement.

REFERENCES

Allakhverdiev, S.I., Nishiyama, Y., Takahashi, S., Miyairi, S., Suzuki, I., Murata, N. (2005). Systematic analysis of the relation of electron transport and ATP synthesis to the photodamage and repair of photosystem II in Synechocystis. Plant Physiology **137**, 263-273.

Alonso, J.M., Stepanova, A.N., Leisse, T.J., Kim, C.J., Chen, H., Shinn, P., Stevenson, D.K., Zimmerman, J., Barajas, P., Cheuk, R., Gadrinab, C., Heller, C., Jeske, A., Koesema, E., Meyers, C.C., Parker, H., Prednis, L., Ansari, Y., Choy, N., Deen, H., Geralt, M., Hazari, N., Hom, E., Karnes, M., Mulholland, C., Ndubaku, R., Schmidt, I., Guzman, P., Aguilar-Henonin, L., Schmid, M., Weigel, D., Carter, D.E., Marchand, T., Risseeuw, E., Brogden, D., Zeko, A., Crosby, W.L., Berry, C.C., Ecker, J.R. (2003). Genome-wide insertional mutagenesis of *Arabidopsis thaliana*. Science **301**, 653-657.

Biswal, U.C., Biswal, B., Mukesh, R.K. (2003). Chloroplast biogenesis. From proplastid to gerontoplast. Dordrecht: Kluver Academic Press.

Boldt, R., Zrenner, R. (2003). Purine and pyrimidine biosynthesis in higher plants. Physiolgia Plantarum **117**, 297-304.

Campisi, L., Yang, Y., Yi, Y., Heilig, E., Herman, B., Cassista, A.J., Allen, D.W., Xiang, H., Jack, T. (1999). Generation of enhancer trap lines in Arabidopsis and characterization of expression patterns in the inflorescence. Plant Journal **17**, 699-707.

Chen, G., Bi, Y.R., Li, N. (2005). EGY1 encodes a membrane-associated and ATP-independent metalloprotease that is required for chloroplast development. Plant Journal **41**, 364-375.

Clough, S.J., Bent, A.F. (1998). Floral dip: a simplified method for Agrobacterium-mediated transformation of *Arabidopsis thaliana*. Plant Journal **16**, 735-743.

Cobbett, C.S. (2000). Phytochelatins and their roles in heavy metal detoxification. Plant Physiology **123**, 825-832.

Connolly, E.L., Campbell, N.H., Grotz, N., Prichard, C.L., Guerinot, M.L. (2003). Overexpression of the FRO2 ferric chelate reductase confers tolerance to growth on low iron and uncovers posttranscriptional control. Plant Physiology **133**, 1102-1110.

Connolly, E.L., Fett, J.P., Guerinot, M.L. (2002). Expression of the IRT1 metal transporter is controlled by metals at the levels of transcript and protein accumulation. Plant Cell **14**, 1347-1357.

Edwards, K., Johnstone, C., Thompson, C. (1991). A simple and rapid method for the preparation of plant genomic DNA for PCR analysis. Nucleic Acids Research **19**, 1349.

Emanuelsson, O., Nielsen, H., Brunak, S., von Heijne, G. (2000). Predicting subcellular localization of proteins based on their N-terminal amino acid sequence. Journal of Molecular Biology **300**, 1005-1016.

Greene, E., Codomo, C., Taylor, N., Henikoff, J., Till, B., Reynolds, S., Enns, L., Burtner, C., Johnson, J., Odden, A., Comai, L., Henikoff, S. (2003). Spectrum of chemically induced mutations from a large-scale reverse-genetic screen in Arabidopsis. Genetics **164**, 731-740.

Hung, W-F., Chen, L-J., Boldt, R., Sun, C-W., Li, H-m. (2004). Characterization of Arabidopsis glutamine phosphoribosyl pyrophosphate amidotransferase-deficient mutants. Plant Physiology **135**, 1314-1323.

Ito, T., Shiraishi, H., Okada, K., Shimura, Y. (1994). Two amidophosphoribosyltransferase genes of *Arabidopsis thaliana* expressed in different organs. Plant Molecular Biology **26**, 529-533.

Jander, G., Norris, S.R., Rounsley, S.D., Bush, D.F., Levin, I.M., Last, R.L. (2002). Arabidopsis map-based cloning in the post-genome era. Plant Physiology **129**, 440-450.

Kraemer, U. (2003). Phytoremediation to phytochelatin - plant trace metal homeostasis. New Phytologist **158**, 4-6.

Lahner, B., Gong, J., Mahmoudian, M., Smith, E.L., Abid, K.B., Rogers, E.E., Guerinot, M.L., Harper, J.F., Ward, J.M., McIntyre, L., Schroeder, J.I., Salt, D.E. (2003). Genomic scale profiling of nutrient and trace elements in *Arabidopsis thaliana*. Nature Biotechnology **21**, 1215-1221.

Li, L., Kaplan, J. (2004). A mitochondrial-vacuolar signaling pathway in yeast that affects iron and copper metabolism. Journal of Biological Chemistry **279**, 33653-33661.

Lukowitz, W., Gillmor, C.S., Scheible, W-R. (2000). Positional cloning in Arabidopsis. Why it feels good to have a genome initiative working for you. Plant Physiology **123**, 795-806.

Maathuis, F.J.M., Filatov, V., Herzyk, P., Krijger, G.C., Axelsen, K.B., Chen, S., Green, B.J., Li, Y., Madagan, K.L., Sanchez-Fernandez, R., Forde, B.G., Palmgren, M.G., Rea, P.A., Williams, L.E., Sanders, D., Amtmann, A. (2003). Transcriptome analysis of root transporters reveals participation of multiple gene families in the response to cation stress. Plant Journal **35**, 675-692.

Marschner, H. (1995). Mineral nutrition of higher plants, second edition. Academic Press, London.

Olsen, L., Theg, S., Selman, B., Keegstra, K. (1989). ATP is required for the binding of precursor proteins to chloroplasts. Journal of Biological Chemistry **264**, 6724-6729.

Petit, J-M., Briat, J-F., Lobreaux, S. (2001). Structure and differential expression of the four members of the *Arabidopsis thaliana* ferritin gene family. Biochemical Journal **359**, 575-582.

Robinson, N.J., Procter, C.M., Connolly, E.L., and Guerinot, M.L. (1999). A ferric-chelate reductase for iron uptake from soils. Nature **397,** 694-697.

Rogers, E.E., Ausubel, F.M. (1997). Arabidopsis enhanced disease susceptibility mutants exhibit enhanced susceptibility to several bacterial pathogens and alterations in PR-1 gene expression. Plant Cell **9**, 305-306.

Rogers, E.E., Guerinot, M.L. (2002). FRD3, a member of the multidrug and toxin efflux family, controls iron deficiency responses in Arabidopsis. Plant Cell **14**, 1787-1799.

Salt, D.E. (2004). Update on plant ionomics. Plant Physiology **136**, 2451-2456.

Sambrook, J., Russell, D.W. (2001). Molecular cloning: a laboratory manual. Cold Spring Harbor, NY: Cold Spring Harbor Laboratory Press.

Schultes, N.P., Brutnell, T.P., Allen, A., Dellaporta, S.L., Nelson, T., Chen, J. (1996). Leaf permease1 gene of maize is required for chloroplast development. Plant Cell **8**, 463-475.

Shaul, O. (2002). Magnesium transport and function in plants: the tip of the iceberg. BioMetals **15**, 307-321.

Shikanai, T., Muller-Moule, P., Munekage, Y., Niyogi, K.K., Pilon, M. (2003). PAA1, a P-Type ATPase of Arabidopsis, functions in copper transport in chloroplasts. Plant Cell **15**, 1333-1346.

Smith, P.M.C., Atkins, C.A. (2002). Purine biosynthesis. Big in cell division, even bigger in nitrogen assimilation. Plant Physiology **128**, 793-802.

Terry, N. (1983). Limiting factors in photosynthesis. Plant Physiology **71**, 855-860.

Terry, N, Low, G. (1982). Leaf chlorophyll content and its relation to the intracellular localization of iron. Journal of Plant Nutrition **5**, 301-310.

The Arabidopsis Genome Initiative. (2000). Analysis of the genome sequence of the flowering plant *Arabidopsis thaliana*. Nature **408**, 796-815.

Theg, S., Bauerle, C., Olsen, L., Selman, B., Keegstra, K. (1989). Internal ATP is the only energy requirement for the translocation of precursor proteins across chloroplastic membranes. Journal of Biological Chemistry **264**, 6730-6736.

Thompson, J.D., Higgins, D.G., Gibson, T.J. (1994). CLUSTAL W: improving the sensitivity of progressive multiple sequence alignment through sequence weighting, position-specific gap penalties and weight matrix choice. Nucleic Acids Research **22**, 4673-4680.

van der Graaf, E., Hooykaas, P., Lein, W., Lerchl, J., Kunze, G., Sonnewald, U., Boldt, R. (2004). Molecular analysis of "de novo" purine biosynthesis in solanaceous species and in *Arabidopsis thaliana*. Frontiers in Bioscience **9**, 1803-1816.

Vert, G.A., Briat, J-F., Curie, C. (2003). Dual regulation of the Arabidopsis high-affinity root iron uptake system by local and long-distance signals. Plant Physiology **132**, 796-804.

Verwoerd, T.C., Dekker, B.M., Hoekema, A. (1989). A small-scale procedure for the rapid isolation of plant RNAs. Nucleic Acids Research **17**, 2362.

Wintz, H., Fox, T., Wu, Y-Y., Feng, V., Chen, W., Chang, H-S., Zhu, T., Vulpe, C. (2003). Expression profiles of *Arabidopsis thaliana* in mineral deficiencies reveal novel transporters involved in metal homeostasis. Journal of Biological Chemistry **278**, 47644-47653.

Yi, Y., Guerinot, M.L. (1996). Genetic evidence that induction of root Fe(III) chelate reductase activity is necessary for iron uptake under iron deficiency. Plant Journal **10**, 835-844.

Young, M.E., Keegstra, K., Froehlich, J.E. (1999). GTP promotes the formation of early-import intermediates but is not required during the translocation step of protein import into chloroplasts. Plant Physiology **121**, 237-244.

VITA

Alberto Maurer was born in Lima, Peru in 1970. He attended Pestalozzi Private School and then was admitted to La Molina National Agriculture University in Lima where he obtained a Bachelor of Science degree in Agricultural Engineering in 1994. His thesis work dealt with the adaptation of new varieties of Barley to the high Andes environment. After finishing his degree, he was hired by the Ag division of Novartis Peru as a Regional Manager, position he held for four years. Alberto came to the University of Missouri–Columbia in August 1999 to pursue his dream of obtaining a PhD in Genetics, goal reached in May 2006.